Dark Matter from rotating axions

Géraldine SERVANT
DESY/U.Hamburg

CERN TH Institute,
14-06-2024

CLUSTER OF EXCELLENCE
QUANTUM UNIVERSE

Universität Hamburg

This talk

Based on:

Rotating axions :
Beyond the standard misalignment mechanism

[Eroncel, Soerensen, Sato, Servant, 2206.14259]

[Eroncel, Soerensen, Sato, Servant, 2406.xxxx]

Gravitational signatures (axion mini-clusters)

[Eroncel, Servant 2207.10111]

Impact on primordial gravitational-wave backgrounds

[Gouttenoire, Servant, Simakachorn, 1912.02569, 2108.10328 , 2111.01150]

Axion fragmentation

[Fonseca, Morgante, Sato, Servant, 1911.08472]

[Chatrchyan, Eroncel, Koschnitzke, Servant, 2305.03756]

Axions & Axion-Like-Particles

Axions could arise either as a higher dimensional gauge field, or as a Pseudo Nambu Goldstone boson (PNGB) from spontaneous breaking of global symmetry which is not exact but broken weakly.

In this talk I assume the second possibility as a simple benchmark. (for a discussion of rotating stringy axions see Krippendorf, Muia, Quevedo 1806.04690)

Important for cosmology: Axion is accompanied by its partner, the radial mode of a complex scalar field.

Axion-Like-Particles (ALPs).

Consider complex scalar field

$$\Phi = \phi e^{i\theta}$$

charged under anomalous U(1) global symmmetry (Peccei-Quinn symmetry)

Spontaneously broken at scale f_a

$$V(\varphi) = \lambda \left(|\varphi|^2 - \frac{f_a^2}{2} \right)^2$$

$$\langle \boldsymbol{\varphi} \rangle = f_a / \sqrt{2}$$

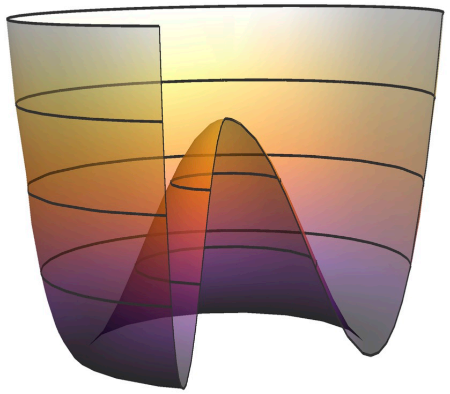

Axion as Goldstone boson

$$\theta \rightarrow \theta + \mathrm{const.}$$

$$\boxed{\theta = a / f_a}$$

ALPs.

Non-perturbative effects at energy $\Lambda_b \ll f_a$ break the shift symmetry and generate a potential/mass for the axion

$$V = m_a^2(T) f_a^2 \left[1 - \cos(\theta)\right]$$

$$m_a = \Lambda_b^2 / f_a$$

QCD axion

$$m_a^2 f_a^2 \approx (76\ \mathrm{MeV})^4$$

Generic ALP

m_a and f_a : free parameters

The hunt for axions.

Mainly through Axion-photon coupling

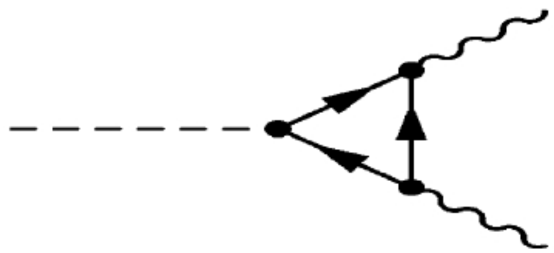

$$\frac{a}{f_a} F_{\mu\nu} \tilde{F}^{\mu\nu}$$

In a background magnetic field:
axion<->photon conversion

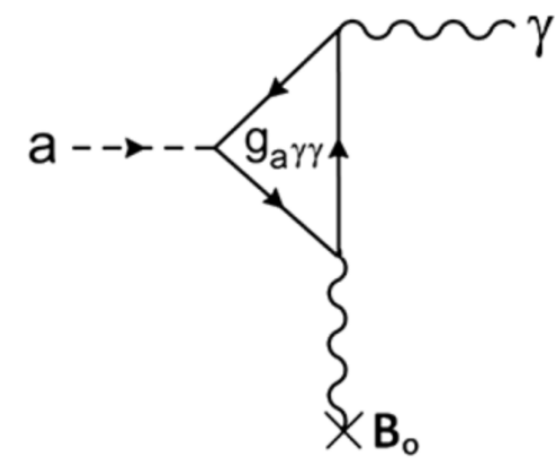

Lifetime ~ f_a^2 / m_a^3

If long-lived: Dark Matter candidate

Lifetime depends on axion-photon coupling.
However, relic abundance only depends on f_a

Three main ways to search for ALPs.

All rely on ALP-photon mixing in magnetic field

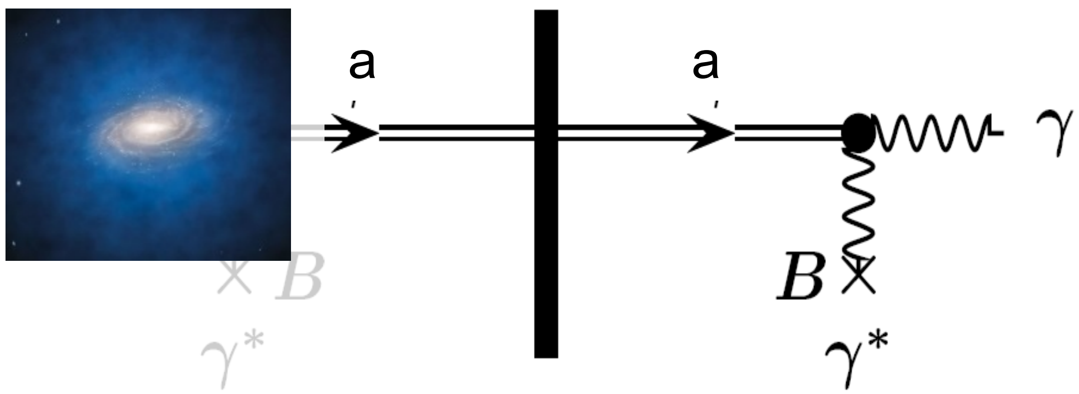

Haloscopes

looking for dark matter constituents, microwaves

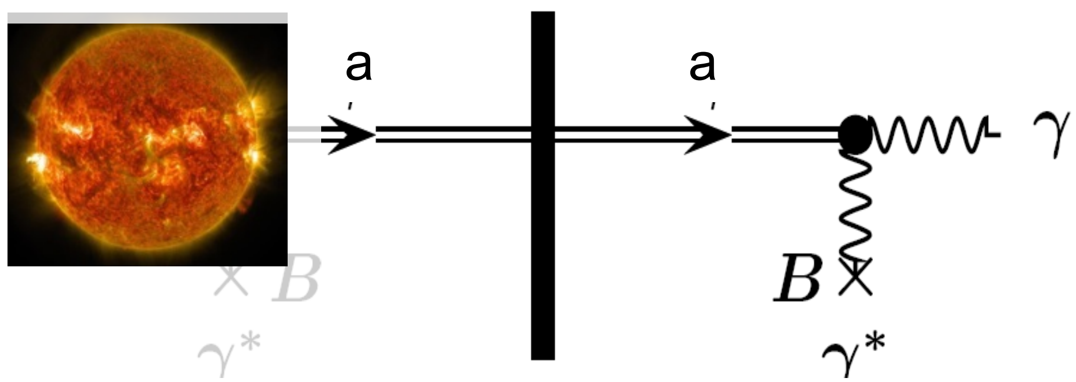

Helioscopes
Axions emitted by the sun, X-rays

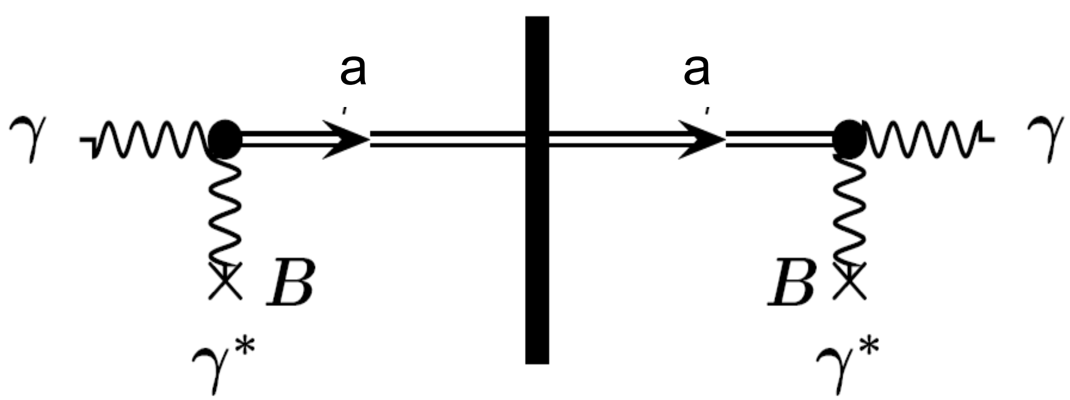

Purely laboratory experiments

“light-shining-through-walls”,

microwaves, optical photons

The Axion-Like-Particle (ALP) parameter space.

If axions are given an interaction to photons then a long list of constraints from ALP searches apply

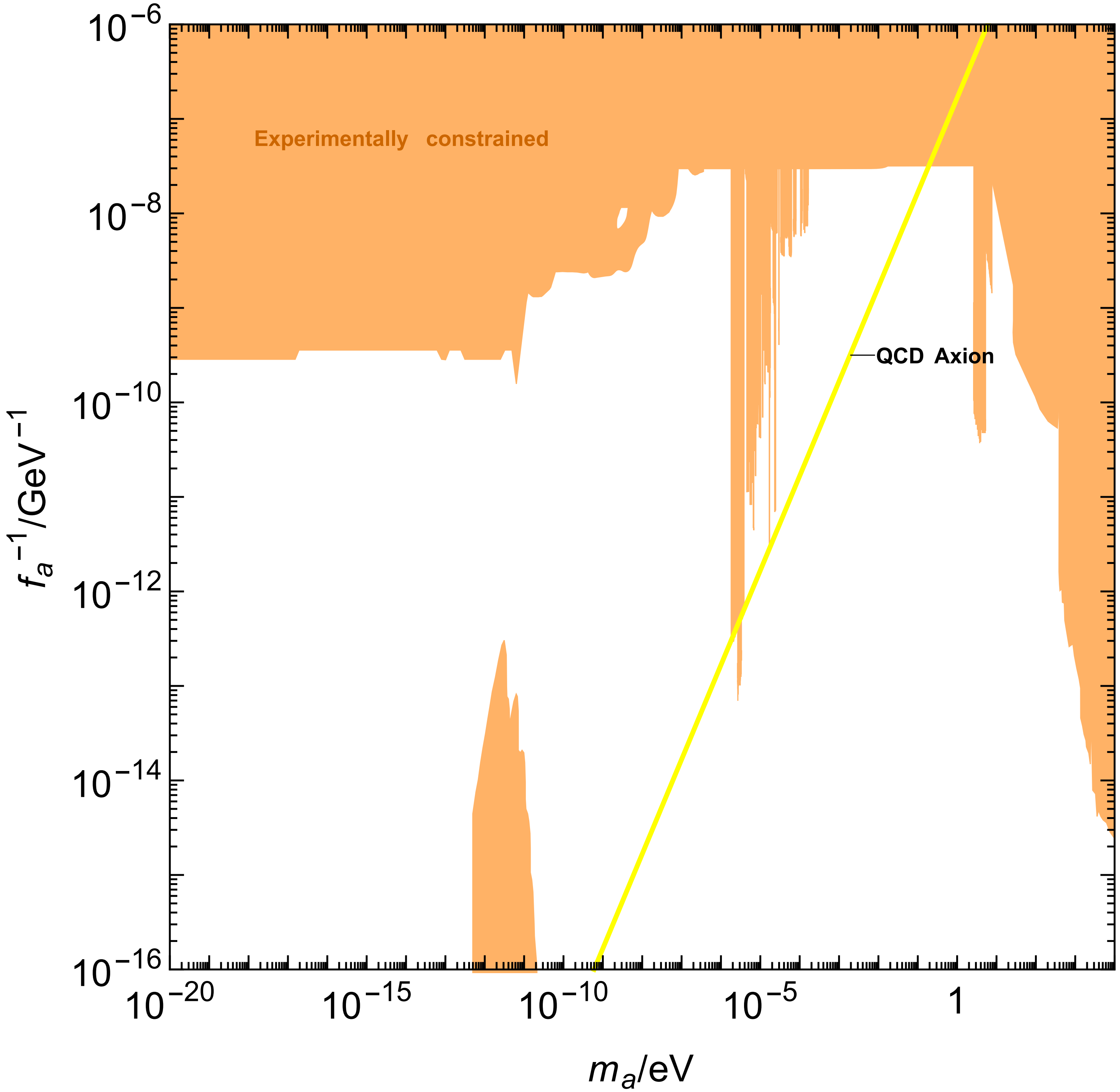

$$\frac{f_\gamma}{f_a} \approx 0.5 \times 10^3$$

assuming KSVZ-like coupling

The hunt for axions.

Any ALP

Only DM

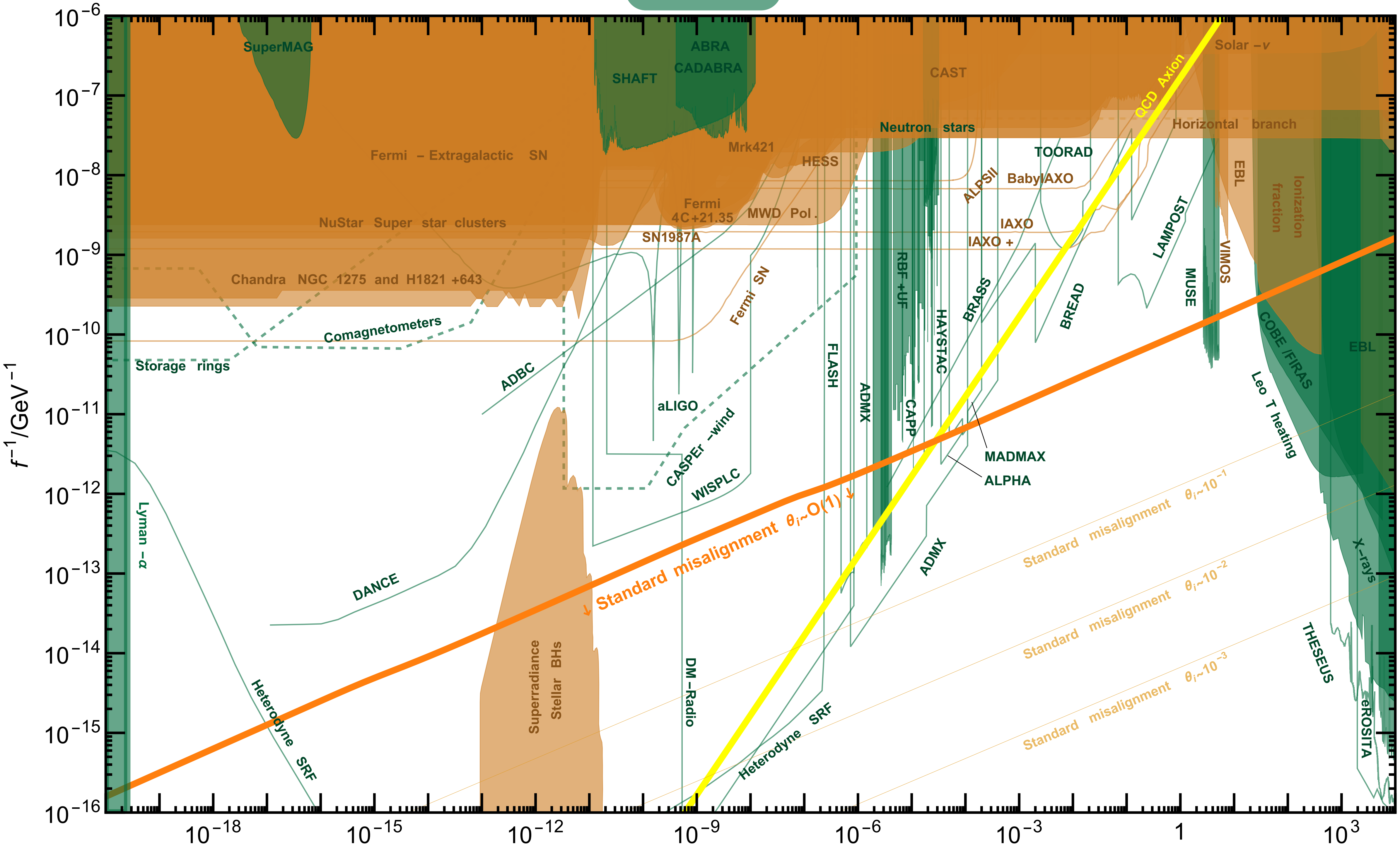

m_0/eV

(KSVZ-like coupling)

2206.14259

$$g_{\theta\gamma} = (\alpha_{\text{em}}/2\pi)(1.92/f)$$

A whole set of experiment constraints.

All data can be found here: C. O'Hare, *cajohare/axionlimits: Axionlimits*, https://cajohare.github.io/AxionLimits/ (2020) [10.5281/zenodo.3932430].

All experiments also listed in tables 1 and 2 of 2206.14259:

Experiment:	Principle	DM?	Ref.
Haloscope constraints			
ABRACADABRA-10cm	Haloscope	DM	[76]
ADMX	Haloscope	DM	[77–83]
BASE	Haloscope (Cryogenic Penning Trap)	DM	[84]
CAPP	Haloscope	DM	[85–87]
CAST-RADES	Haloscope	DM	[88]
DANCE	Haloscope (Optical cavity polarization)	DM	[89]
Grenoble Haloscope	Haloscope	DM	[90]
HAYSTAC	Haloscope	DM	[91, 92]
ORGAN	Haloscope	DM	[93]
QUAX	Haloscope	DM	[94, 95]
RBF	Haloscope	DM	[96]
SHAFT	Haloscope	DM	[97]
SuperMAG	Haloscope (Using terrestrial magnetic field)	DM	[98]
UF	Haloscope	DM	[99]
Upload	Haloscope	DM	[100]
Haloscope projections			
ABDC	Haloscope	DM	[101]
ADMX	Haloscope	DM	[102]
aLIGO	Haloscope	DM	[103]
ALPHA	Haloscope (Plasma haloscope)	DM	[104]
BRASS	Haloscope	DM	[105]
BREAD	Haloscope (Parabolic reflector)	DM	[106]
DANCE	Haloscope (Optical cavity polarization)	DM	[107]
DMRadio	Haloscope (All stages: 50L, m^3 and GUT)	DM	[108, 109]
FLASH	Haloscope (Formerly KLASH)	DM	[110, 111]
Heterodyne SRF	Haloscope (Superconduct. Resonant Freq.)	DM	[112, 113]
LAMPOST	Haloscope (Dielectric)	DM	[114]
MADMAX	Haloscope (Dielectric)	DM	[115]
ORGAN	Haloscope	DM	[93]
QUAX	Haloscope	DM	[116]
TOORAD	Haloscope (Topological anti-ferromagnets)	DM	[117, 118]
WISPLC	Haloscope (Tunable LC circuit)	DM	[119]
LSW and optics			
ALPS	Light-shining-through wall	Any	[120]
ALPS II	Light-shining-through wall (projection)	Any	[121]
CROWS	Light-shining-through wall (microwave)	Any	[122]
OSQAR	Light-shining-through wall	Any	[123]
PVLAS	Vacuum magnetic birefringence	Any	[124]
Helioscopes			
CAST	Helioscope	Any	[125, 126]
babyIAXO	Helioscope (projection)	Any	[1, 127, 128]
IAXO	Helioscope (projection)	Any	[1, 127, 128]
IAXO+	Helioscope (projection)	Any	[1, 127, 128]

Table 1. List of experimental searches for axions and ALPs. The table is continued in table 2. All experiments here rely on the axion-photon coupling.

Experiment:	Principle	DM?	Reference
Astrophysical constraint			
4C+21.35	Photon-ALP oscillation on the γ-rays from blazars	Any	[129]
Breakthrough Listen	ALP $\to$ radio γ in neutron star magn. fields	DM	[130]
Bullet Cluster	Radio signal from ALP DM decay	DM	[131]
Chandra	AGN X-ray prod. in cosmic magn. field	Any	[132–135]
BBN + $N_{\rm eff}$	ALP thermal relic perturbing BBN and $N_{\rm eff}$	Any	[136]
Chandra MWD	X-rays from Magnetic White Dwarf ALP prod.	Any	[137]
COBE/FIRAS	CMB spectral distortions from DM relic decay	DM	[138]
Distance ladder	ALP $\leftrightarrow \gamma$ perturbing luminosity distances	Any	[139]
Fermi-LAT	SN ALP product. $\to \gamma$-rays in cosmic magn. field	Any	[140–142]
Fermi-LAT	AGN X-ray production $\to$ ALP in cosmic magn. field	Any	[143]
Haystack Telescope	ALP DM decay $\to$ microwave photons	DM	[144]
HAWC TeV Blazars	$\gamma \to$ ALP $\to \gamma$ conversion reducing γ-ray attenuation	Any	[145]
H.E.S.S.	AGN X-ray production $\to$ ALP in cosmic magn. field	Any	[146]
Horizontal branch stars	stellar metabolism and evolution	Any	[147]
LeoT dwarf galaxy	Heating of gas-rich dwarf galaxies by ALP decay	DM	[148]
Magnetic white dwarf pol.	$\gamma \to$ ALP conversion polarizing light from MWD stars	Any	[149]
MUSE	ALP DM decay $\to$ optical photons	DM	[150]
Mrk 421	Blazar γ-ray $\to$ ALP $\to \gamma$-ray in cosmic magn. field	Any	[151]
NuStar	Stellar ALP production $\to \gamma$ in cosmic magn. fields	Any	[152, 153]
NuStar, Super star clusters	Stellar ALP production $\to \gamma$ in cosmic magn. fields	Any	[153]
Solar neutrinos	ALP energy loss $\to$ changes in neutrino production	Any	[154]
SN1987A ALP decay	SN ALP production $\to \gamma$ decay	Any	[155]
SN1987A gamma rays	SN ALP production $\to \gamma$ in cosmic magnetic field	Any	[156, 157]
SN1987A neutrinos	SN ALP luminosity less than neutrino flux	Any	[157, 158]
Thermal relic compilation	Decay and BBN constraints from ALP thermal relic	Any	[159]
VIMOS	Thermal relic ALP decay $\to$ optical photons	Any	[160]
White dwarf mass relation	Stellar ALP production perturbing WD metabolism	Any	[161]
XMM-Newton	Decay of ALP relic	DM	[162]
Astrophysical projections			
eROSITA	X-ray signal from ALP DM decay	DM	[163]
Fermi-LAT	SN ALP production $\to \gamma$ in cosmic magnetic field	Any	[164]
IAXO	Helioscope detection of supernova axions	Any	[165]
THESEUS	ALP DM decay $\to$ x-ray photons	DM	[166]
Neutron coupling:			
CASPEr-wind	NMR from oscillating EDM (projection)	DM	[167, 168]
CASPEr-ZULF-Comag.	NMR from oscillating EDM	DM	[168, 169]
CASPEr-ZULF-Sidechain	NMR (constraint & projection)	DM	[168, 170]
NASDUCK	ALP DM perturbing atomic spins	DM	[171]
nEDM	Spin-precession in ultracold neutrons and Hg	DM	[168, 172]
K-3He	Comagnetometer	DM	[173]
Old comagnetometers	New analysis of old comagnetometers	DM	[174]
Future comagnetometers	Comagnetometers	DM	[174]
SNO	Solar ALP flux from deuterium dissociation	Any	[175]
Proton storage ring	EDM signature from ALP DM	DM	[176]
Neutron Star Cooling	ALP production modifies cooling rate	Any	[177]
SN1987 Cooling	ALP production modifies cooling rate	Any	[178]
Coupling independent:			
Black hole spin	Superradiance for stellar mass black holes	Any	[72–74]
Lyman$-\alpha$	Modification of small-scale structure	DM	[60]

Table 2. List of experimental searches for axions and ALPs.

Which of these axions can make Dark Matter ?

Pre- and post-inflationary scenarios.

Potential of full complex PQ scalar field

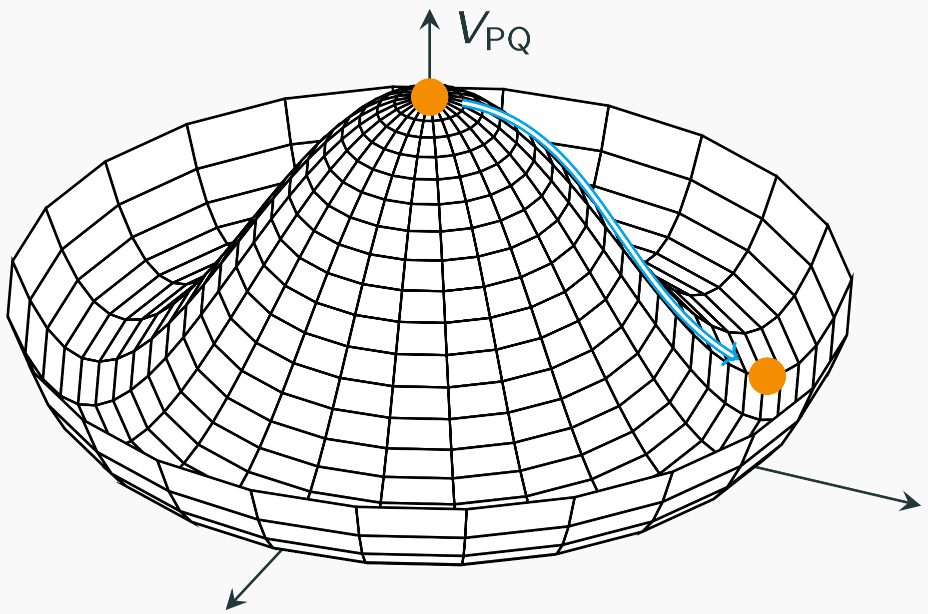

Post-inflationary scenario

- Different initial angle in each Hubble patch.
- Inhomogeneous including topological defects.

Pre-inflationary scenario

- Random initial angle in the observable universe.
- Initially homogeneous w/o topological defects.

Pre- and post-inflationary scenarios.

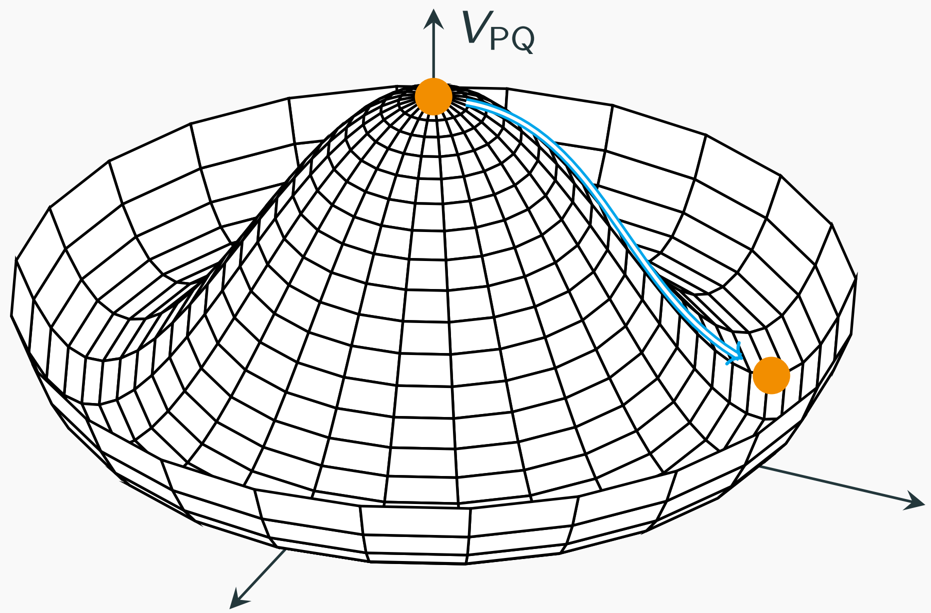

Post-inflationary scenario

- Different initial angle in each Hubble patch.
- Inhomogeneous including topological defects.

Pre-inflationary scenario

- Random initial angle in the observable universe.
- Initially homogeneous w/o topological defects.

↓

GLOBAL (axionic) COSMIC STRINGS

↓

primordial GW bgd

Usual story.

(Most axion cosmology literature is about the rather late cosmology from moment axion gets a mass)

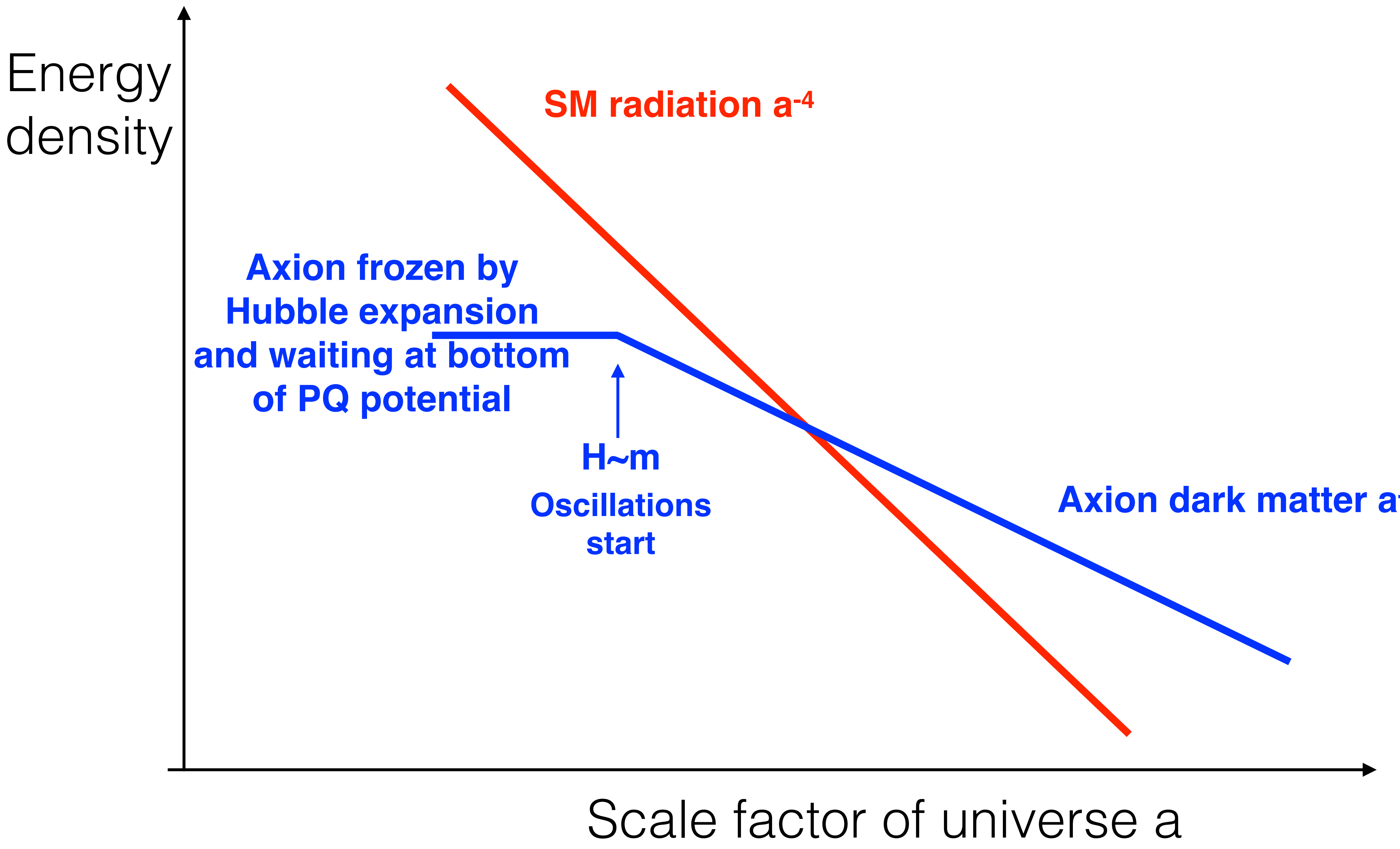

Axions from the misalignment mechanism.

Axion late cosmology

a

Neglecting fluctuations, the homogeneous zero-mode satisfies

$$\ddot{\Theta} + 3H\dot{\Theta} + m_{\rm a}^2(T)\sin(\Theta) = 0,$$

$$ds^2 = dt^2 - a^2(t)\left[\frac{dr^2}{1-kr^2} + r^2 d\Omega^2\right]$$

With initial conditions: $\Theta(t_i) = \Theta_i, \quad \dot{\Theta}(t_i) = 0.$ *standard assumption*

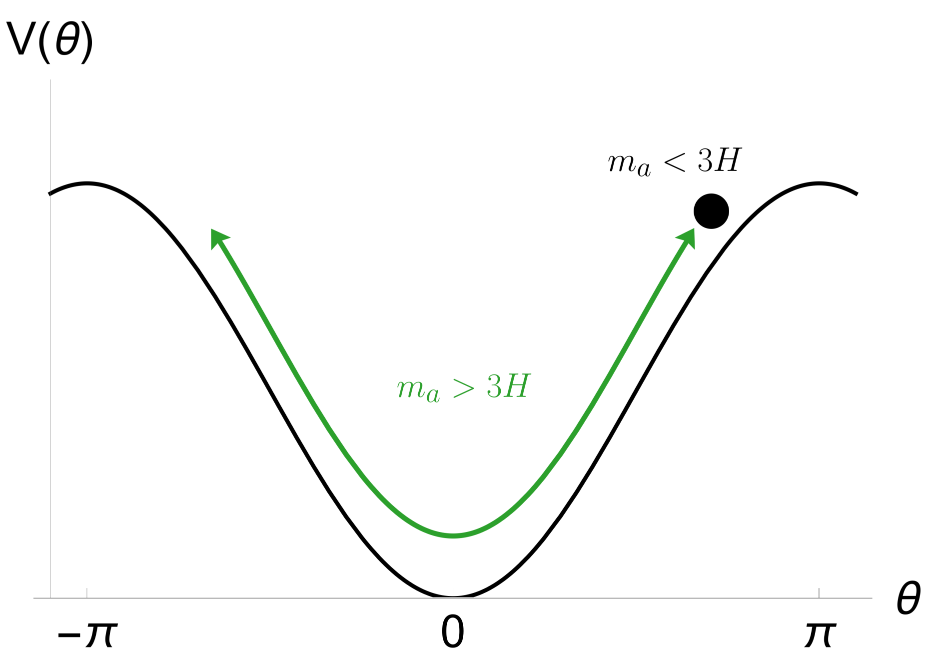

- $m_a \ll 3H \iff \rho_a \propto a^0$ (Frozen)
- $m_a \gg 3H \iff \rho_a \propto a^{-3}$ (Oscillating)

—> standard misalignment mechanism

For $\Theta_i \sim 1 \qquad \rho_{\rm DM} \sim \rho_{osc}\left(\frac{a_{osc}}{a_0}\right)^3 \sim m_a^2 f_a^2 \left(\frac{T_0}{T_{osc}}\right)^3$

$$T_{osc} \sim \sqrt{m_a M_{Pl}}$$

$\rho_{\rm DM}$ grows with f_a —> Axion Dark Matter overabundance for too large f_a

Conventional misalignment makes too little DM for low f_a.

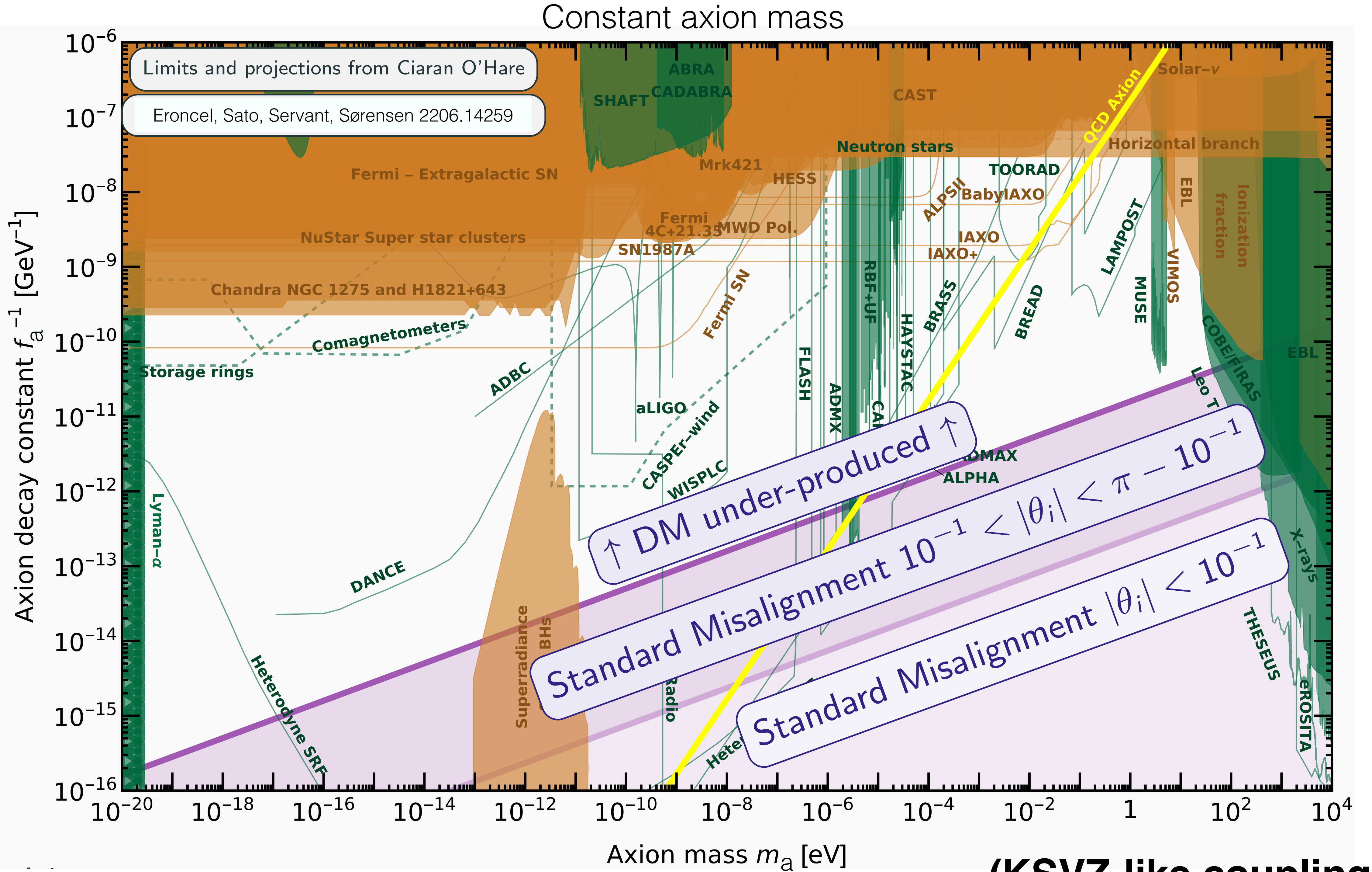

(KSVZ-like coupling)

$g_{\theta\gamma} = (\alpha_{\mathbf{em}}/2\pi)(1.92/f)$

A way out: switch on initial velocity for the axion

Standard versus kinetic Misalignment.

Two ways to delay the onset of oscillations

Initial field value tuned to top of potential:

Standard (Large) misalignment

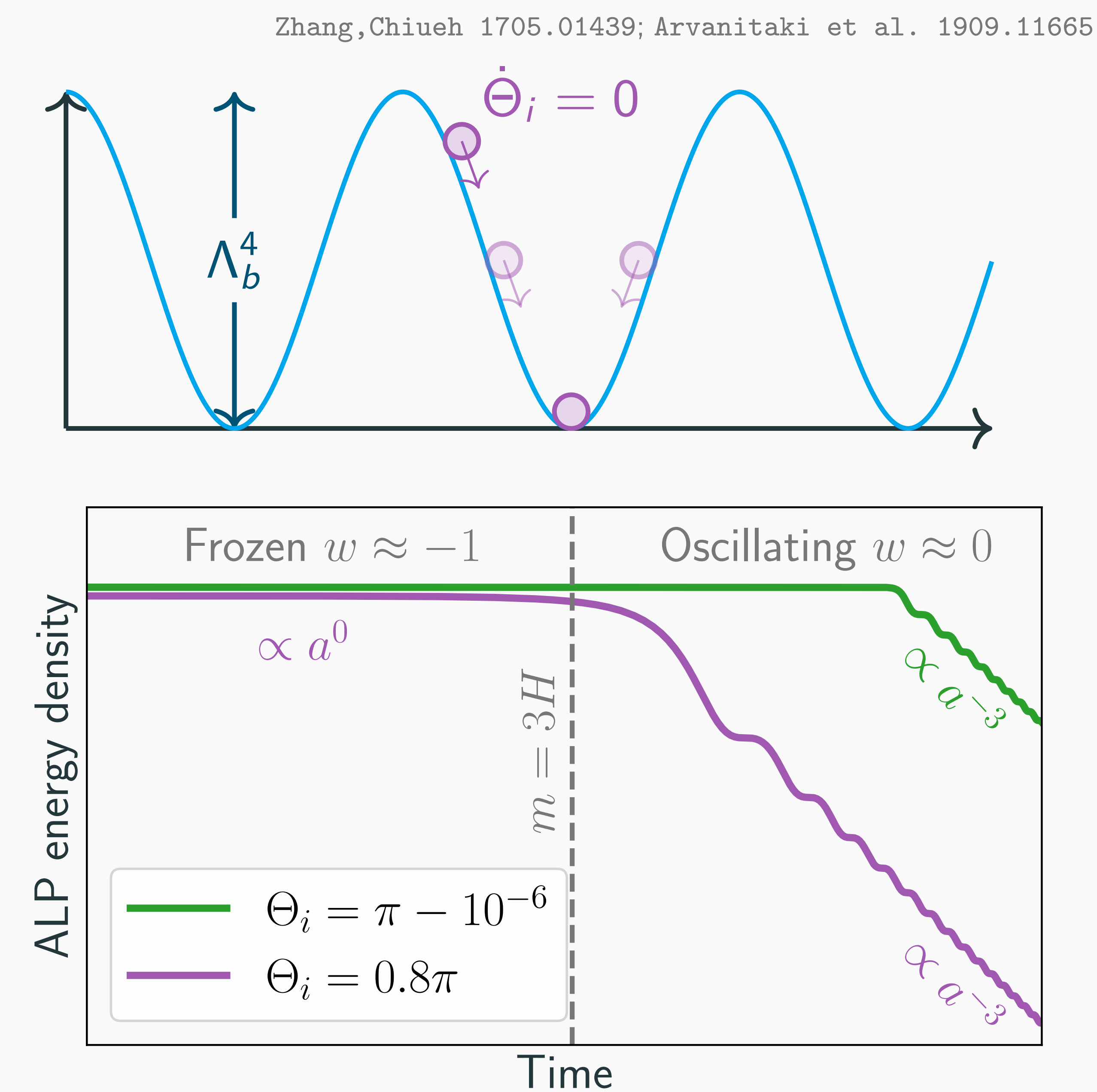

Large initial velocity

Kinetic misalignment

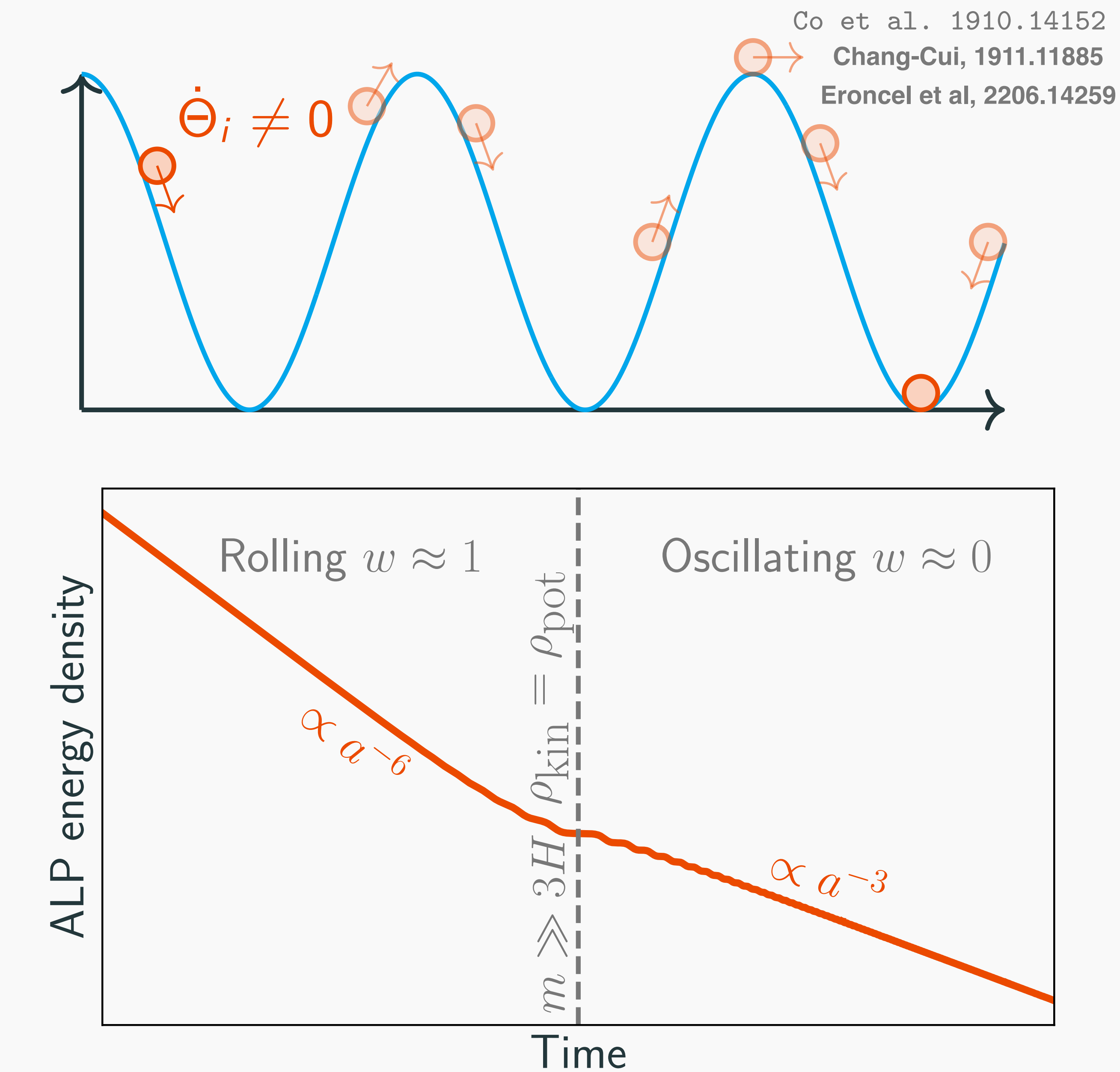

A third way to delay the onset of oscillations: a non-periodic potential.

1906.06352, 2305.03756

$$V(\theta) = \frac{m_\phi^2 f_\phi^2}{2p}\left[\left(1+\theta^2\right)^p - 1\right], \quad p < 1.$$

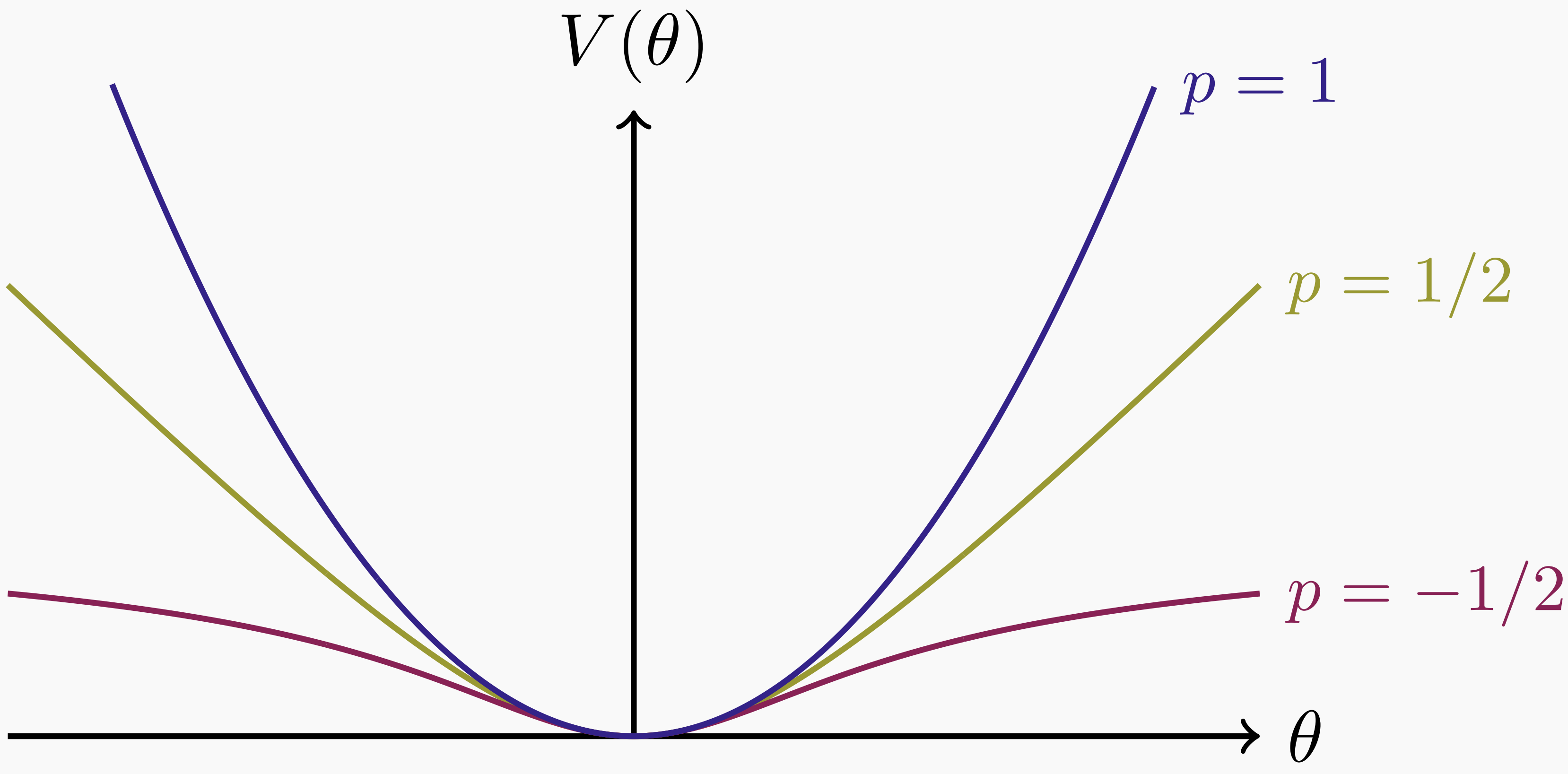

Common property of all these cases: onset of oscillations is delayed which boosts the dark matter abundance, and extends the ALP dark matter parameter space to lower decay constants.

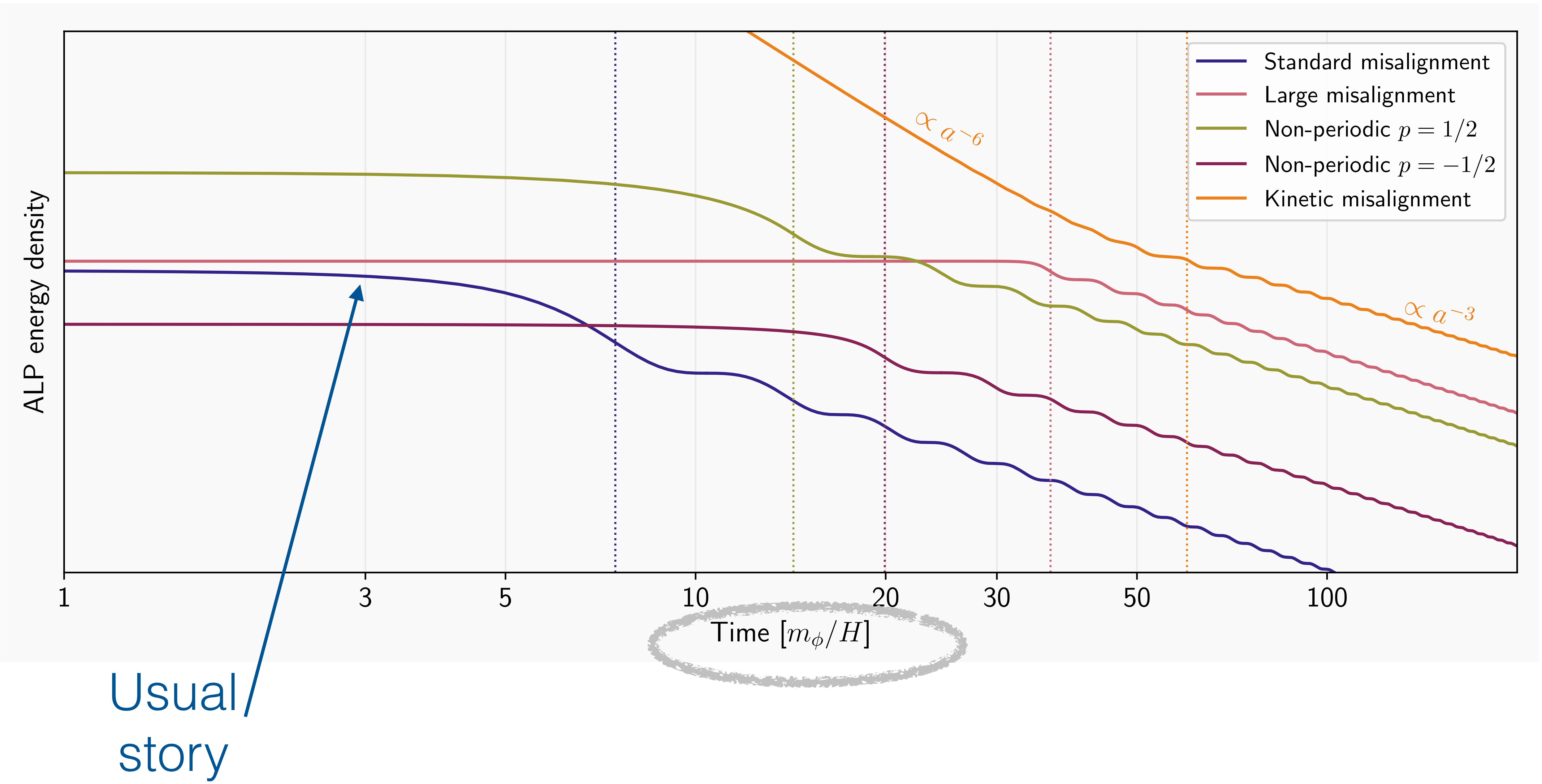

ALP DM parameter space.

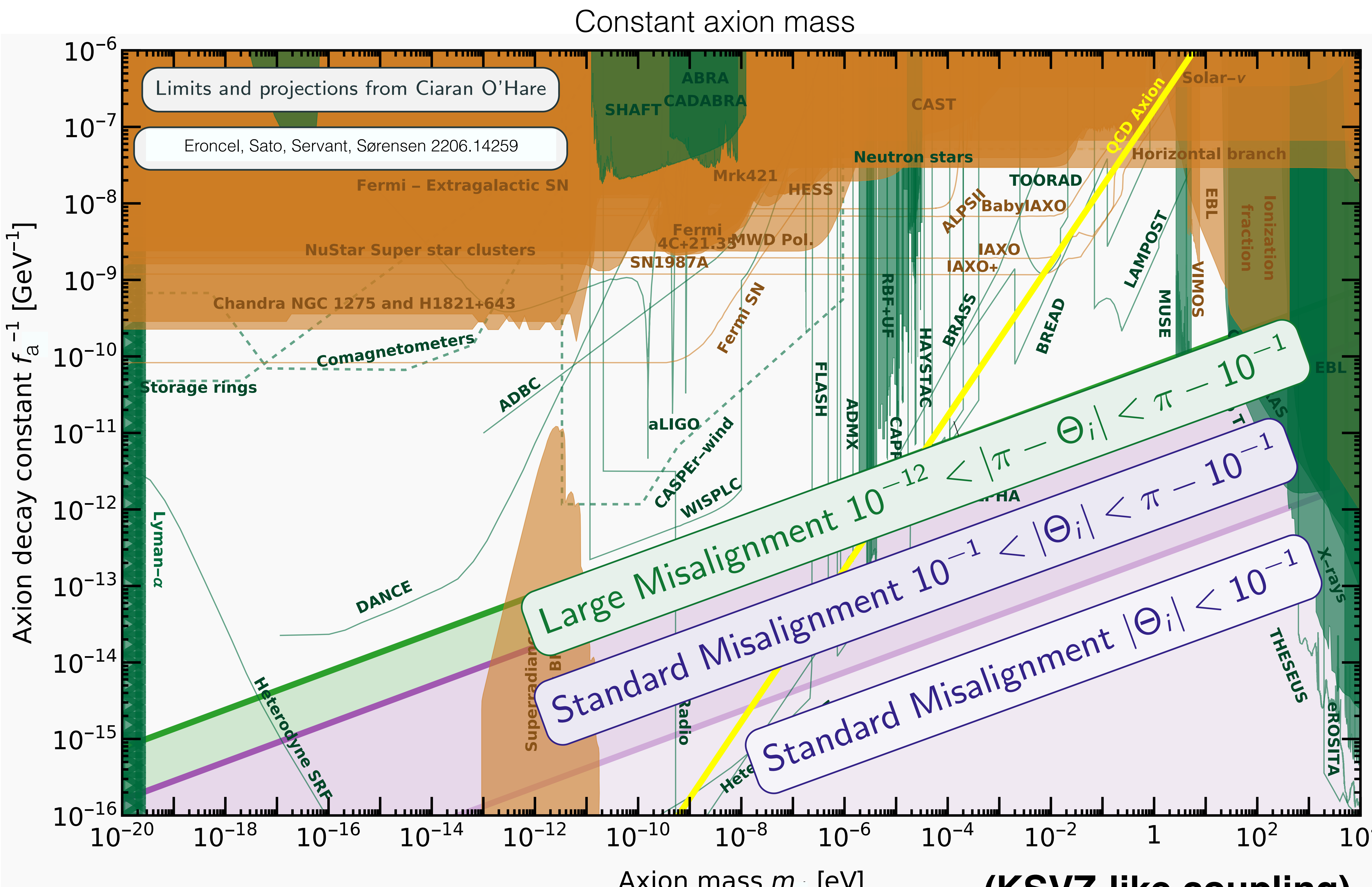

(KSVZ-like coupling)

$$g_{\theta\gamma} = (\alpha_{\mathbf{em}}/2\pi)(1.92/f)$$

Kinetic misalignment.

Add kinetic energy to delay onset of oscillations

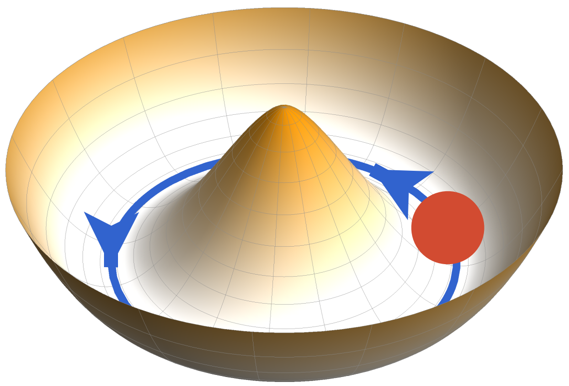

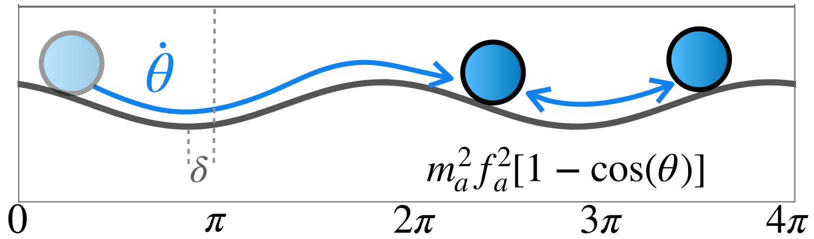

> Delay oscillations
$\Rightarrow$ less redshift
$\Rightarrow$ more DM
$\Rightarrow$ lower f_a

-> ALP can be DM for low f_a

Co, Hall, Harigaya et al '19'20
Chang, Cui'19
Eröncel et al, '22

Axion cosmology.

“Common” story:

Starts at $\langle\phi\rangle=0$

Studies axion cosmology ignoring the radial mode

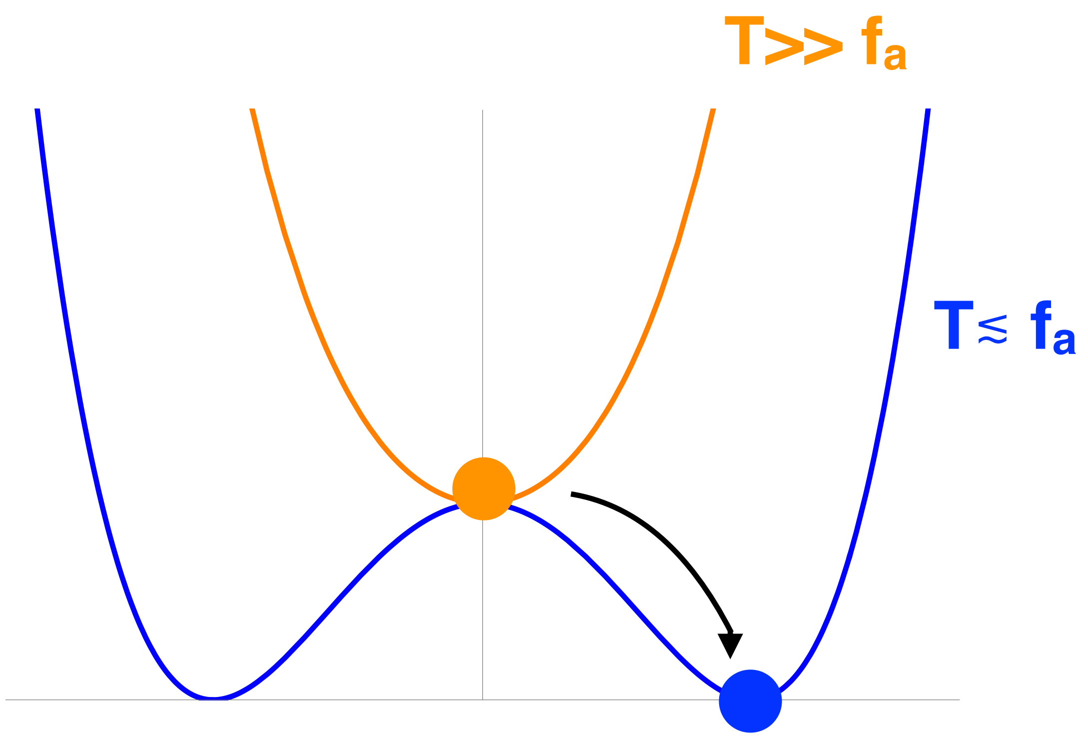

Alternative:

Starts at $\langle\phi\rangle \gg f_a$

(field can be driven naturally to these large field values during inflation due to a negative Hubble-induced mass term)

Radial mode /axion interplay

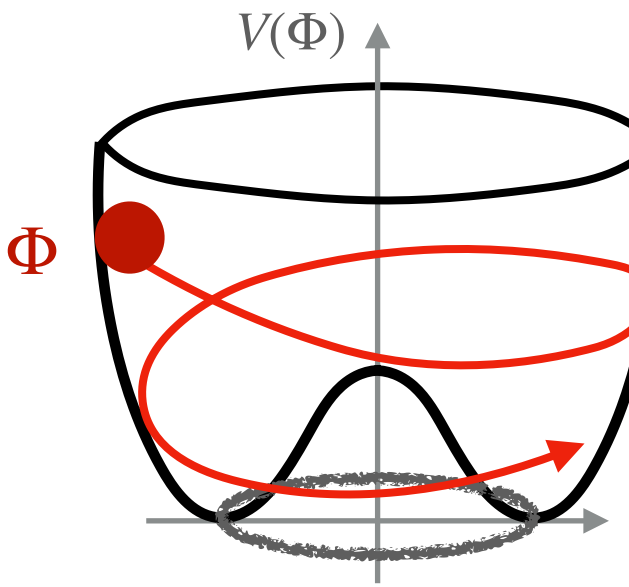

How did the axion acquire a kick?

If PQ symmetry is broken explicitly at high energies
—> mexican hat potential is tilted

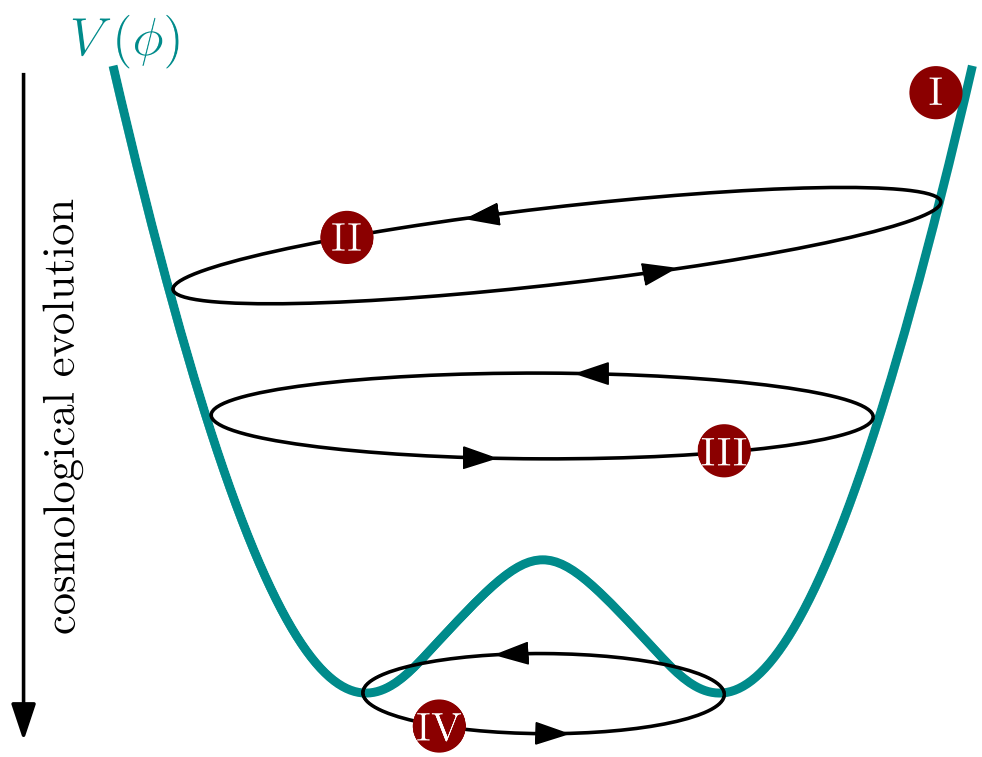

Figure by P. Simakachorn

If radial mode of PQ field starts at large VEV, the angular mode gets a large kick in the early universe

With initial conditions: $$\frac{1}{2}\dot{\Theta}_i^2 \gg 2m^2(T_i)$$ **Delayed axion oscillations !**

-> kinetic misalignment mechanism

[Co, Harigaya, Hall'19] 1910.14152

2004.00629

Initial conditions.

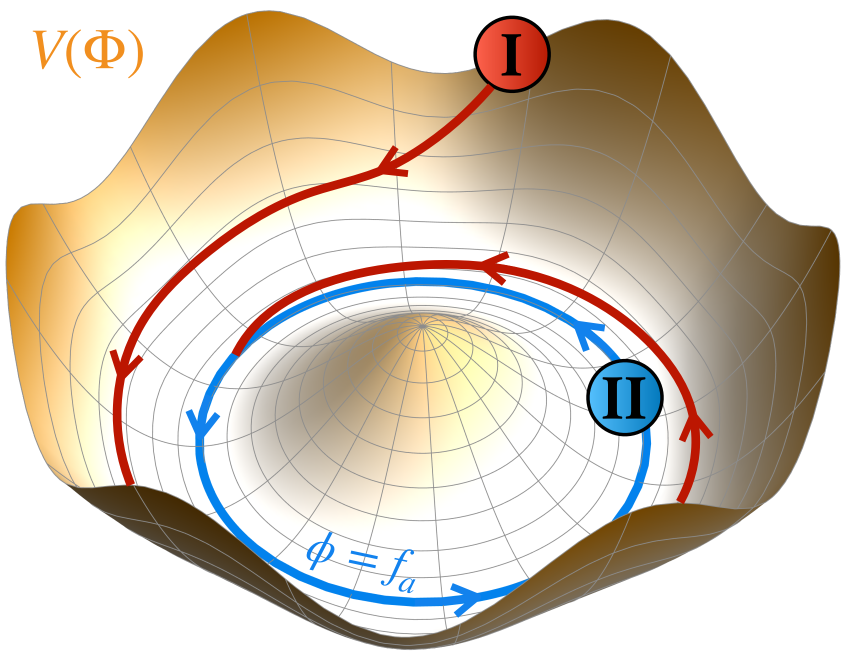

Similar to Affleck-Dine ’85 scenario

At early times, ϕ is driven away from ϕ =0,
towards $\langle\phi\rangle \gg f_a$
by negative Hubble-induced mass term $H \gg m_\phi$

$$V_H(\Phi, H) \supset -cH^2|\Phi|^2$$

Dine, Randall, Thomas ‘95

+ explicit U(1) breaking term transfers radial mode motion into kick for the axion

Usual story.

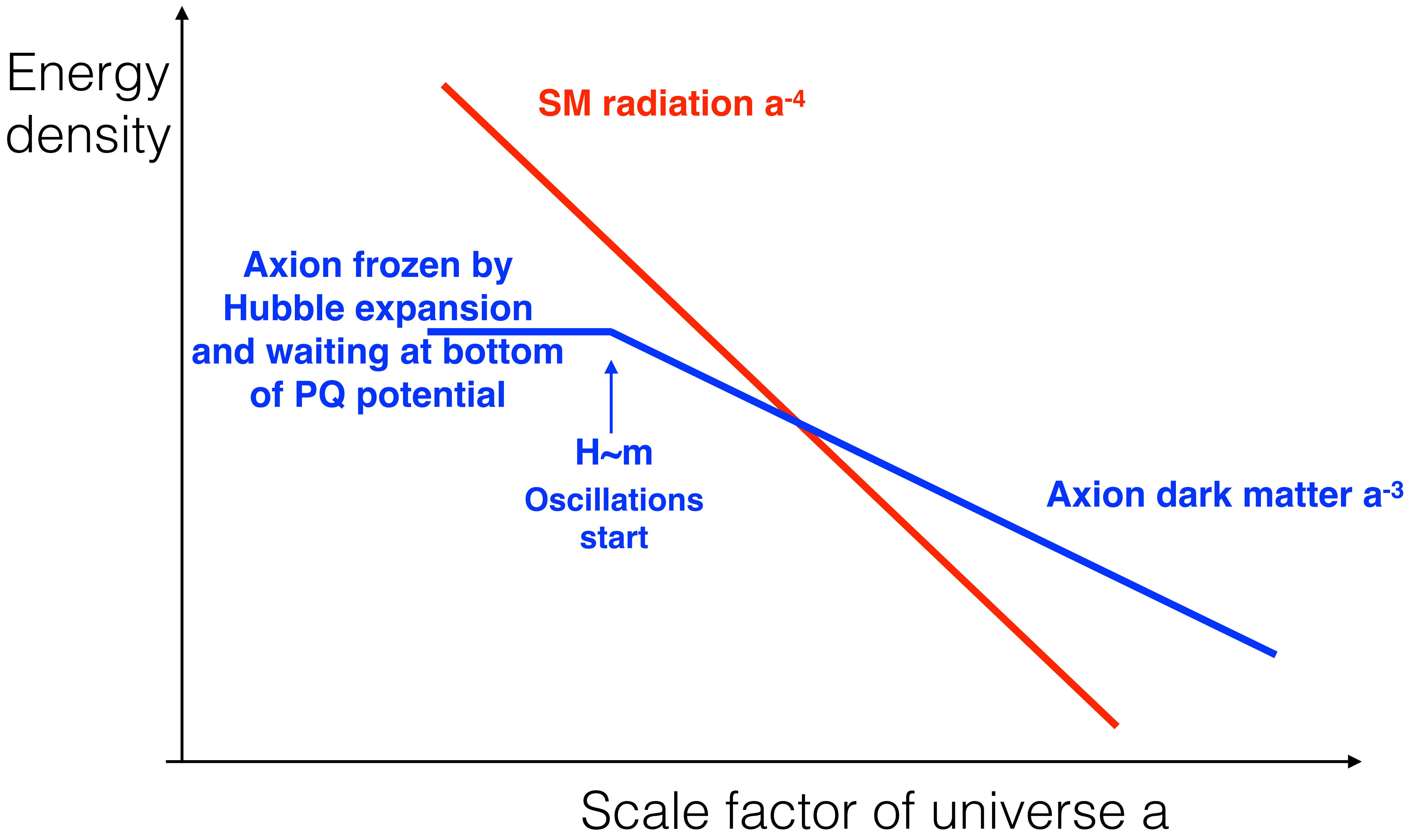

Energy density
SM radiation a-4
Axion frozen by Hubble expansion and waiting at bottom of PQ potential
H~m
Oscillations start
Axion dark matter a-3
Scale factor of universe a

New story.

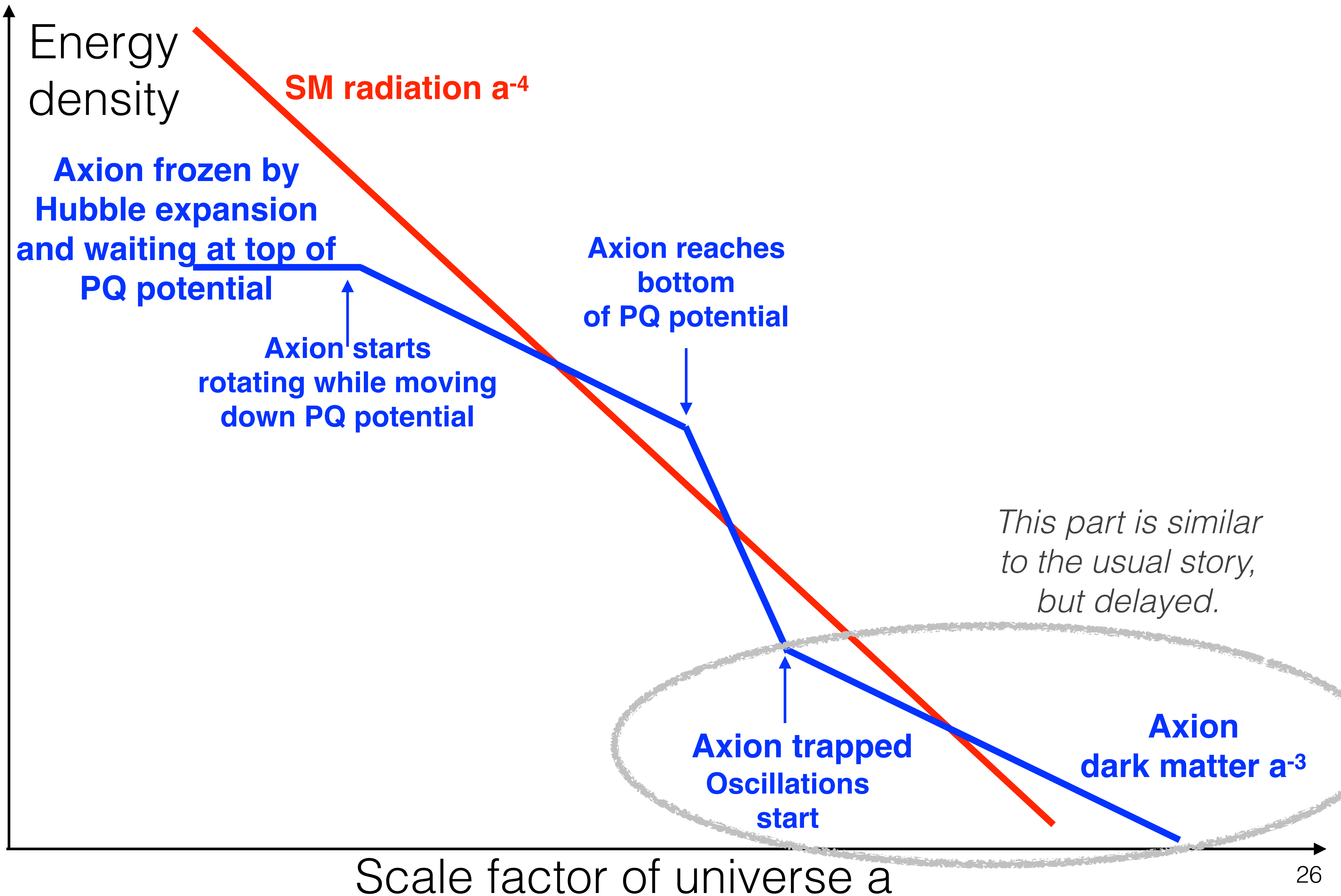

Energy density
SM radiation a-4
Axion frozen by Hubble expansion and waiting at top of PQ potential
Axion starts rotating while moving down PQ potential
Axion reaches bottom of PQ potential
This part is similar to the usual story, but delayed.
Axion trapped Oscillations start
Axion dark matter a-3
Scale factor of universe a

New story.

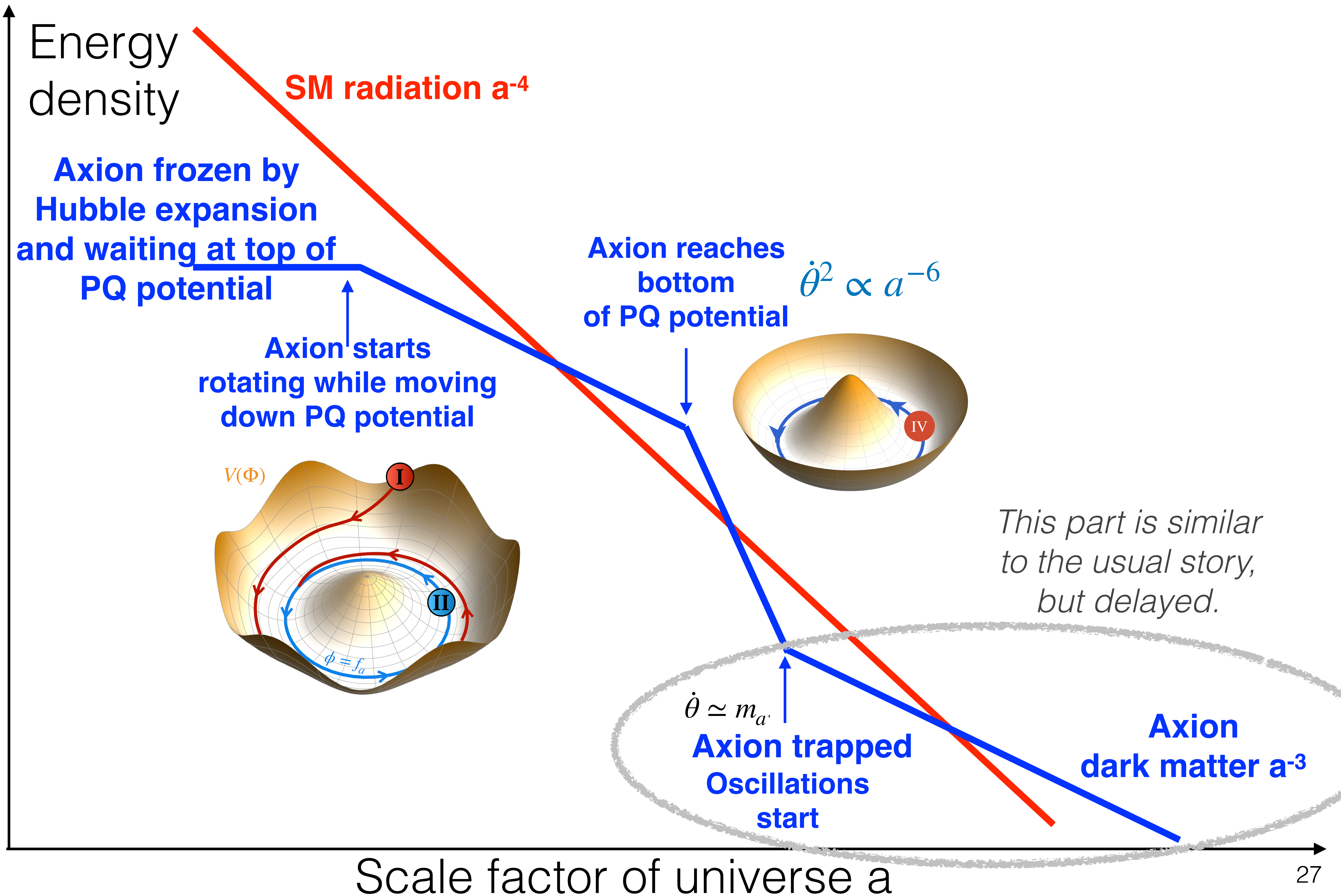

Energy density
SM radiation a-4
Axion frozen by Hubble expansion and waiting at top of PQ potential
Axion starts rotating while moving down PQ potential
V(Φ)
I
II
$\phi = f_a$
Axion reaches bottom of PQ potential
$\dot{\theta}^2 \propto a^{-6}$
IV
This part is similar to the usual story, but delayed.
$\dot{\theta} \simeq m_a$
Axion trapped Oscillations start
Axion dark matter a-3
Scale factor of universe a

ALP DM parameter space.

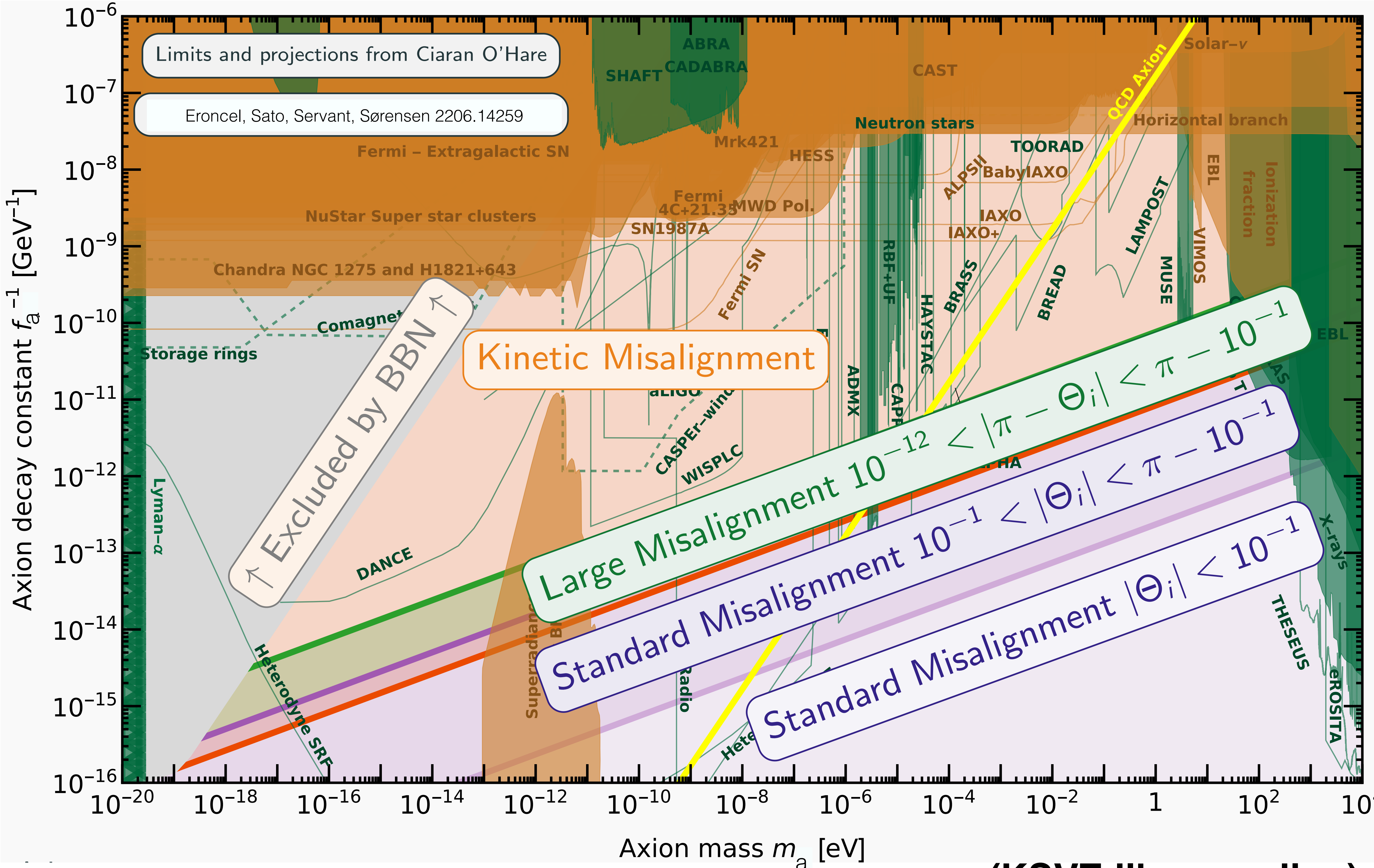

(KSVZ-like coupling)

$$g_{\theta\gamma} = (\alpha_{\mathbf{em}}/2\pi)(1.92/f)$$

ALP DM parameter space.

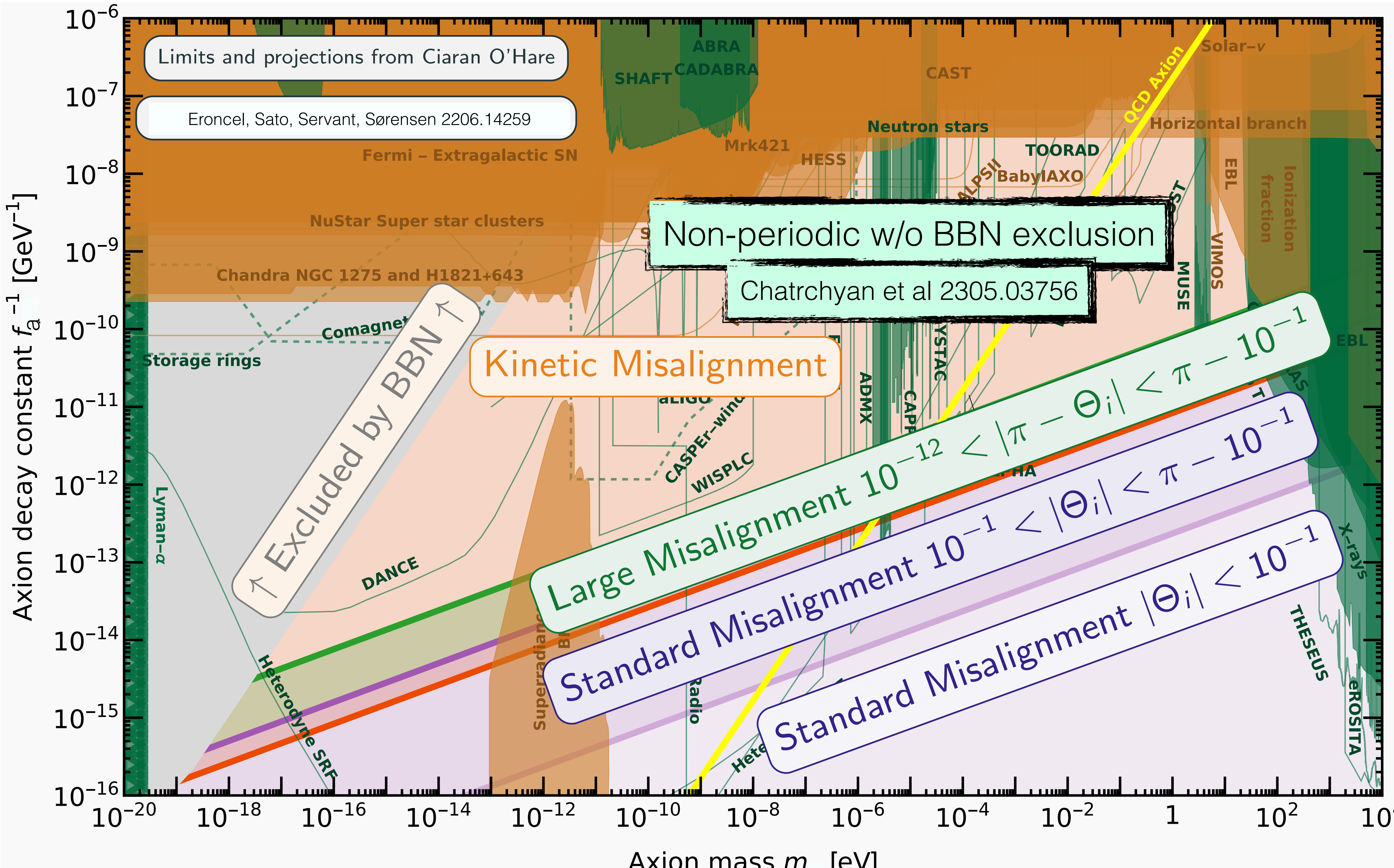

(KSVZ-like coupling)

$g_{\theta\gamma} = (\alpha_{\mathbf{em}}/2\pi)(1.92/f)$

Axion kinetic misalignment:

↓

Axion fragmentation.

↓

Compact axion halos.

Axion fragmentation

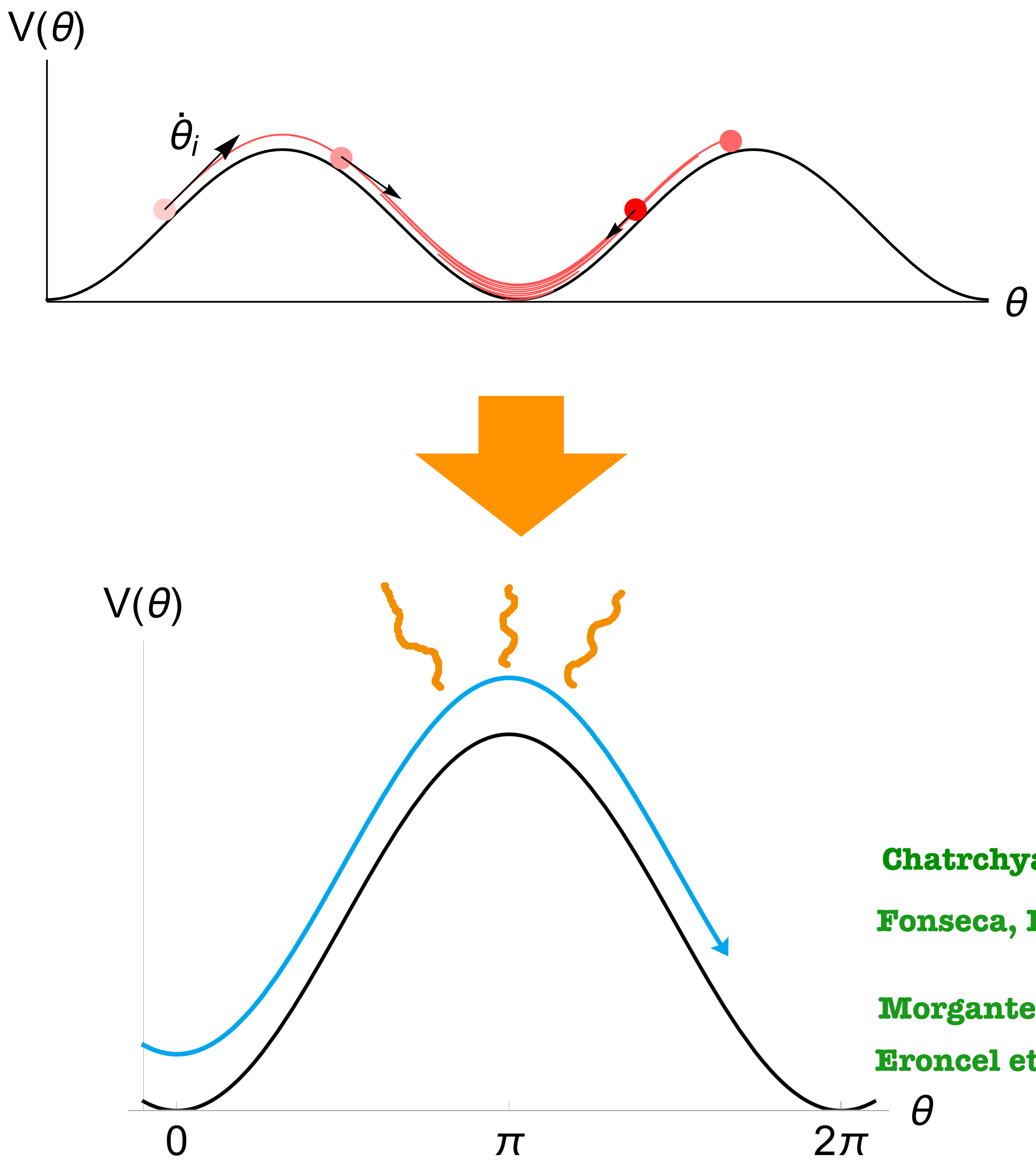

Chatrchyan et al, 1903.03116, 2004.07844

Fonseca, Morgante, Sato, Servant, 1911.08472, 1911.08473

Morgante et al, 2109.13823

Eroncel et al' 2206.14259, 23065.103756

Axion Fragmentation.

Not considered in usual axion phenomenology with oscillations around one minimum: Fragmentation suppressed unless the field starts very close to the top of the potential ("large misalignment mechanism") or for specific potentials with more than one cosine -> parametric resonance.

Greene, Kofman, Starobinsky, hep-ph/9808477
Chatrchyan et al, 1903.03116, 2004.07844
Arvanitaki et al, 1909.11665

However, becomes very relevant when field crosses many wiggles, with interesting implications, e.g. for the relaxion mechanism, but also as a new axion Dark Matter production mechanism.

Chatrchyan et al, 1903.03116, 2004.07844
Fonseca,Morgante,Sato, Servant'19
Morgante et al, 2109.13823

Generalization Eroncel et al, 2206.14259, 23065.103756
(fragmentation before and after trapping + detailed application to DM)

ALP fluctuations.

- Even in pre-inflationary scenario, ALP field has some fluctuations on top of the homogeneous background, which can be described by the mode functions in the Fourier space.

$$\theta(t, x) = \Theta(t) + \int \frac{d^3k}{(2\pi)^3} \theta_k e^{i\vec{k}\cdot\vec{x}} + \text{h.c.}$$

- Even though the fluctuations are small initially, they can be enhanced exponentially later via parametric resonance yielding to fragmentation.

- In the case of efficient fragmentation, all the energy of the homogeneous mode can be transferred to the fluctuations. [Fonseca et al. 1911.08472; Morgante et al. 2109.13823]

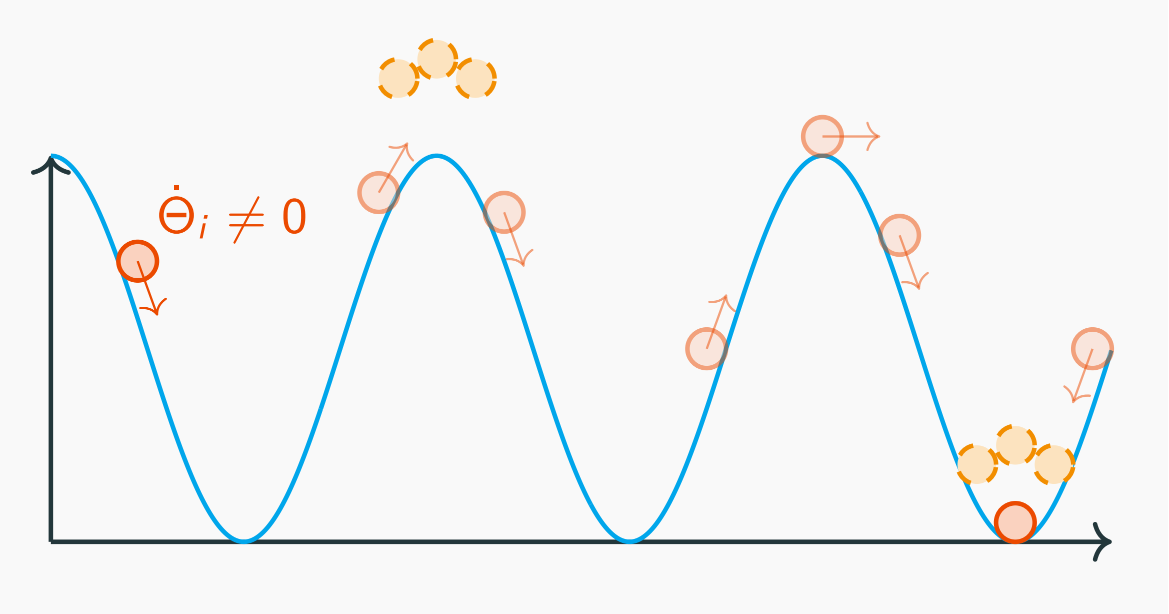

Fragmentation regions in ALP parameter space.

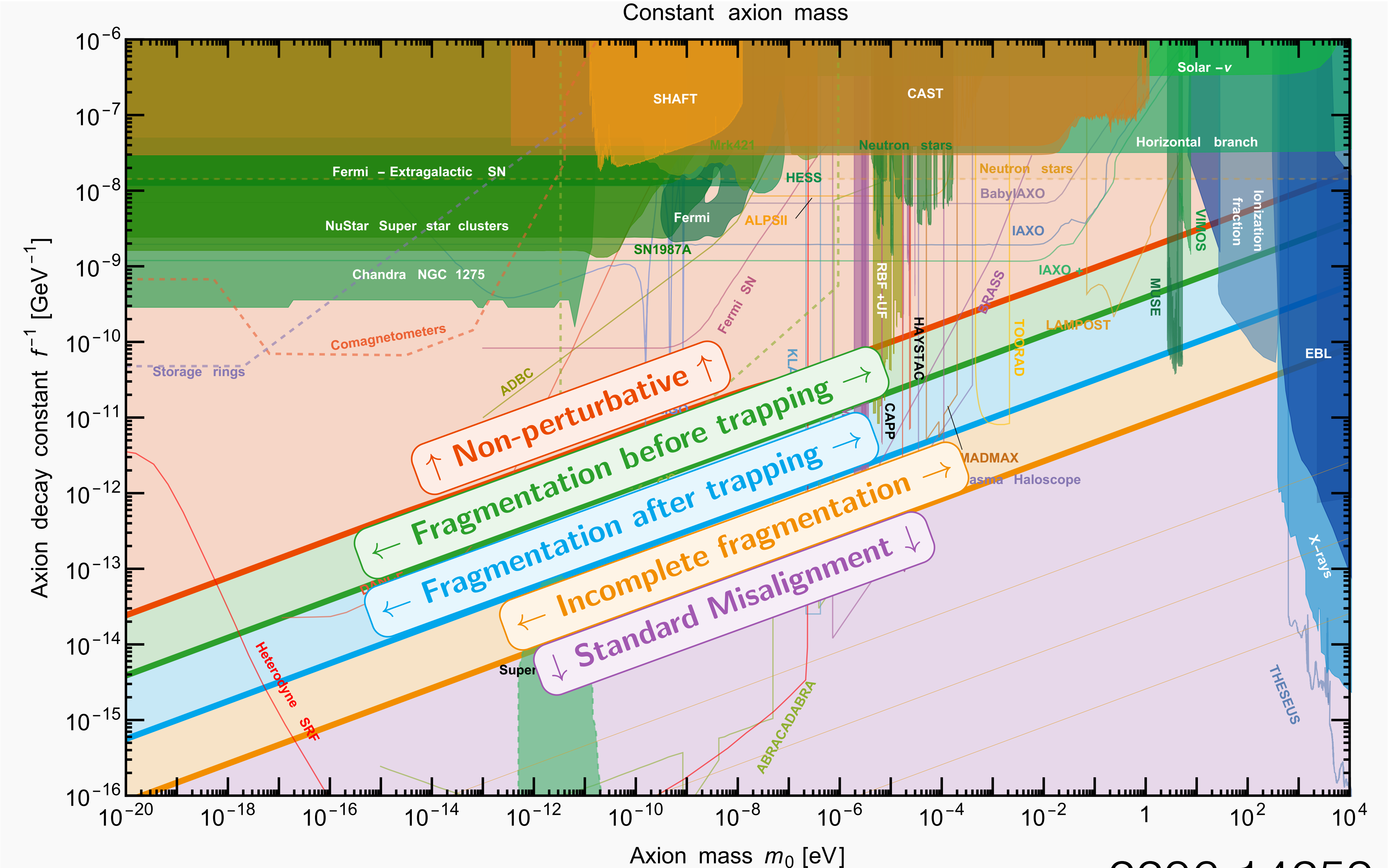

2206.14259

Fragmentation regions in ALP parameter space.

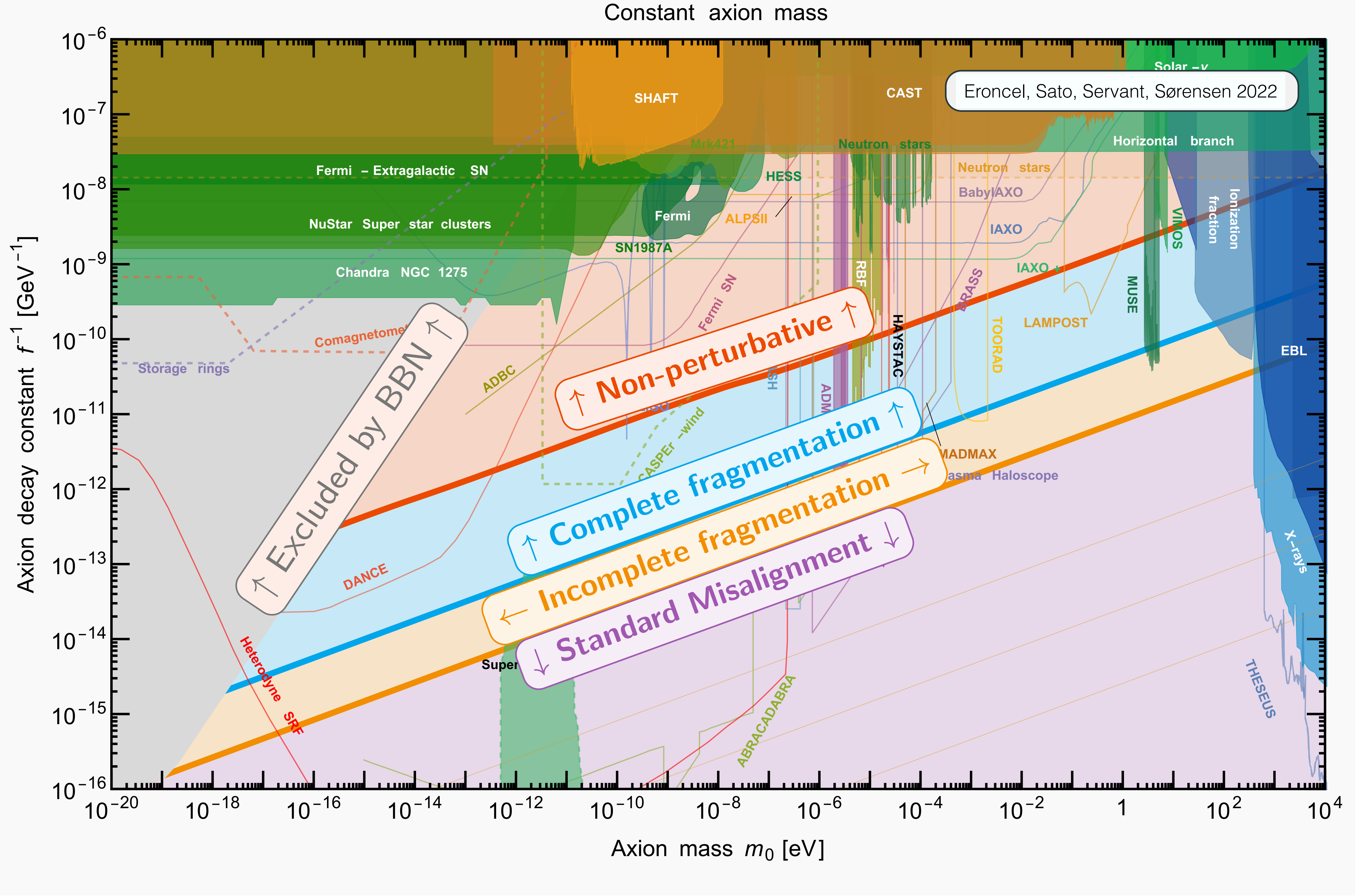

ALP fluctuations.

$$\phi(t,\mathbf{x}) = \bar{\phi}(t) + \int \frac{\mathrm{d}^3k}{(2\pi)^3}\phi_k e^{i\vec{k}\cdot\vec{x}} + \text{h.c.}$$

EoM for the unavoidable adiabatic perturbations :

$$\ddot{\phi}_k + 3H\dot{\phi}_k + \underbrace{\left[\frac{k^2}{a^2} + V''(\phi)\Big|_{\bar{\phi}}\right]}_{\text{eff. frequency}}\phi_k = \underbrace{2\,\Phi_k\, V'(\phi)\Big|_{\bar{\phi}} - 4\dot{\Phi}_k\dot{\bar{\phi}}}_{\text{source term}}$$

unstable when the effective frequency

- **becomes negative ⇒ tachyonic instability**
- **is oscillating ⇒ parametric resonance**

Growth rate of the perturbations depends exponentially on $\left.\frac{m_\phi}{H}\right|_{\text{osc}}$

Dense and compact ALP mini-clusters (clums of ALP DM) can also be formed in the pre-inflationary scenario!

Observational tests: compact axion halos.

kinetic misalignment—>axion fragmentation-> structure formation enhancement

Small m → Large mini-cluster

Perturbative analysis +
Press-Schechter formalism

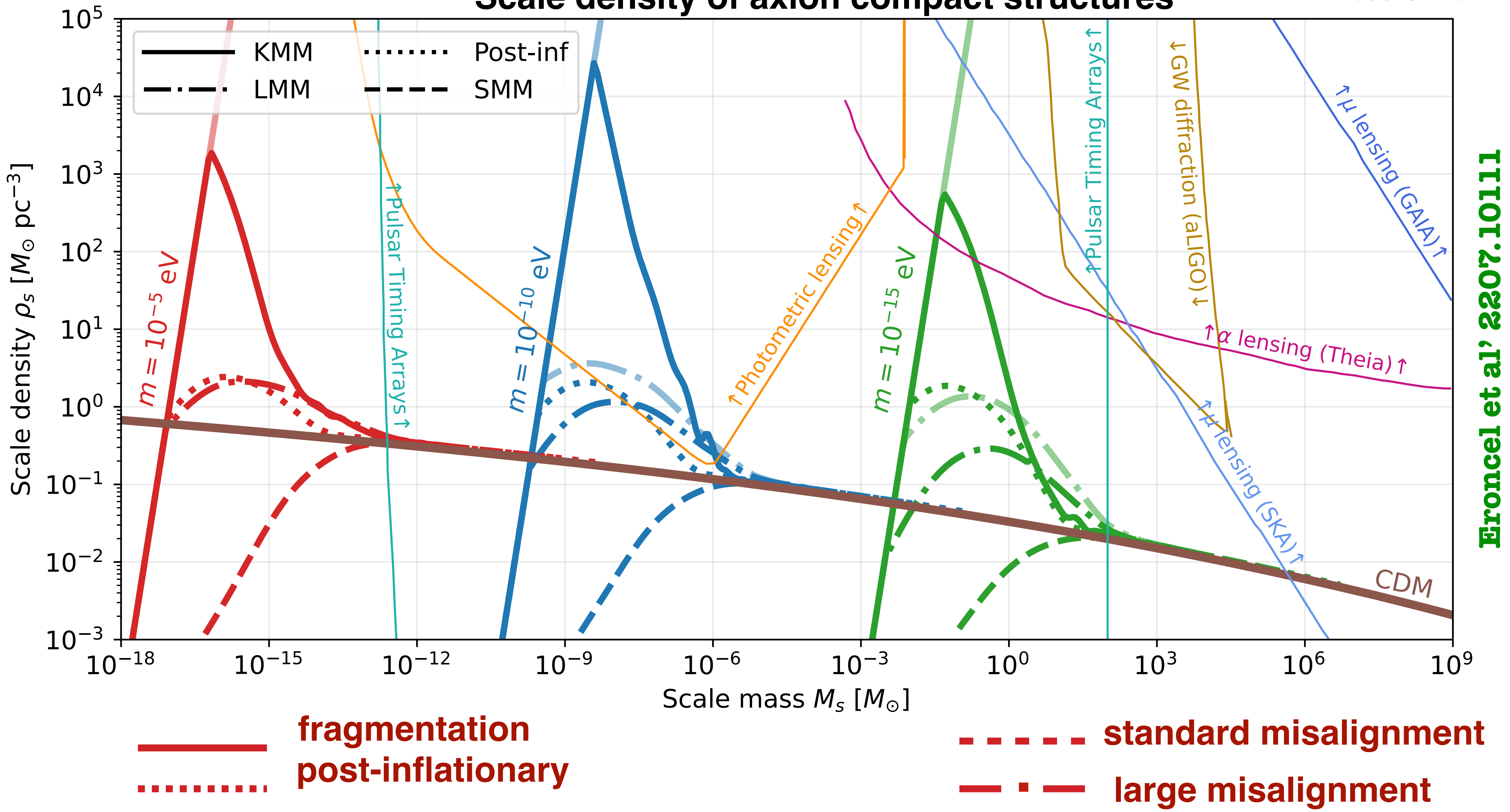

Studied in the context of large misalignment scenario in [Arvanitaki et al'19]

Different in the context of axion kinetic fragmentation [Eroncel et al , 2207.10111]

Parameter space where parametric resonance can create compact halos.

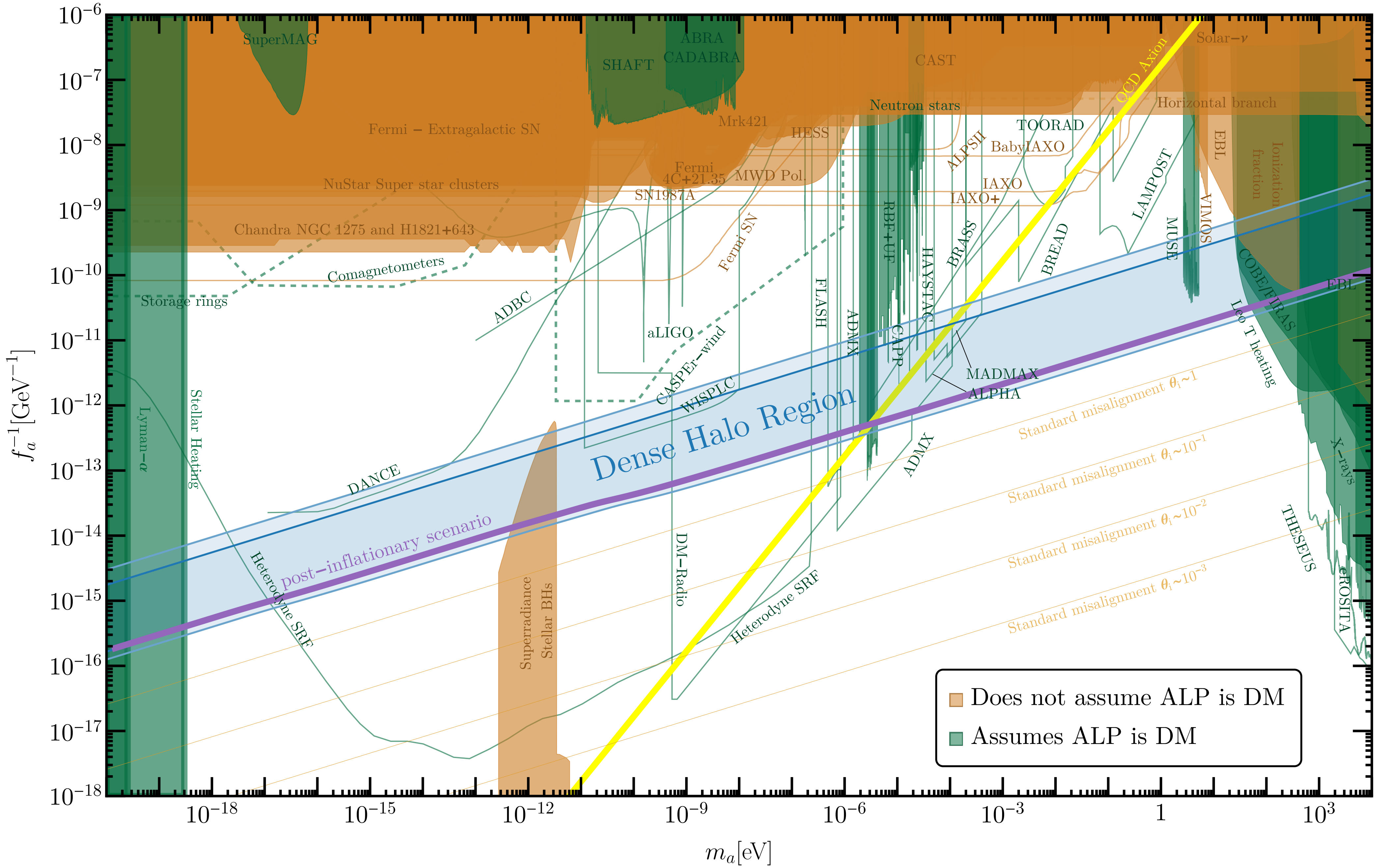

Chatrchyan et al, 2305.03756

Parameter space where parametric resonance can create compact halos (with $\rho_s \gtrsim 10\,M_\odot\,\mathrm{pc}^{-3}$).

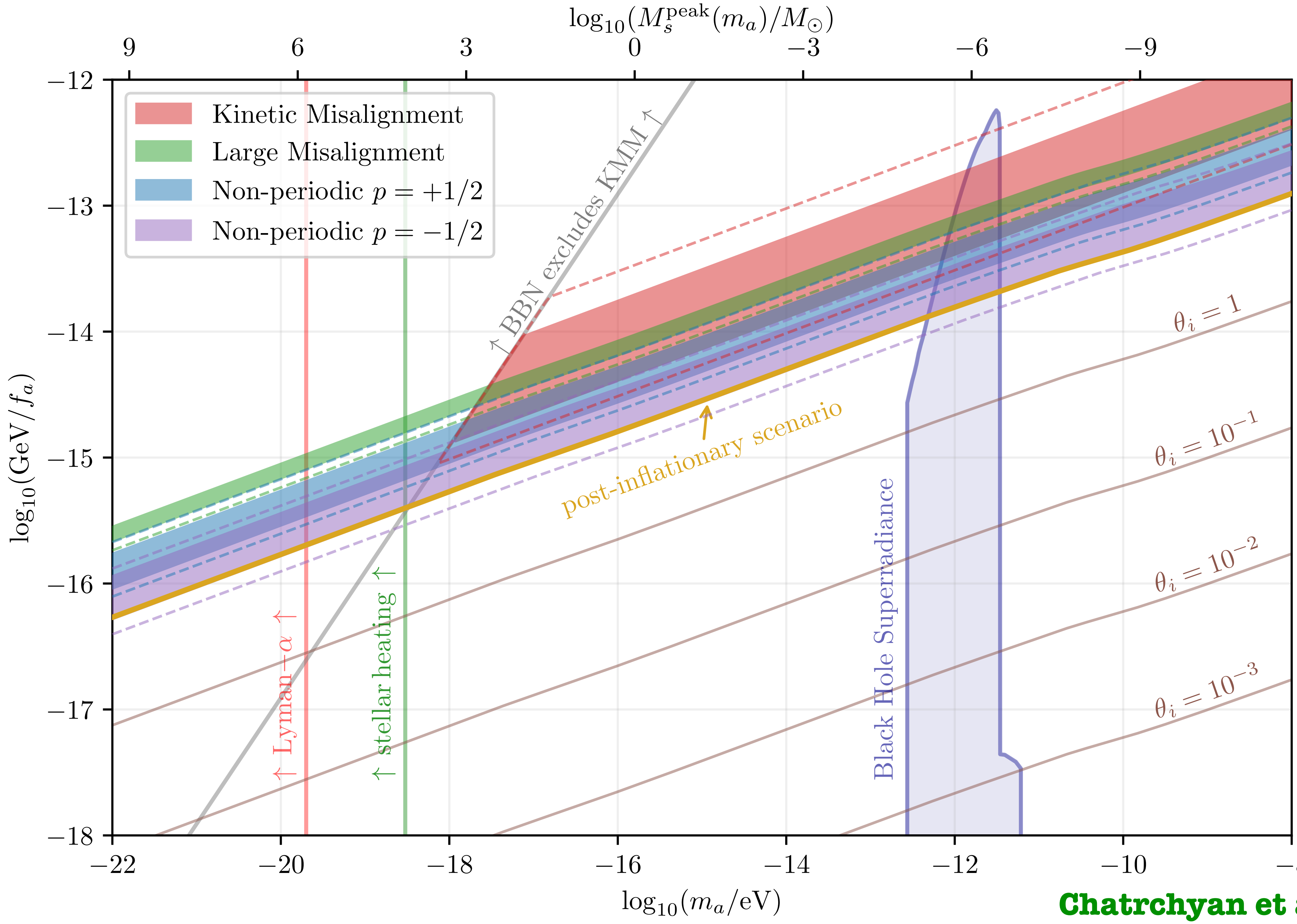

Chatrchyan et al 2305.03756

The dense halo regions from ≠ production mechanisms mostly overlap.
Difficult to infer the producion mechanism from observations.
However, observations of dense structure gives information about f_a even when ALP does not couple to the SM!

Observability of compact halos from kinetic misalignment.

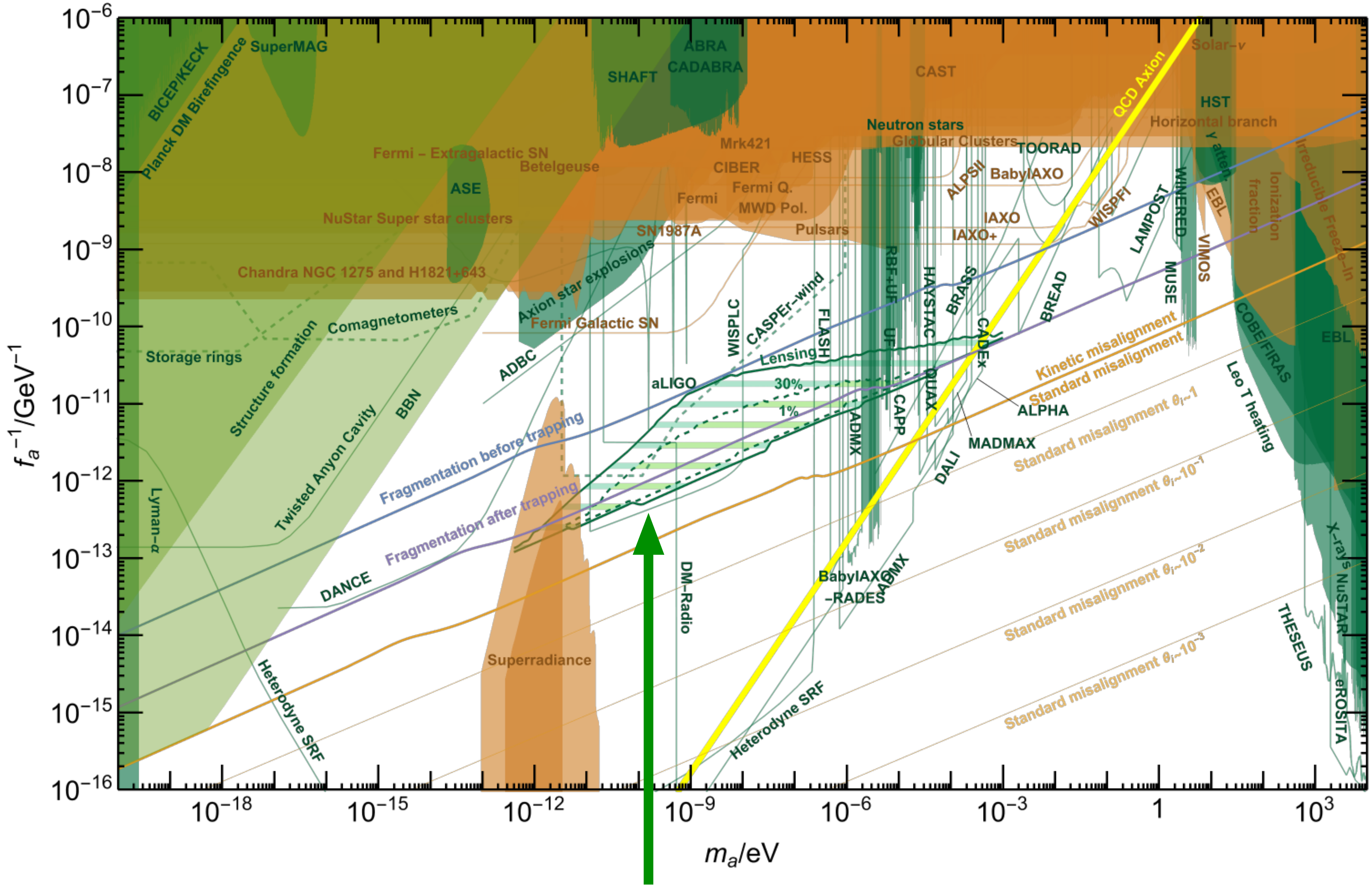

Region that can be probed by photometric lensing

Model implementations of a rotating axion .

Complex scalar field

“Affleck-Dine Baryogenesis” (Affleck, Dine, 1985)
“Axiogenesis” (Co, Hall, Harigaya, et. al., ’19)
“Kination cosmology” (Gouttenoire et al, ’21)

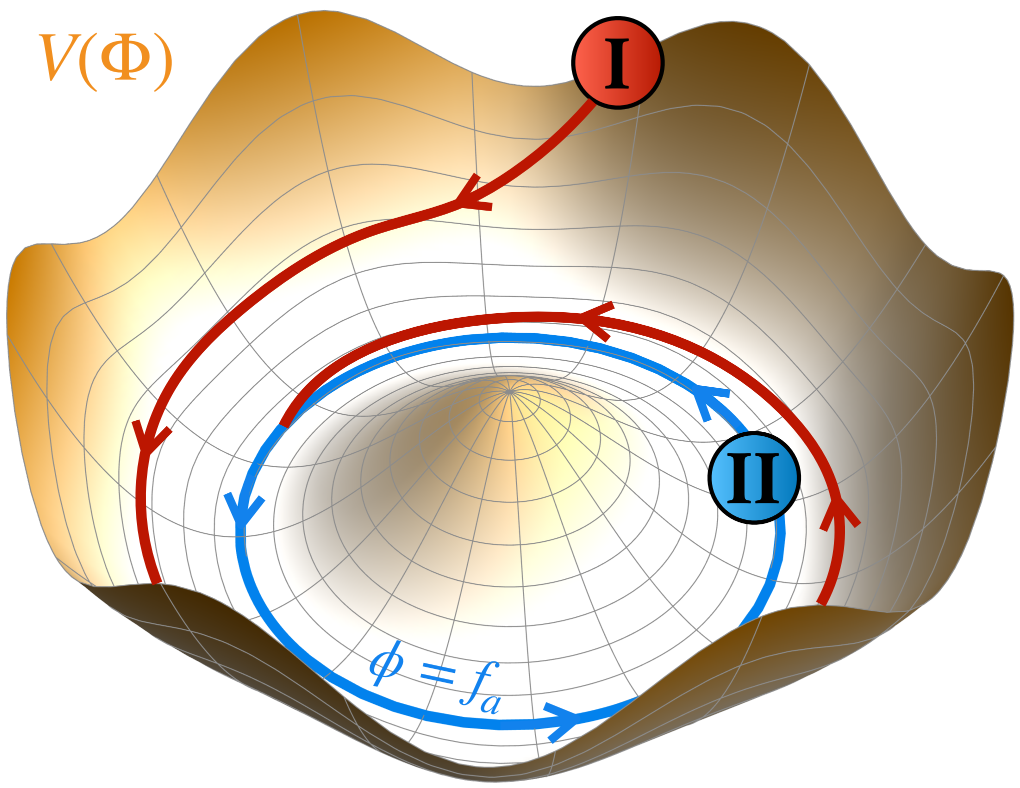

$\Phi \sim \phi e^{i\theta}$ with $U(1)$-symmetry

Radial mode ϕ oscillates in potential with mass $\sqrt{V''(\Phi)}$.

Angular mode θ “axion” spins, with large kinetic energy.

Requirements

1. $U(1)$-symmetric (quadratic) potential with spontaneous symmetry-breaking minimum

2. Large initial scalar VEV

3. Explicit $U(1)$-breaking term (wiggle for angular velocity)

4. Damping of radial motion

Ingredients 1 & 2 : scalar potential

$$V(\Phi) = m_r^2 |\Phi|^2 \left[\log\left(\frac{|\Phi|^2}{f_a^2}\right) - 1\right] + \left[A\frac{\Phi^n}{M_{Pl}^{n-3}}. + h.c\right] + \frac{|\Phi|^{2n-2}}{M_{Pl}^{2n-6}}$$

I. $U(1)$-conserving potential
(quadratic)
with a minimum f_a

(motivated by supersymmetric setups)

$\propto \cos(l\theta)$
II. explicit breaking term
(e.g. $U(1)$ is not exact
at high scales.)

stabilization
i.e., at large $|\Phi|$

$$\phi_{\rm ini} \simeq M_{\rm Pl}\left(\sqrt{\frac{c}{\lambda^2}}\cdot\frac{m_r}{M_{\rm Pl}}\right)^{1/(n-2)}$$

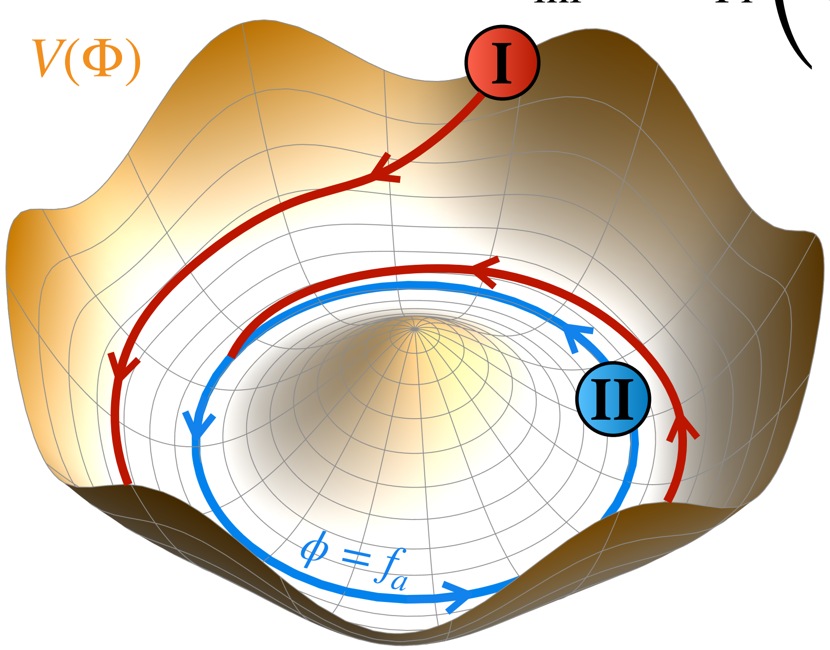

Ingredient 3 : large initial VEV $\phi_{\rm ini}$

By adding a negative Hubble mass

$$V_H(\Phi, H) \supset -cH^2|\Phi|^2$$

ϕ is driven away from $\phi = 0$ at early times ($H \gg m_r$)

(e.g. Dine, Randall, Thomas, 1995, Fujita & Harigaya 1607.07058)

Fate of radial mode.

Radial mode oscillations can overclose universe.

Can be damped.

WHEN: before radial mode dominates → no entropy production

after radial mode dominates → entropy production

HOW: Coupling with fermion χ : $\phi\chi\chi$

Coupling with Higgs : $\phi^2 H^2$

Ingredient 4: Damping

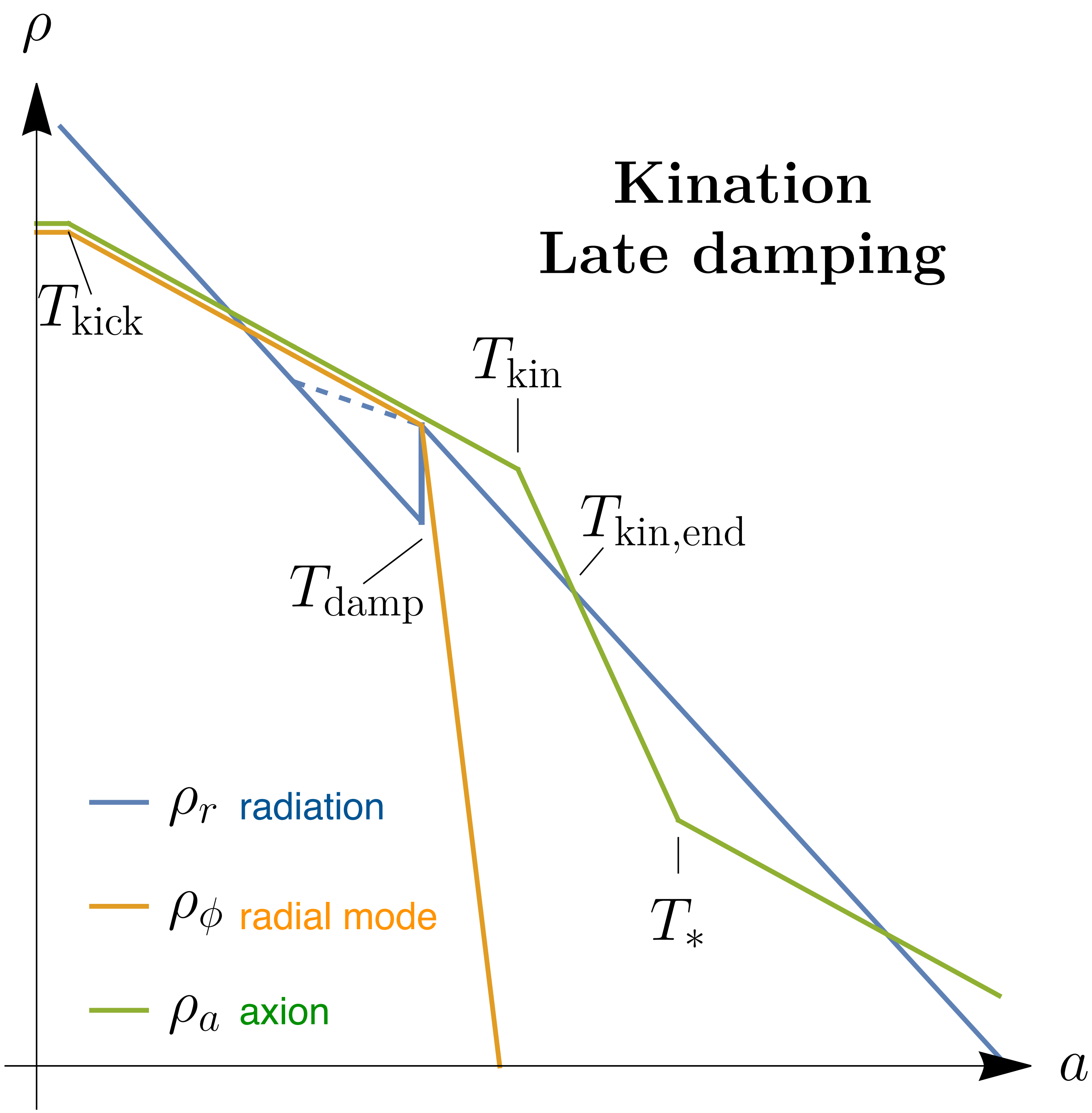

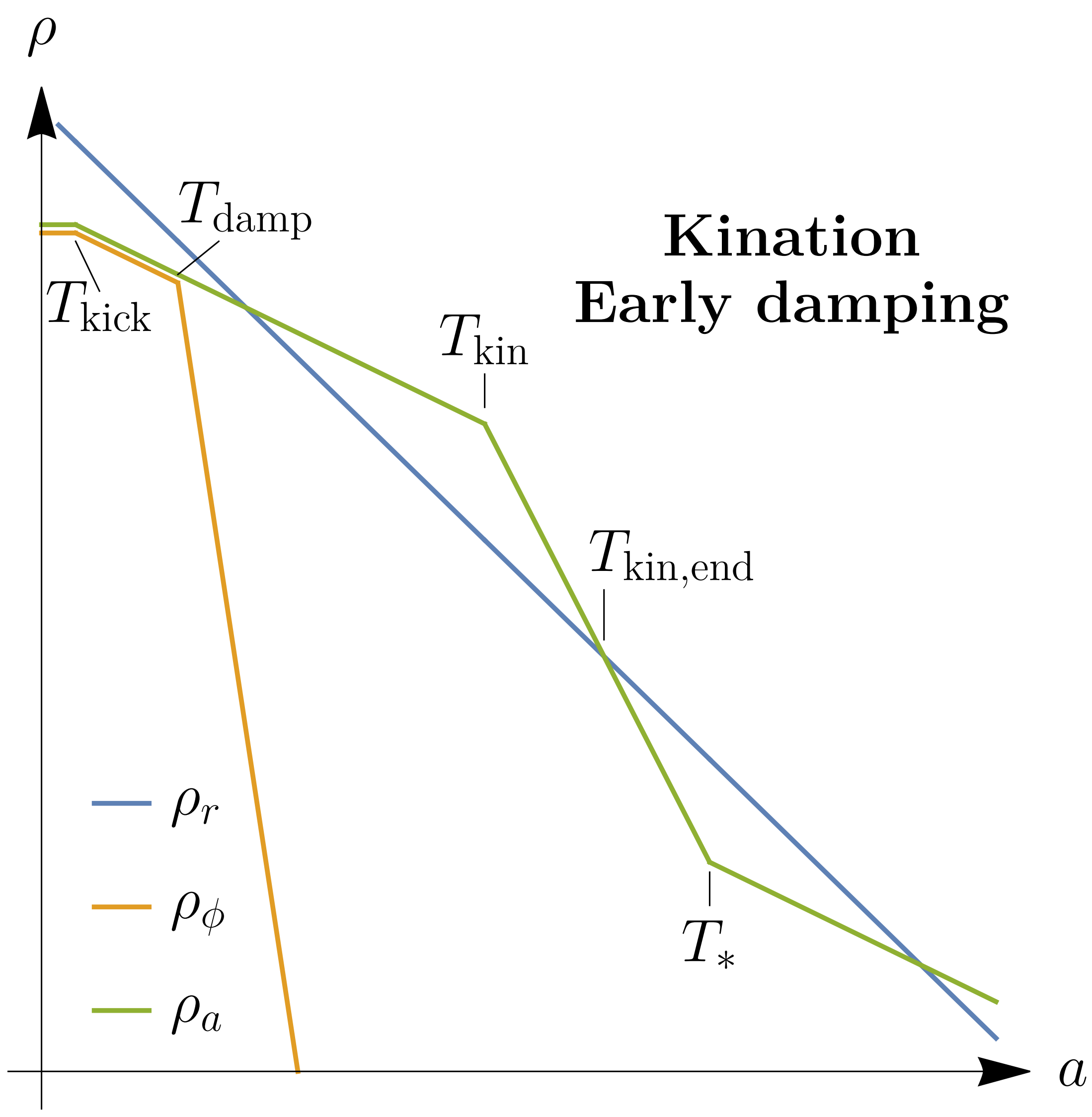

Trapping temperature.

$$T_* \approx (2.12)^{\frac{\gamma}{2+\gamma}} \left(2 \times 10^8\right)^{\frac{2}{6+\gamma}} \left(\frac{g_*}{72}\right)^{-\frac{2}{6+\gamma}} (m_a f_a)^{\frac{1}{2}+\frac{1}{6+\gamma}} \left(\frac{h^2\Omega_{\phi,0}}{h^2\Omega_{\rm DM}}\right)^{-\frac{2}{6+\gamma}},$$

$$m_a^2(T) \approx m_a^2 \times \begin{cases} (T/T_c)^{-\gamma} & \text{if } T > T_c \\ 1 & \text{if } T < T_c \end{cases}, \quad \text{where} \quad \begin{matrix} T_c = 2.12 \times \Lambda_{b,0}, \\ \Lambda_{b,0} = \sqrt{f_a m_a}, \\ \gamma = 8.16, \end{matrix}$$

where:

$$\left(\frac{h^2\Omega_{\phi,0}}{h^2\Omega_{\rm DM}}\right) \approx \left(\frac{m_a}{5 \times 10^{-3}\,{\rm eV}}\right)\left(\frac{Y}{40}\right),$$

$$Y = \frac{n_{\rm PQ}}{s},$$

$$n_{\rm PQ} = \dot{\theta}\phi^2 \propto a^{-3}$$

Our goal: extract predictions for Y for any (m_a,f_a) as a function of the UV parameters of the theory that control the size of the kick, such as the mass of the radial mode m_ϕ and n the dimension of the explicit PQ-breaking higher-dimensional operators

$$T_{kick} \approx \sqrt{m_\phi M_{Pl}}$$

$$\dot{\theta}_{\rm kick} = \mathcal{O}(1) \times m_\phi,$$

$$Y_{\rm kick} = \frac{n_{PQ}}{s} = \epsilon \frac{m_\phi \phi_{\rm kick}^2}{\frac{2\pi^2}{45} g_{*s} T_{\rm kick}^3} \approx 0.8 \times \epsilon \left(\frac{M}{m_{\rm Pl}}\right)^{\frac{2n-6}{n-2}} \left(\frac{m_{\rm Pl}}{m_\phi}\right)^{\frac{n-6}{2n-4}},$$

Kination from a rotating axion

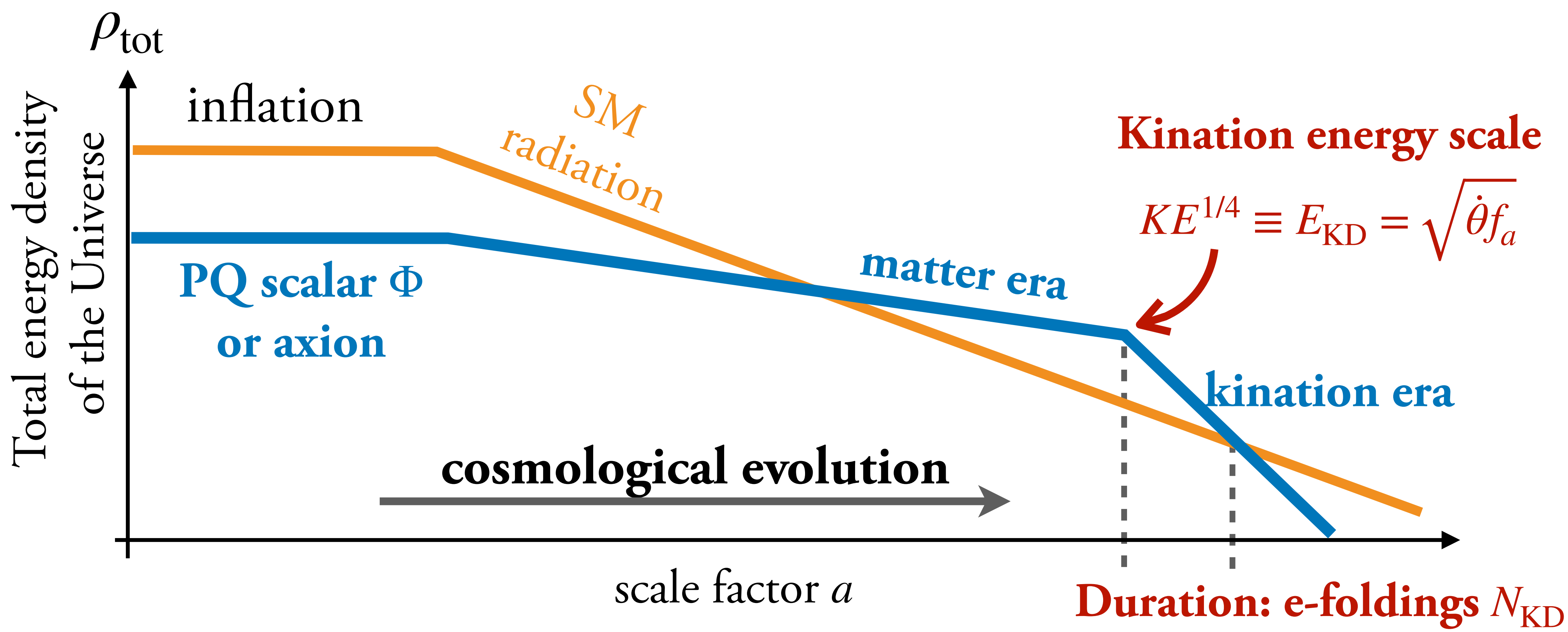

are characterized by
(given the spontaneous symmetry-breaking scale f_a)

1. **kination energy scale** $E_{\rm KD} = \sqrt{\dot{\theta} f_a}$

   (the spinning speed of axion $\dot{\theta}$ when kination starts)

2. **the duration of kination era** $N_{\rm KD} = \log(a_{\rm start}/a_{\rm end})$

   (related to the beginning of the matter era)

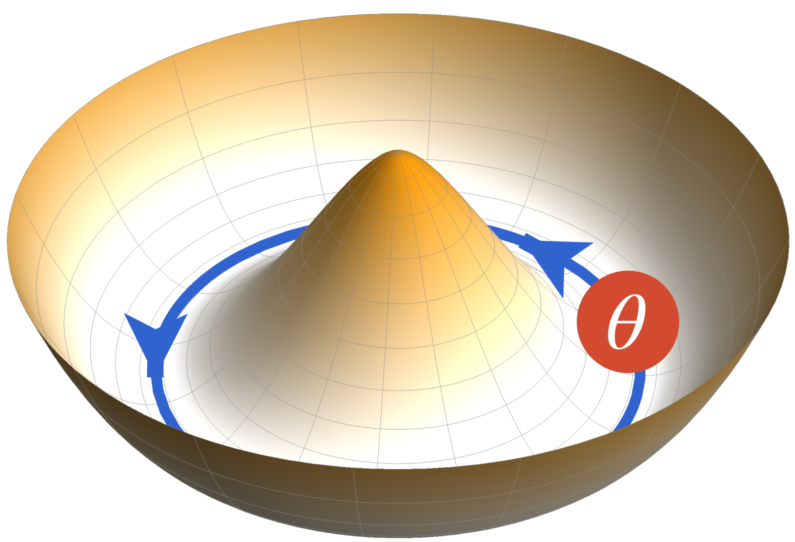

circle of $\phi = f_a$

Once $\langle \phi \rangle = f_a$ $\rho_a \propto \dot{\theta}^2 \propto a^{-6}$

kination

BBN constraint: $T_* \gtrsim 20 \text{ keV}.$

Many other constraints to check:

-perturbativity
-homogeneity
-radial mode abundance and decay
-efficient radial mode damping

Explicit UV completions.

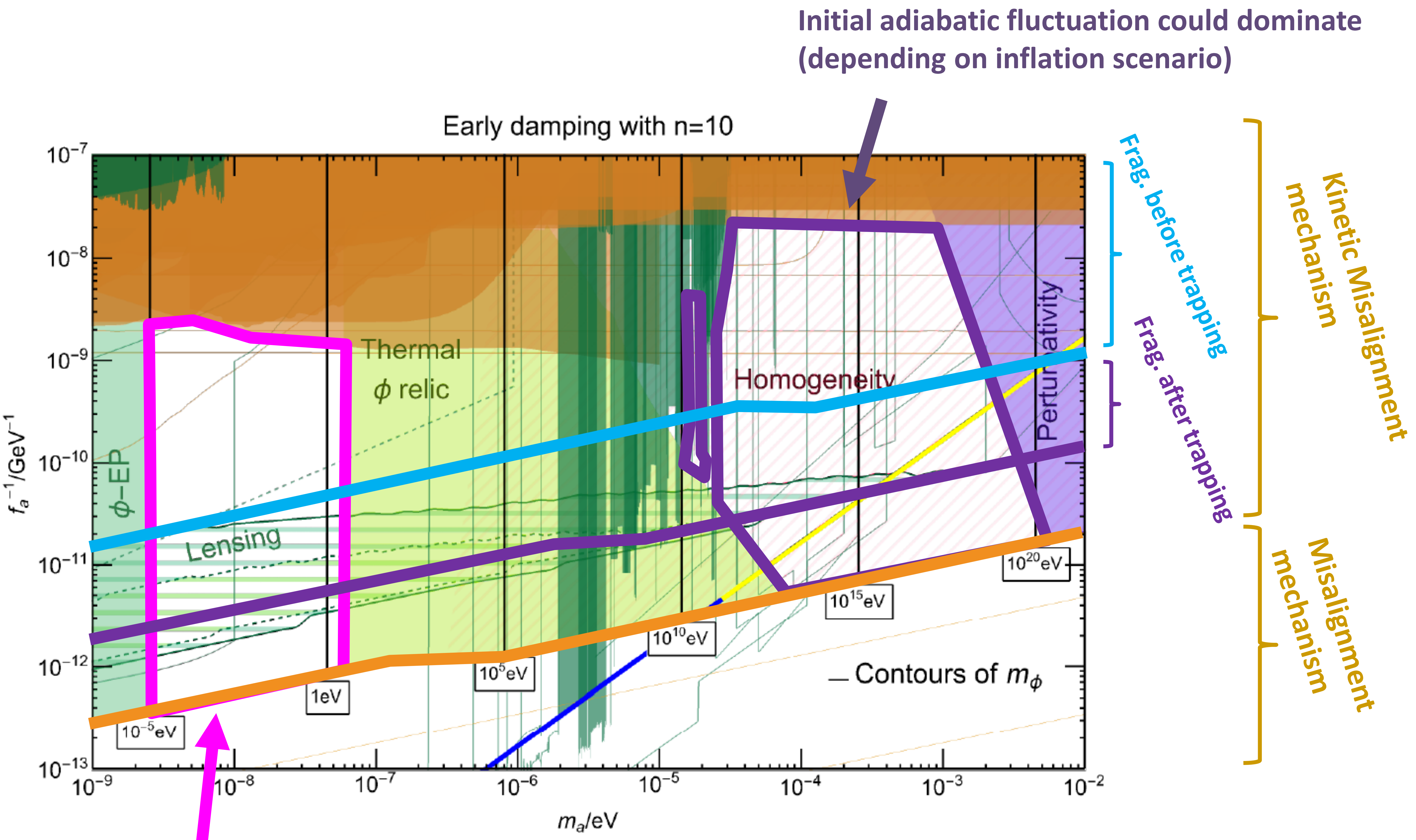

Kinetic misalignment (+ fragmentation)

[Eroncel, Soerensen, Sato, Servant, 2406.xxxxx]

Necessary suppression of A_s

$A_{s,\text{Planck}} \approx 2.1 \times 10^{-9}$ at a pivot scale of $0.05\ \text{Mpc}^{-1}$

Initially $\rho_{\text{fluc}} \sim A_s \rho_a$

Later $\rho_a \propto a^{-6}$

$\rho_{\text{fluc}} \propto a^{-4}$

To avoid domination by axion fluctustions: $A_s(k_{\text{kin}}) \lesssim \left(\frac{a_{\text{kin}}}{a_*}\right)^2$

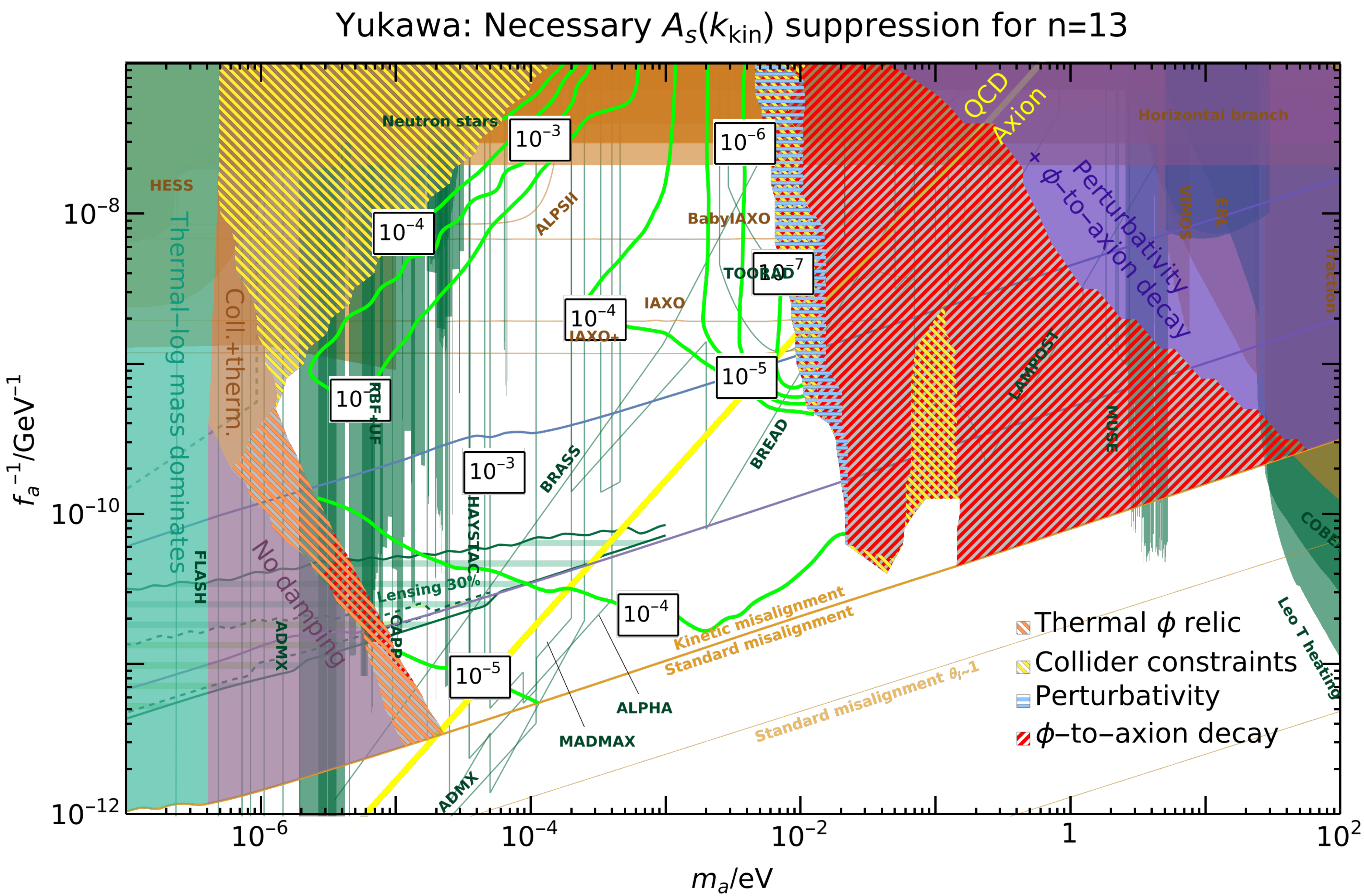

Explicit UV completions realising the axion kinetic misalignment.

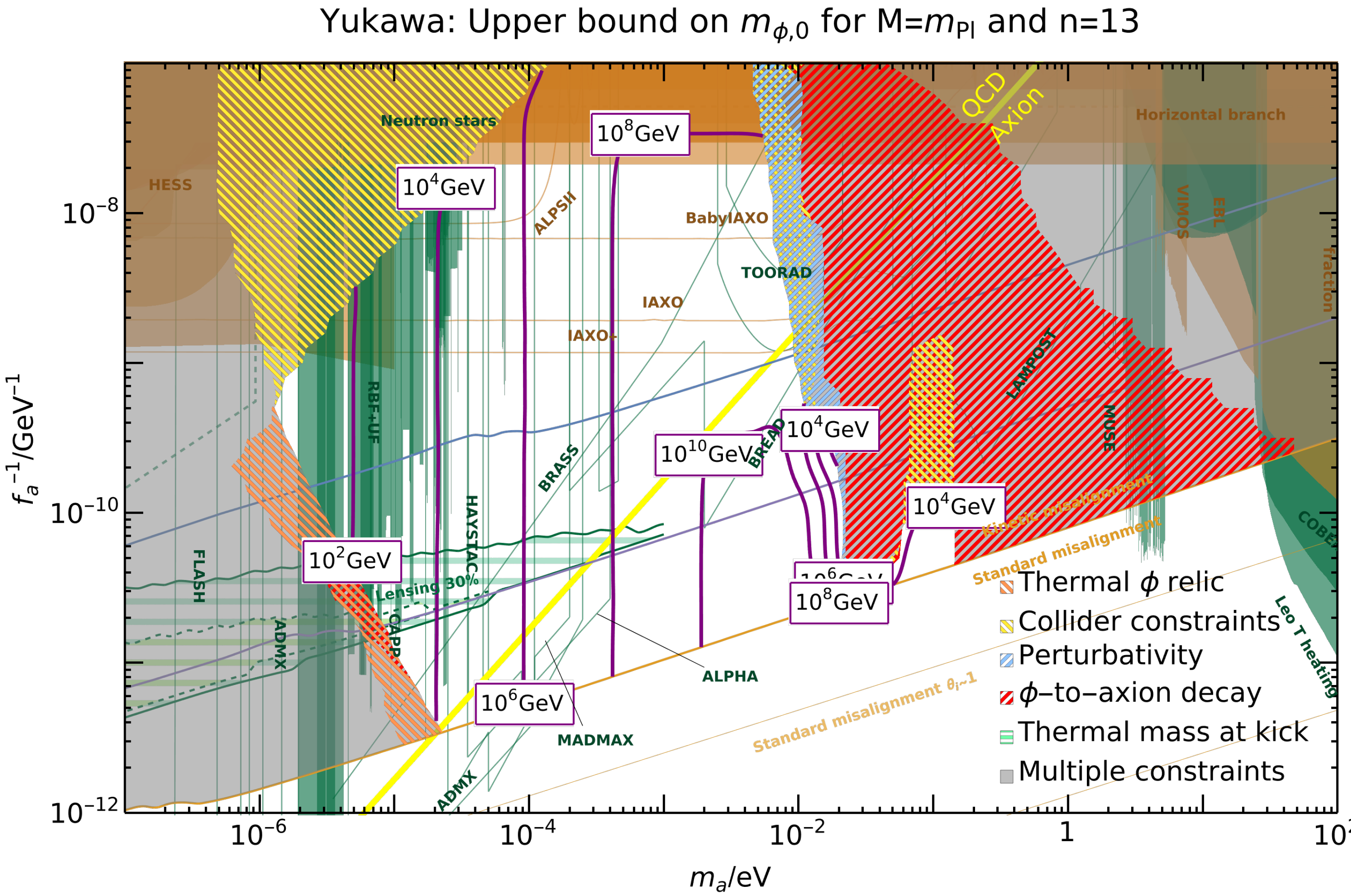

[Eroncel et al, in prep.]

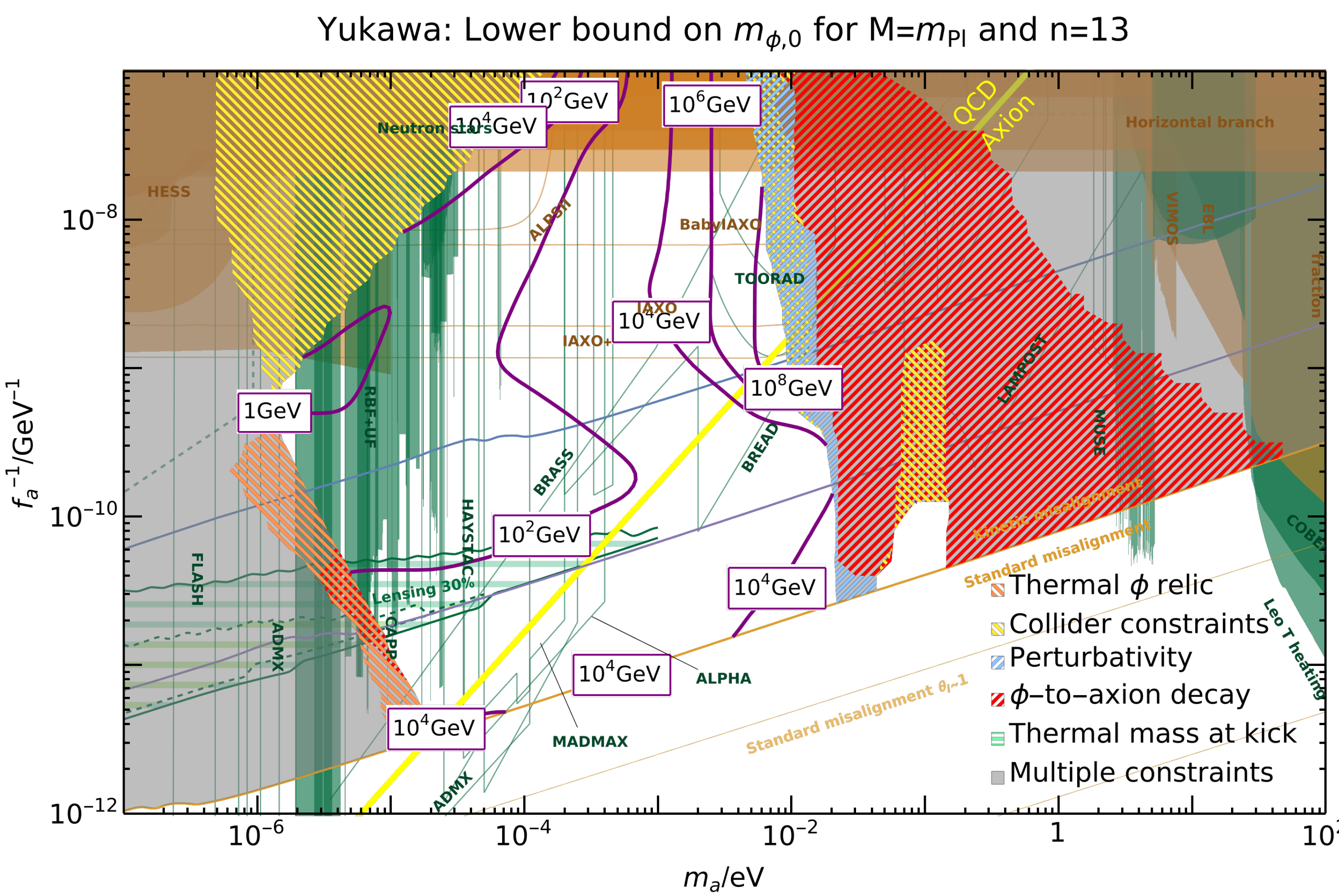

Explicit UV completions realising the axion kinetic misalignment.

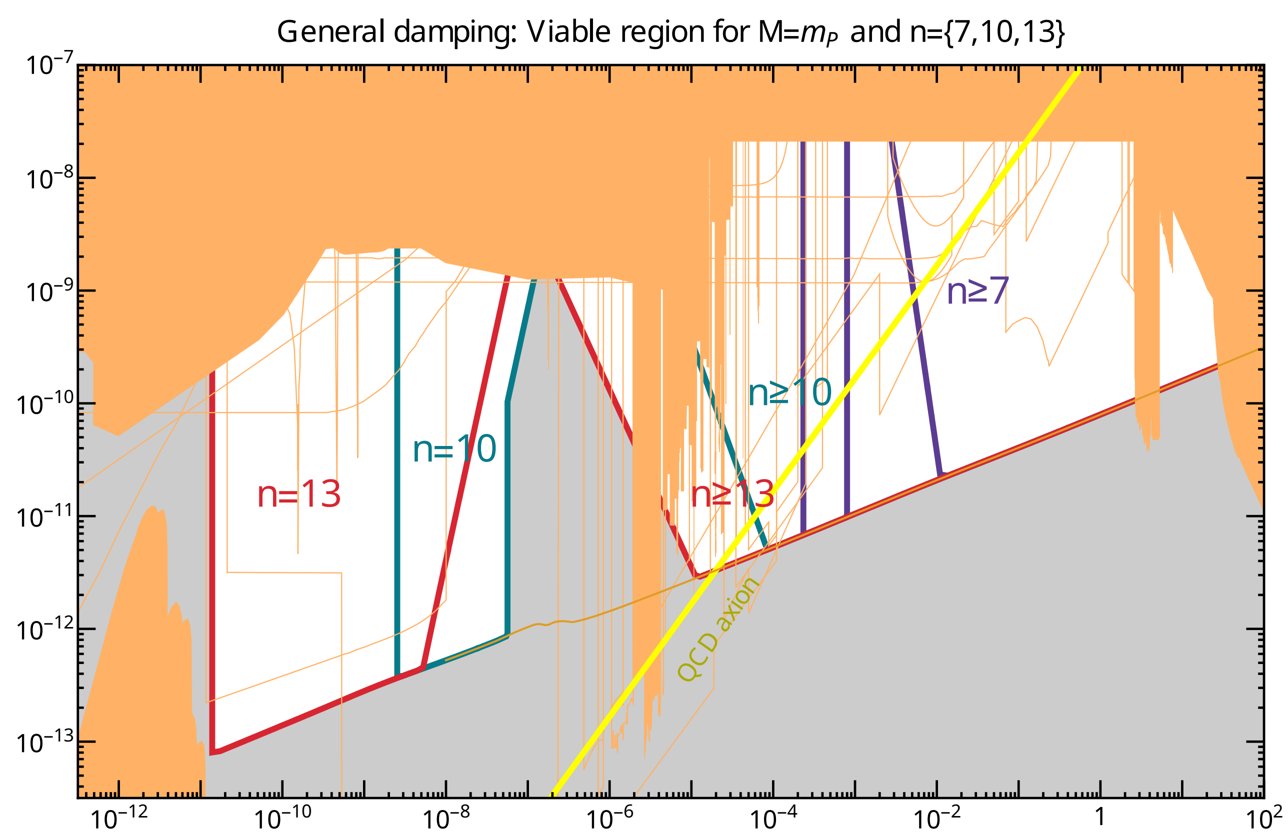

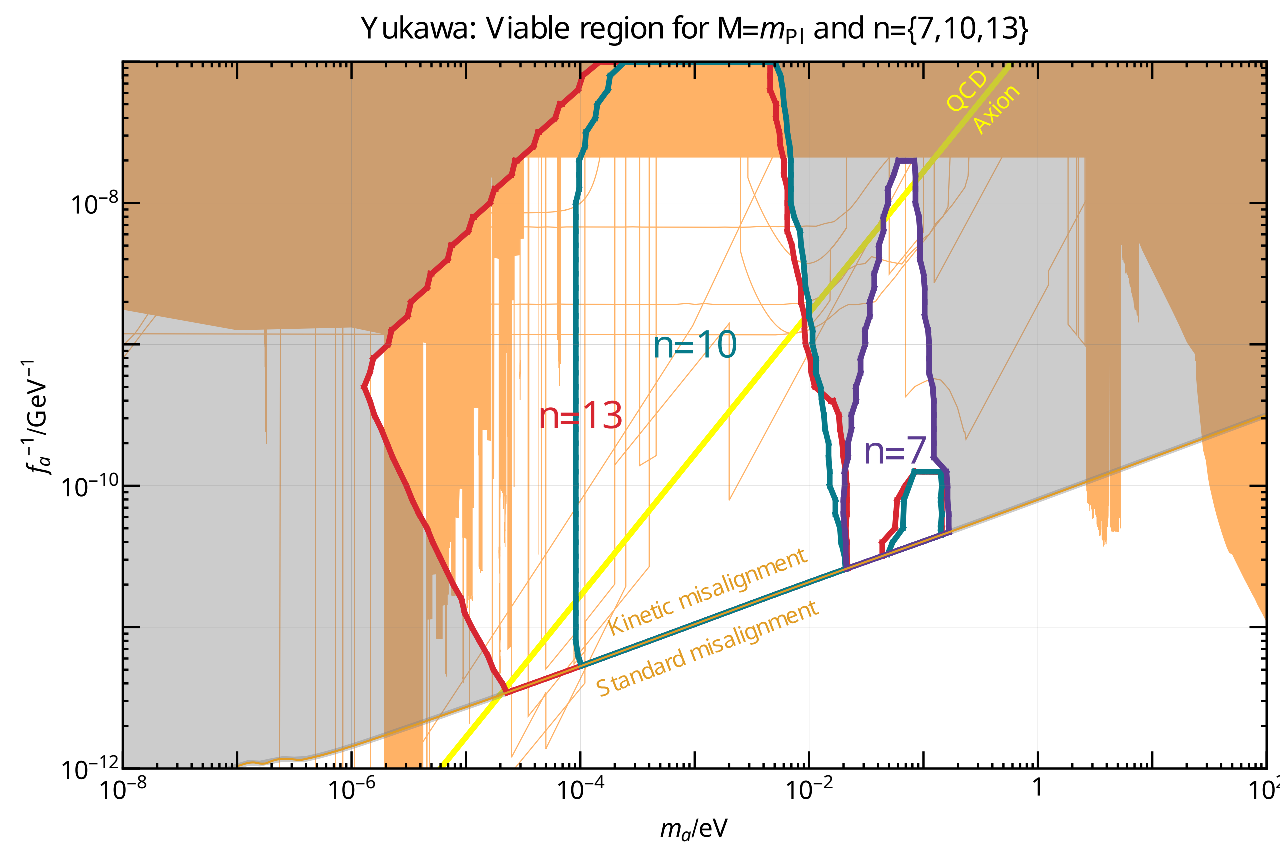

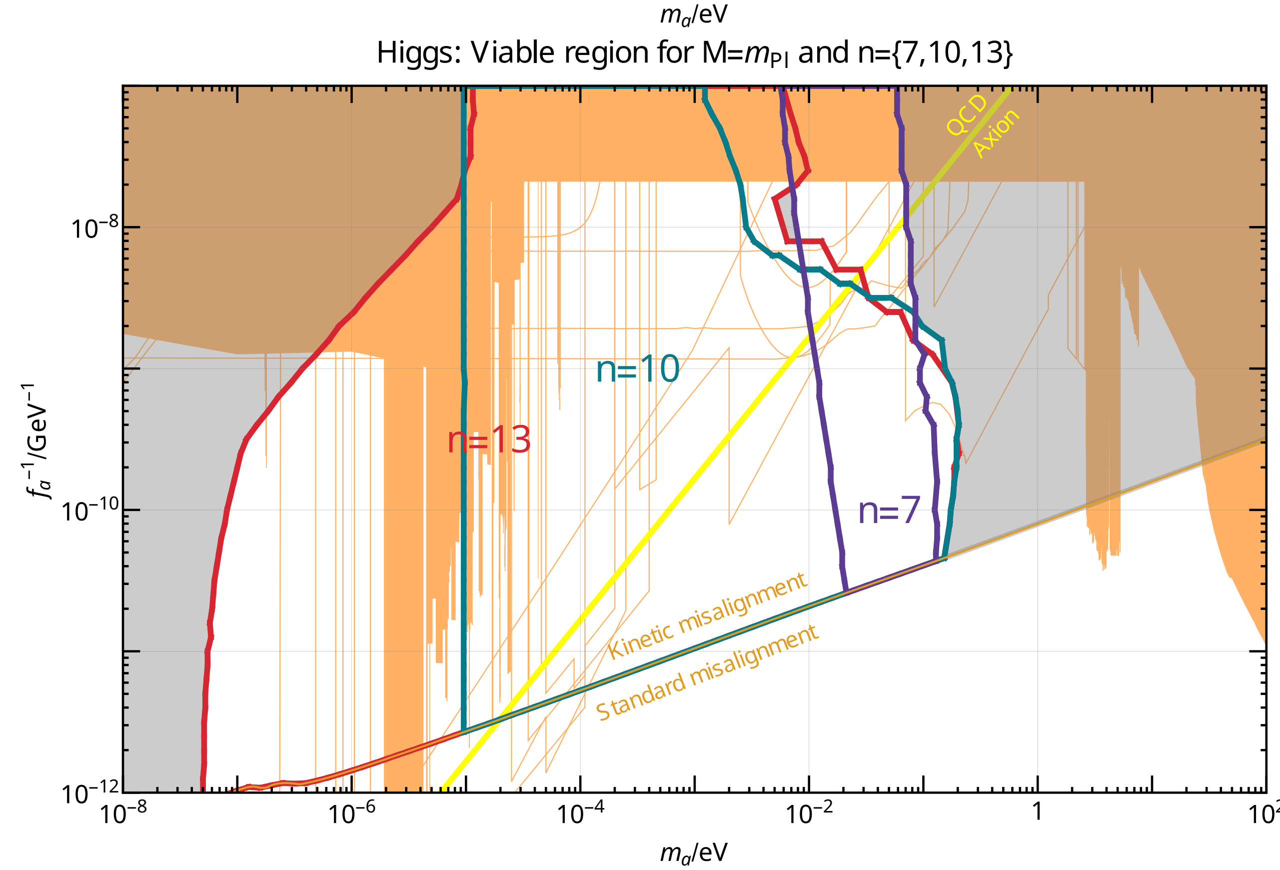

[Eroncel et al, 2406.xxxxx]

Correlations between axion mass and radial-mode mass.

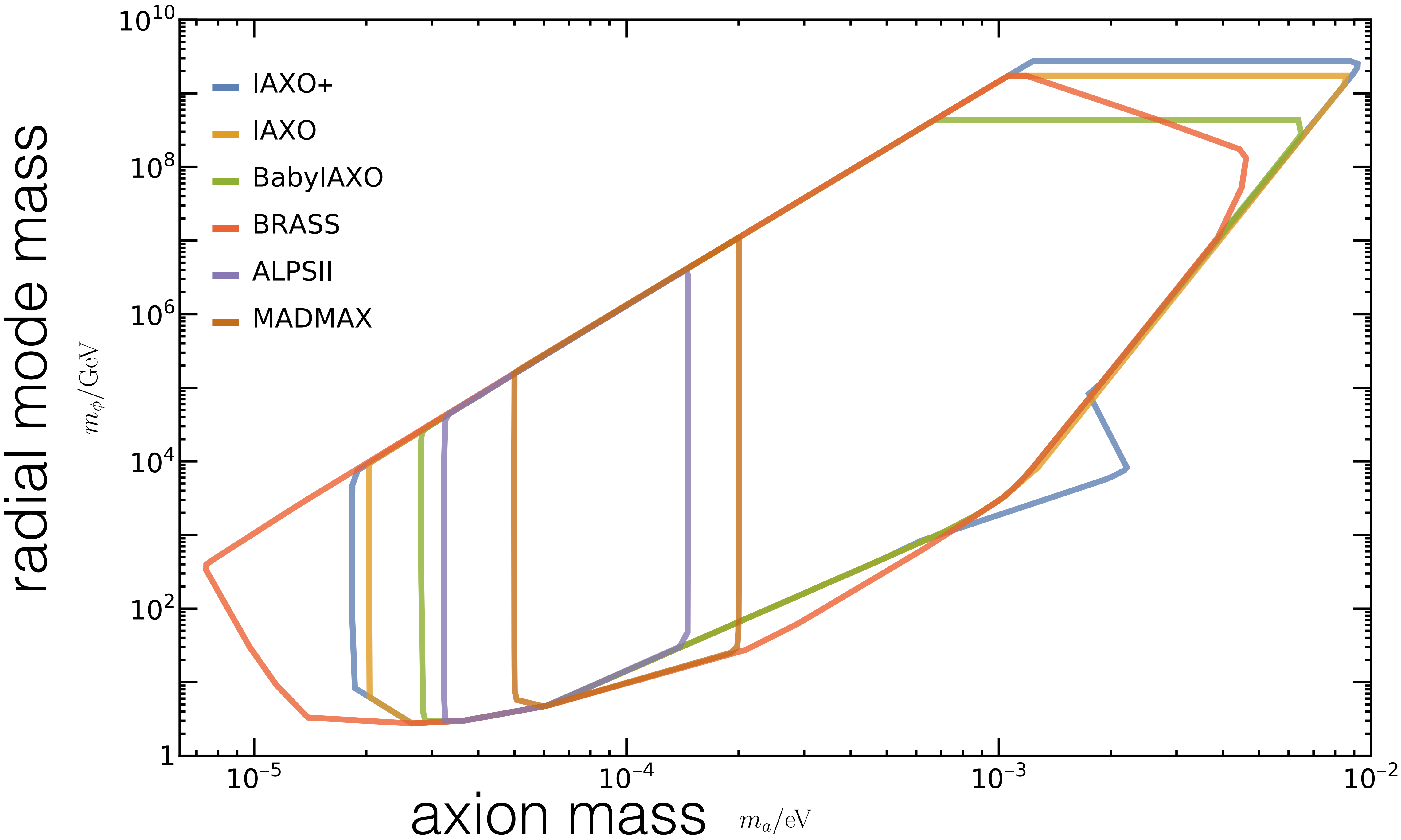

[Eroncel et al, 2406.xxxxx]

GWs from axion fragmentation.

The transfer of energy in the early universe from the homogeneous axion field into axion quantum fluctuations, inevitably produces a stochastic background of gravitational waves of primordial origin with a peak frequency controlled by the axion mass.

$$\ddot{h}_{ij} + 3H\dot{h}_{ij} - \frac{\Delta h_{ij}}{a^2} = \frac{16\pi}{M_{\rm pl}^2}\Pi_{ij}^{\rm TT},$$

$$\Pi_{ij}^{\rm TT}(t,\vec{x}) = \frac{1}{a^2}\left[\partial_i\phi(t,\vec{x})\partial_j\phi(t,\vec{x}) - \frac{1}{3}\delta_{ij}(\partial_k\phi(t,\vec{x})\partial_k\phi(t,\vec{x}))\right]$$

Gravitational waves from ALP DM fragmentation.

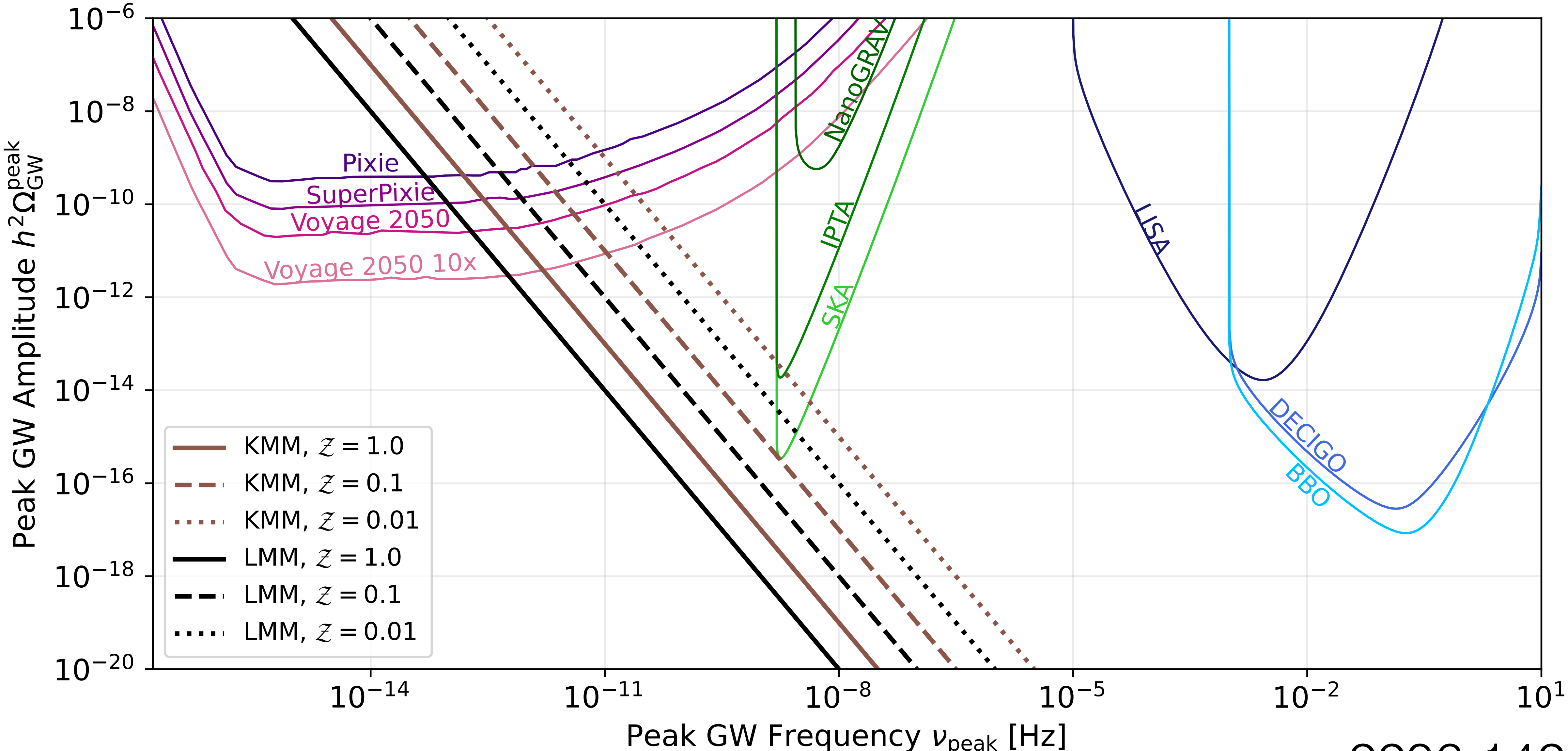

2206.14259

$\mathcal{Z}$ = needed dilution factor of ALP energy density

Conclusion.

-Standard Misalignment Mechanism cannot account for dark matter in the ALP parameter space where the experiments are most sensitive.

-Kinetic Misalignment Mechanism moves the ALP Dark Matter window into testable territory.

-All axion experiments are in principle sensitive to axion dark matter (even helioscopes and light-shining-through-the-wall experiments)
QCD axion Dark Matter inside MADMAX and Iaxo sensitivities

-Axion not alone, e.g, its radial mode partner is a key player

-ALP mini-clusters can be formed even in the pre-inflationary scenario from kinetic fragmentation.

- **Band in the (m_a,f_a)-plane where dense structures can be formed does not depend drastically on the production mechanism.**
- **Existence of this band allows us to obtain information about the decay constant, even if ALP does not couple to the Standard Model.**

- Gravitational waves: not discussed in this talk, however kination leads to a unique amplification of the primordial GW background from inflation & from cosmic strings (2111.01150)

Extra material.

Equation of motion of complex scalar field in expanding universe

$$\ddot{\Phi} - a^{-2}\nabla^2\Phi + 3H\dot{\Phi} + \frac{\partial V}{\partial \Phi^\dagger} = 0$$

with $\Phi = \phi e^{i\theta}$

$$\ddot{\phi} - a^{-2}\nabla^2\phi + 3H\dot{\phi} + V'(\phi) = \phi\dot{\theta}^2 - a^{-2}\phi(\nabla\theta)^2,$$
$$\phi\ddot{\theta} - a^{-2}\phi\nabla^2\theta + 3H\phi\dot{\theta} = -2\dot{\phi}\dot{\theta} + 2a^{-2}\nabla\phi\nabla\theta.$$

For homogeneous field, these are Kepler problem:

centrifugal force

$$\ddot{\phi} + 3H\dot{\phi} + V'(\phi) = \phi\dot{\theta}^2$$

coriolis force

$$\ddot{\theta} + 3H\dot{\theta} = -2\frac{\dot{\phi}}{\phi}\dot{\theta}$$

conservation of charge (angular momentum):

$$\frac{d}{dt}(a^3\phi^2\dot{\theta}) = 0$$

Ingredient 4: Damping

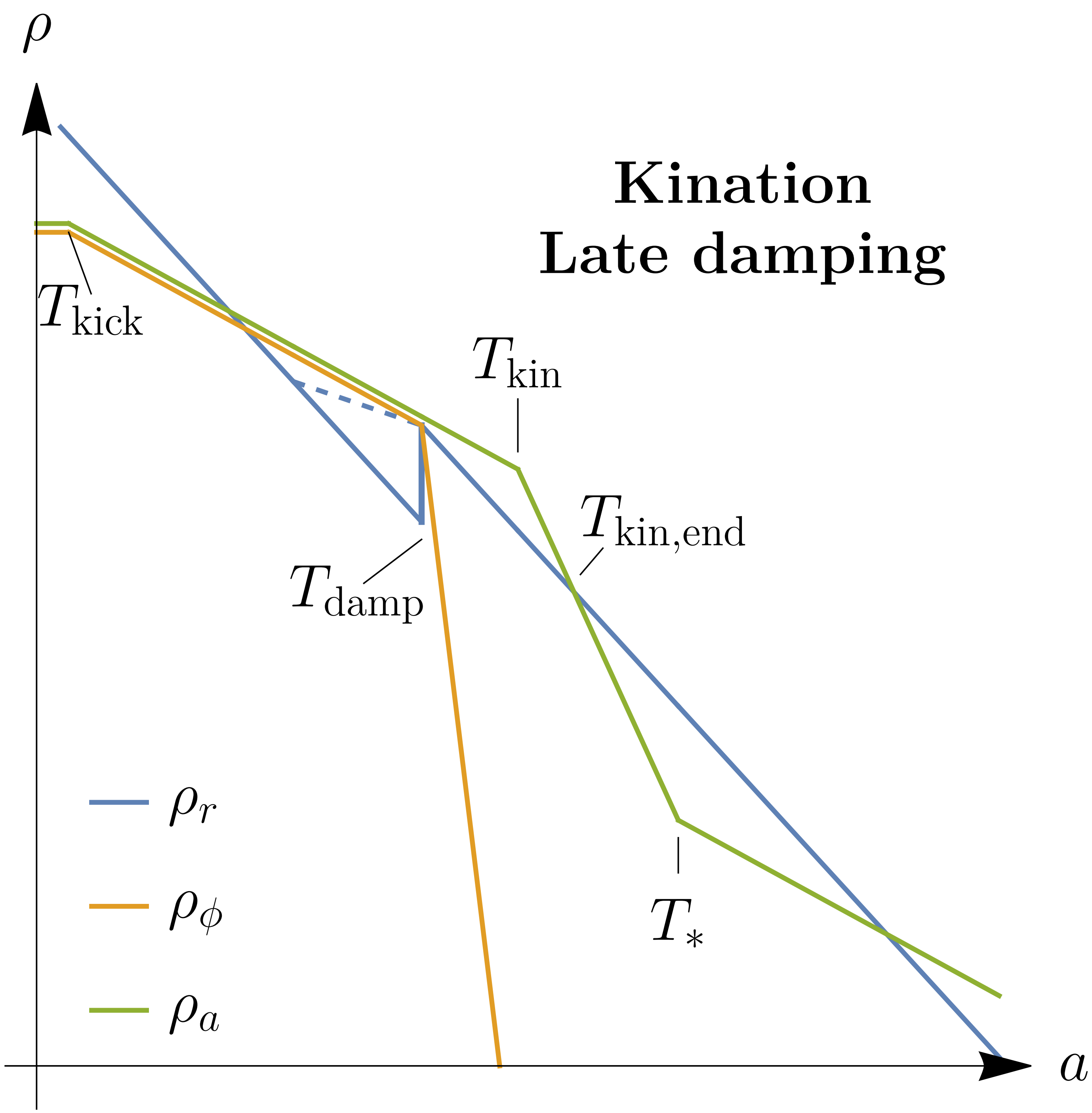

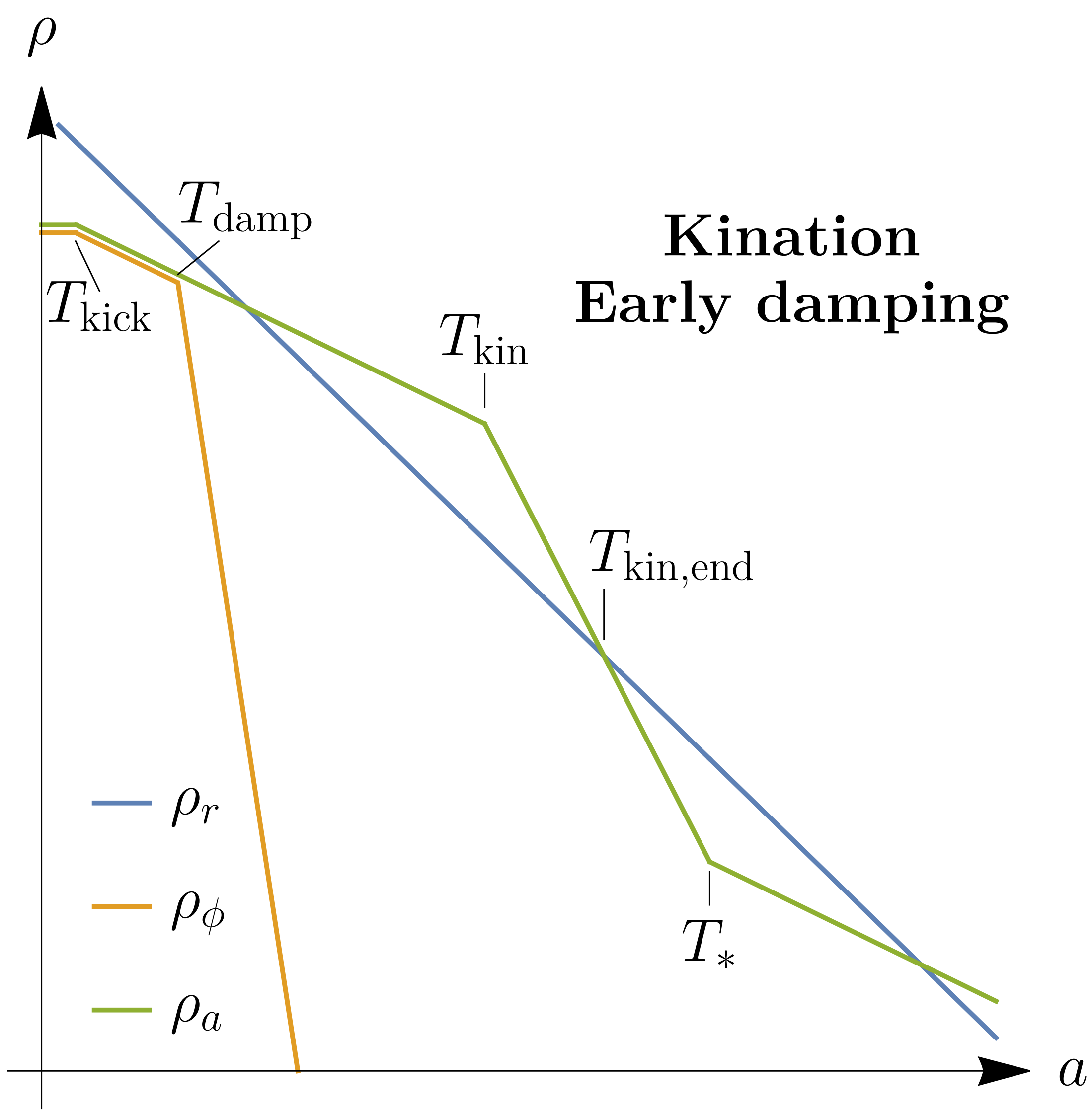

Power spectrum at the end of parametric resonance.

The size of fluctuations is determined by the density contrast:

$$\delta_\rho(\vec{\mathbf{x}}, t) \equiv \frac{\rho(\vec{\mathbf{x}}, t) - \overline{\rho}(t)}{\overline{\rho}(t)}$$

The power spectrum (two-point function) determines the distribution of structures today:

$$\mathcal{P}_\delta(k) = \frac{k^3}{2\pi^2} \left\langle \left| \tilde{\delta}_\rho(\vec{\mathbf{k}}, t) \right|^2 \right\rangle$$

After the parametric resonance the power spectrum can reach to $\mathcal{O}(1)$ values:

Dense and compact ALP mini-clusters can also be formed in the pre-inflationary scenario!

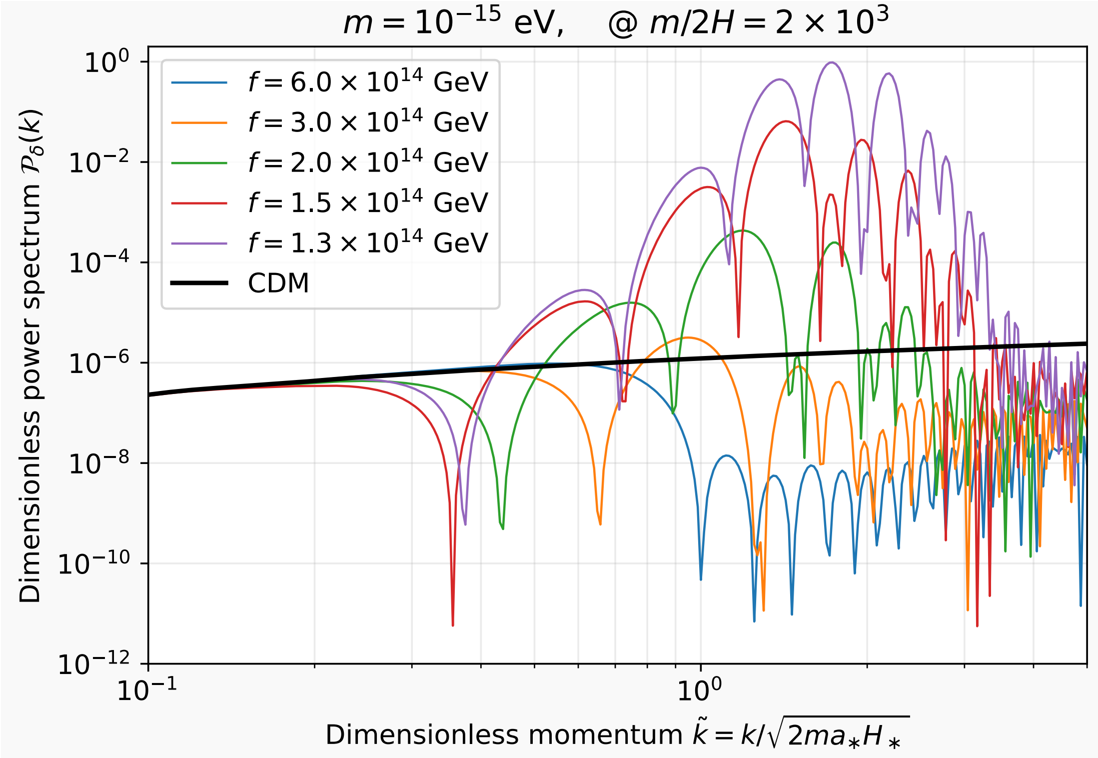

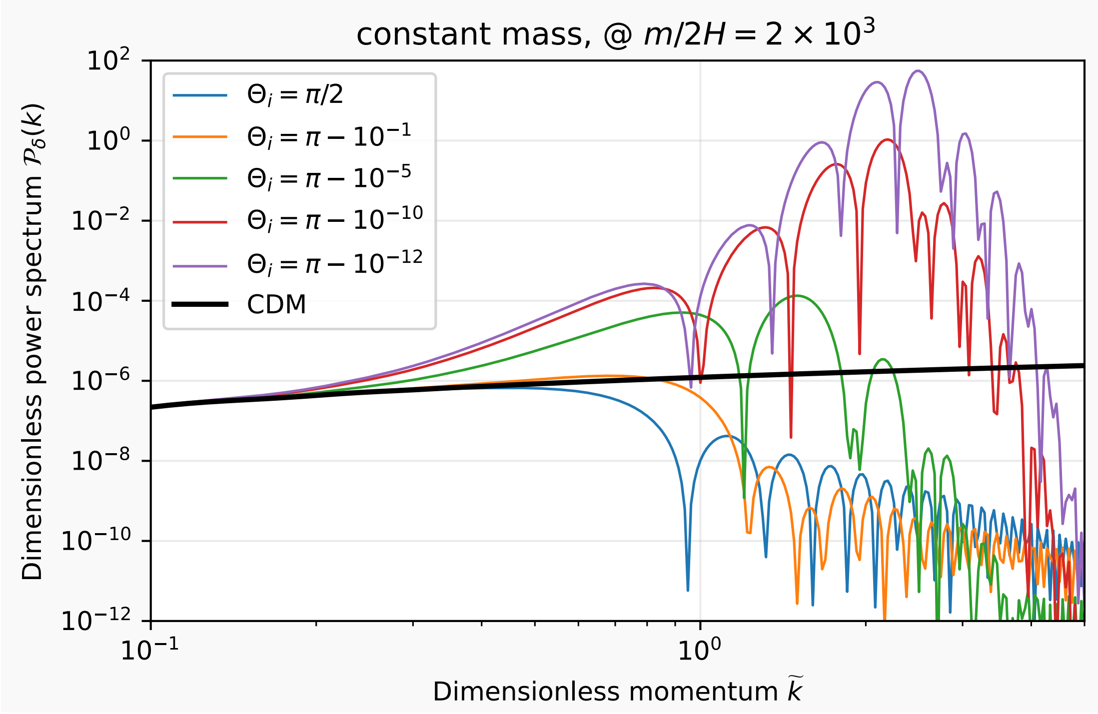

Halo Mass Function X(M).

X(M) = Fraction of DM that resides in halos with mass M

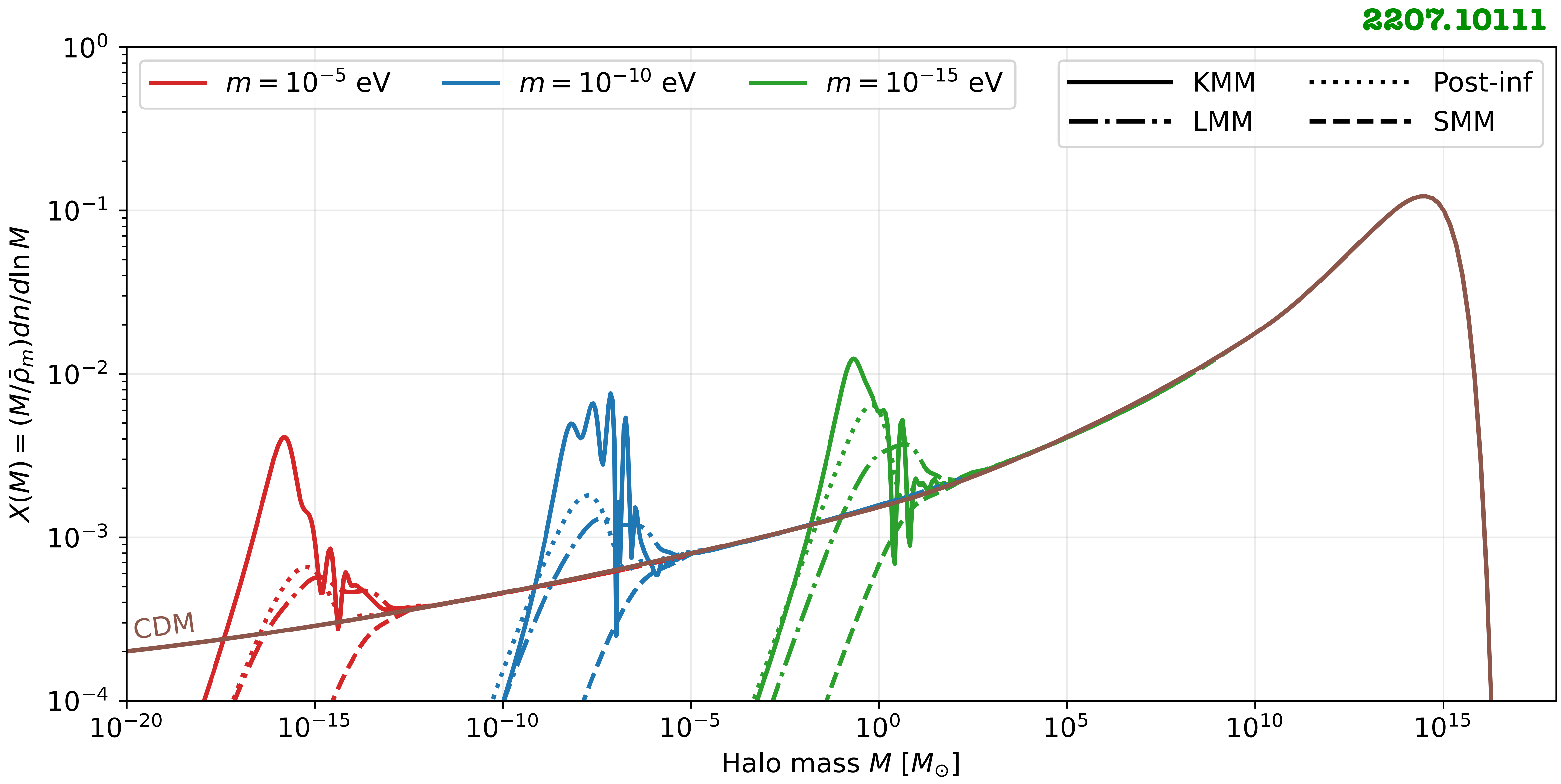

Breakdown of linearity & complete fragmentation.

When power spectrum becomes O(1),

linear perturbation theory breaks down,

—> the ALP field becomes completely fragmented.

The regime can be studied semi-analytically

via energy conservation arguments (Fonseca et al'19, Eroncel et al 2206.14259)

or fully numerically using lattice simulations (Morgante et al, 2109.13823, Chatrchyan et al 2305.03756)

The non-linear effects smoothen the power spectrum:

In the non-linear regime, more efficient parametric

resonance yields a power spectrum with smaller peaks.

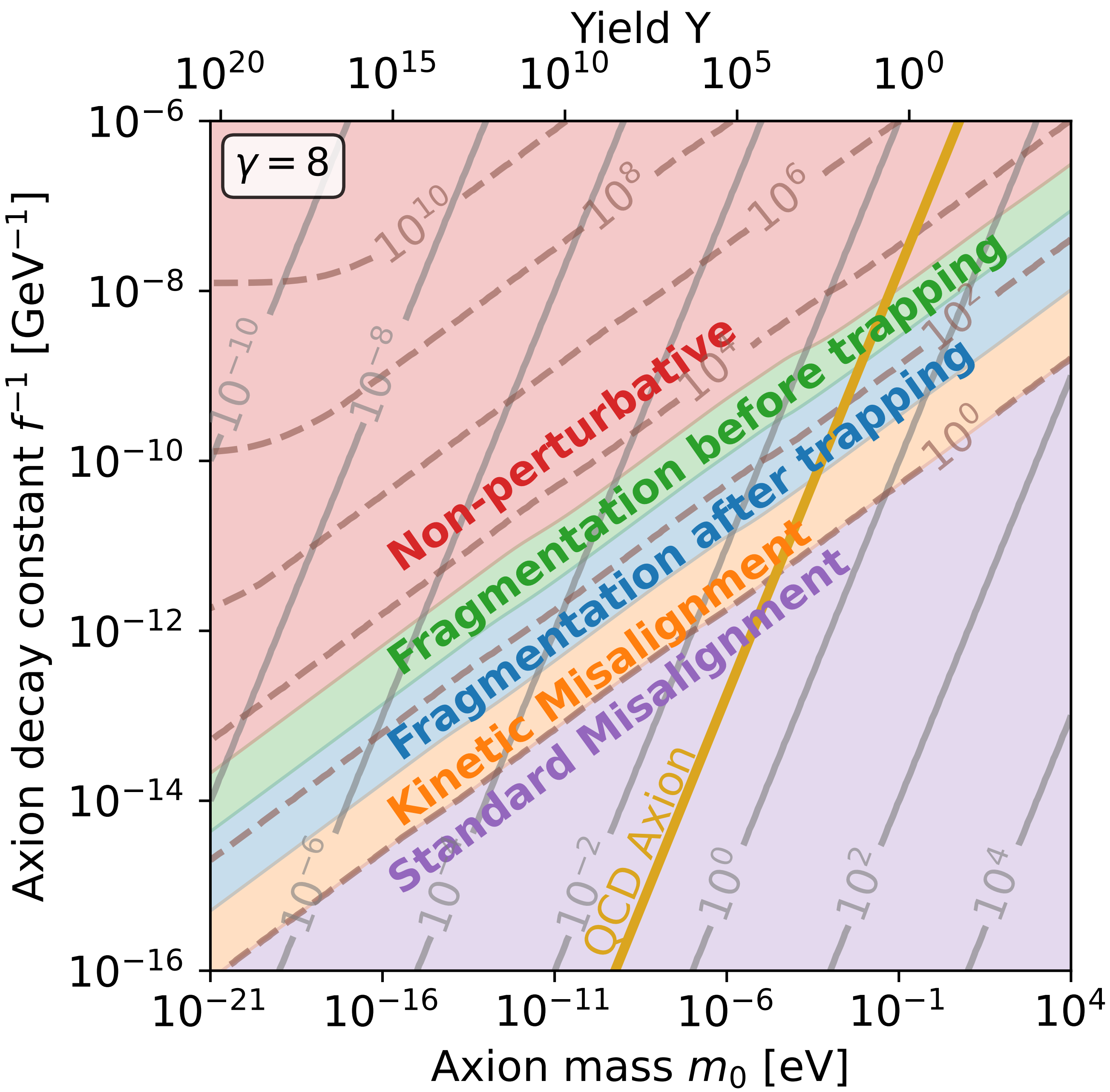

Solid lines: contours of zero-temperature barrier heights,

Dashed lines: (m/3H)_* contours

2206.14259

Contours of trapping temperature in GeV.

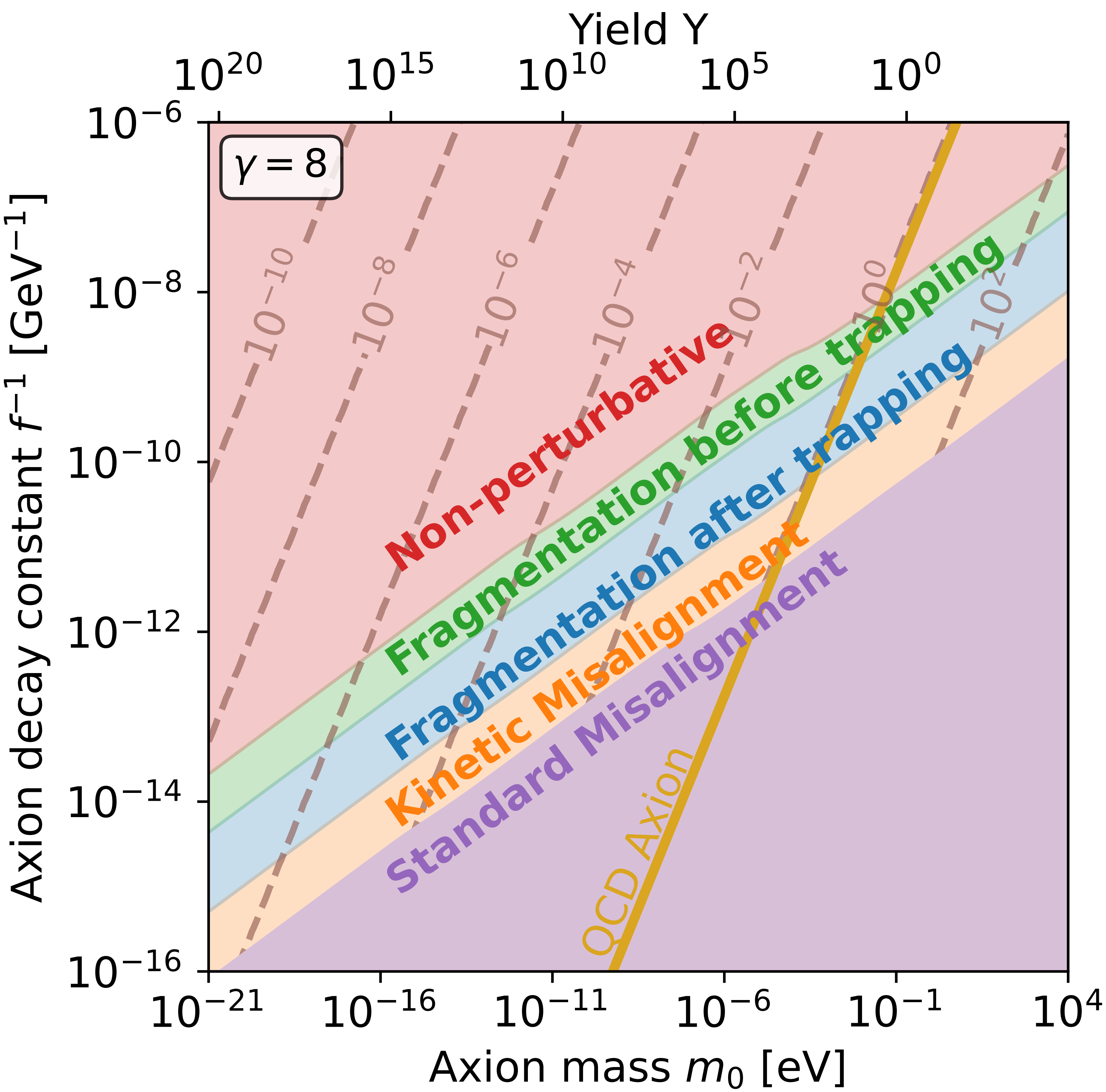

2206.14259

Slide by Marco Gorghetto

ALPs: Targets for haloscopes

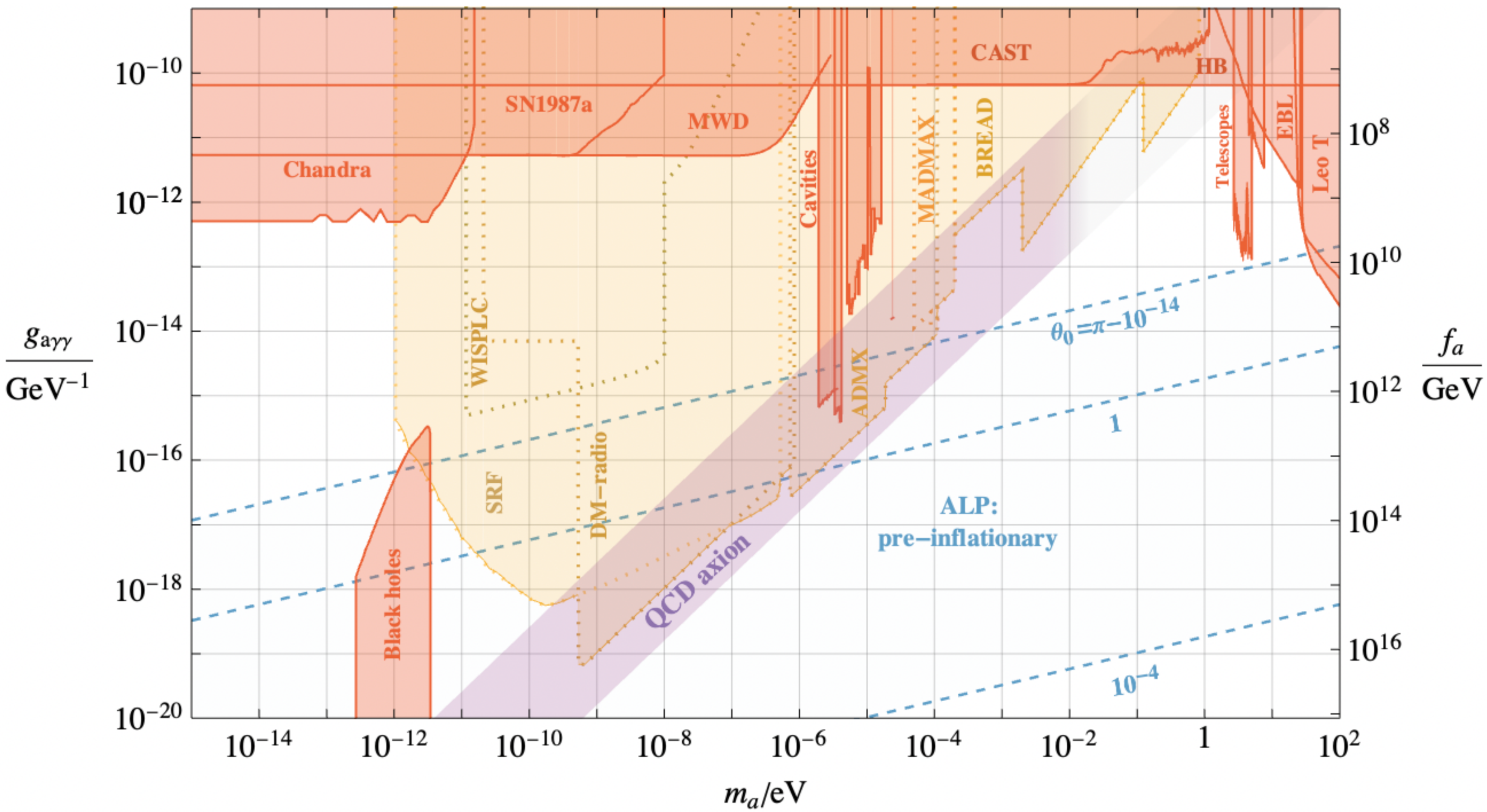

$$\frac{\Omega_a^{\text{mis}}}{\Omega_{\text{DM}}} \simeq 2.2 \cdot 10^{-3} \left(\frac{f_a}{10^{12}\ \text{GeV}}\right)^2 \left(\frac{m_a}{10^{-6}\ \text{eV}}\right)^{1/2} h(\theta_0)\, \theta_0^2$$

$$g_{a\gamma\gamma} \simeq \frac{\alpha_{em}}{2\pi f_a}$$

The case $N_{DW} > 1$.

Slide by Marco Gorghetto

ALPs: Targets for haloscopes

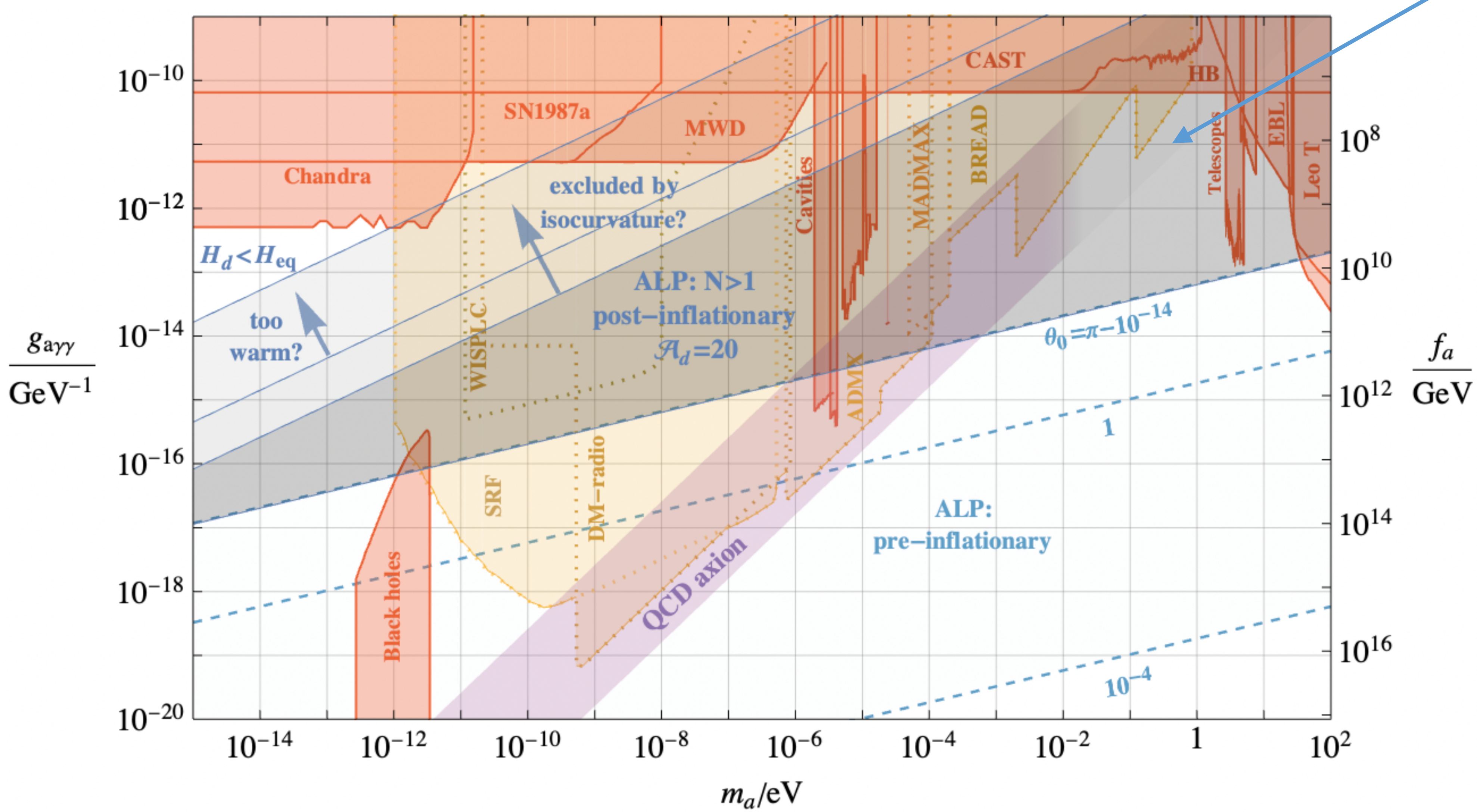

Domain wall number

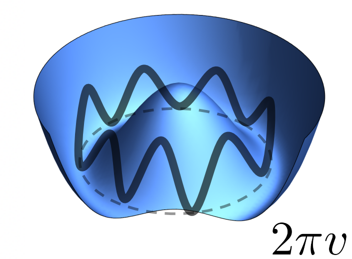

$v = N f_a$

$$\frac{\Omega_a}{\Omega_{DM}} \simeq 2 \left(\frac{\mathcal{A}_d}{20}\right)\left(\frac{m_a}{H_d}\right)^{1/2}\left(\frac{f_a}{10^{12}\ \text{GeV}}\right)^2\left(\frac{m_a}{10^{-6}\ \text{eV}}\right)^{1/2}$$

[2212.13263]

M. Gorghetto, E.Hardy

Gravitational-wave signatures of axion cosmology .

Standard Model sources of primordial GW.

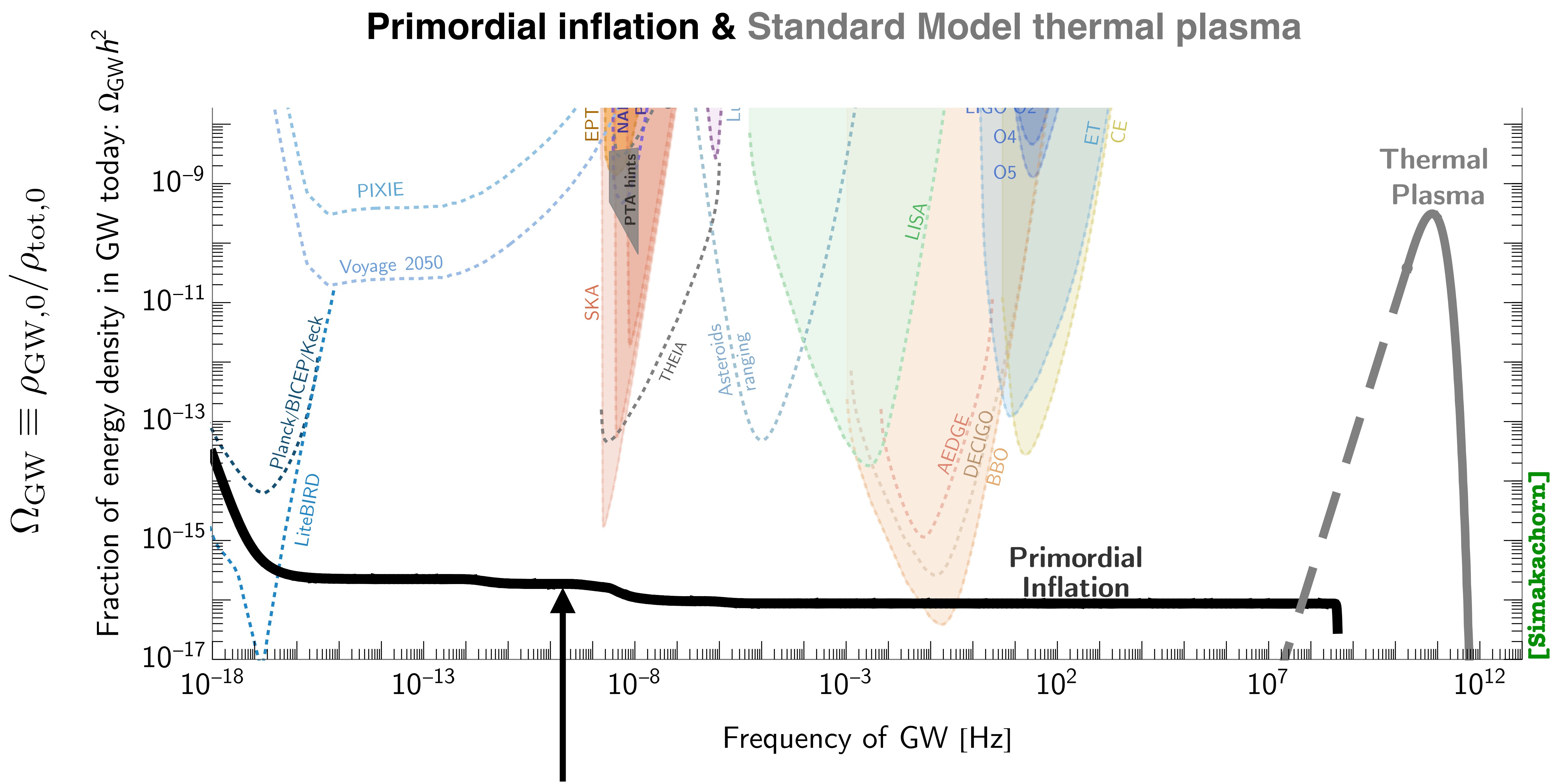

Irreducible GW background from amplification of initial quantum fluctuations of the gravitational field during inflation

Beyond-the-Standard Model sources.

Preheating, first-order phase transitions, cosmic strings

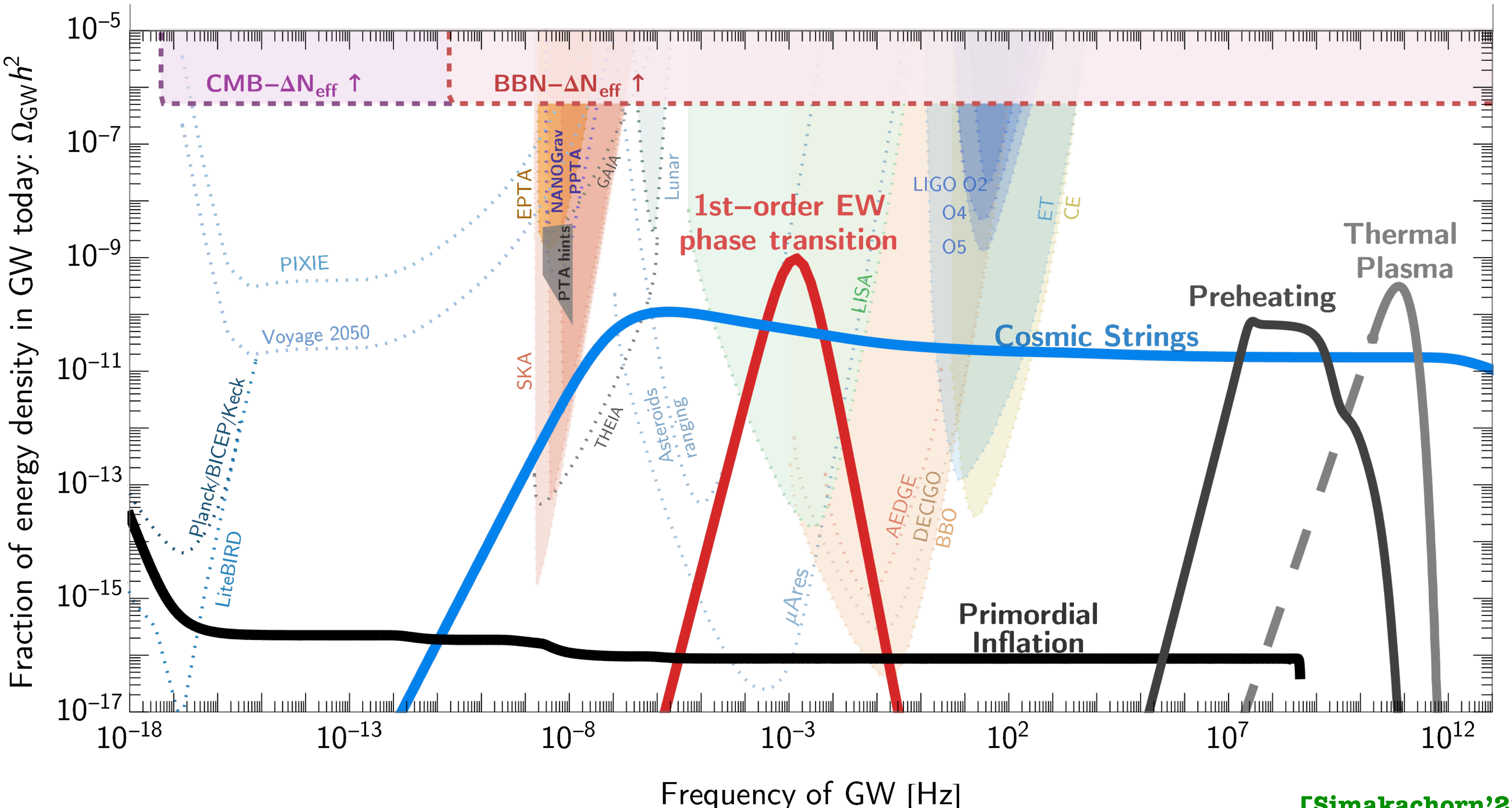

[Simakachorn'22]

Reading the history of the universe.

GW frequency $$f_{\mathrm{GW},0} \simeq \lambda_{\mathrm{GW}}^{-1}\left(\frac{a_{\mathrm{prod}}}{a_0}\right)$$

Low-freq. lim

$f_{\mathrm{GW}}^{\mathrm{min}} \simeq H_0^{-1}$

$\simeq 10^{-18}$ Hz

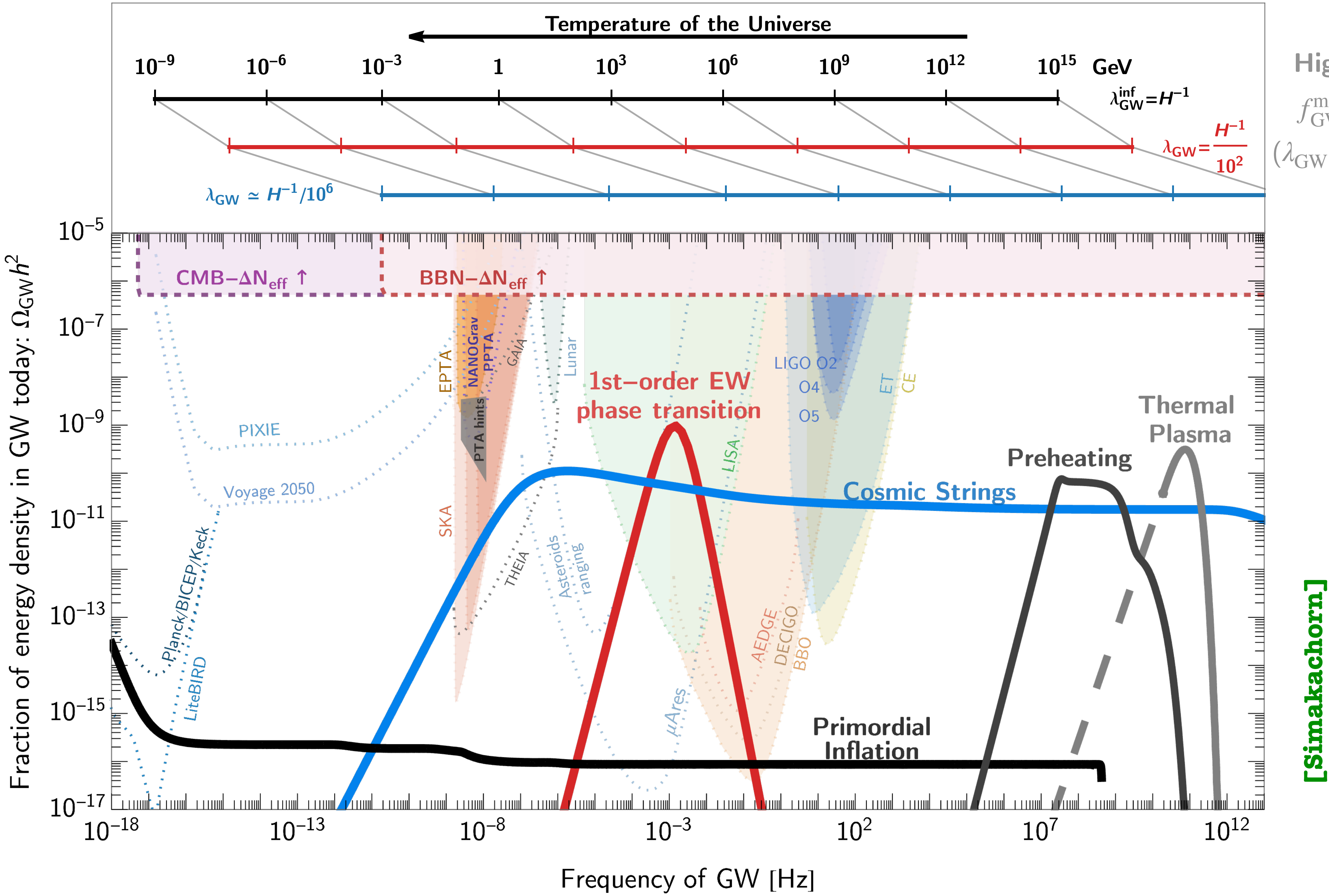

High-freq. limit

$f_{\mathrm{GW}}^{\mathrm{max}} \simeq 10^{13}$ Hz

$(\lambda_{\mathrm{GW}} \sim H^{-1} \sim M_{\mathrm{pl}}^{-1})$

[Simakachorn]

Reading the history of the universe.

GW frequency $f_{\mathrm{GW},0} \simeq \lambda_{\mathrm{GW}}^{-1}\left(\frac{a_{\mathrm{prod}}}{a_0}\right)$

Low-freq. lim

$f_{\mathrm{GW}}^{\min} \simeq H_0^{-1}$

$\simeq 10^{-18}$ Hz

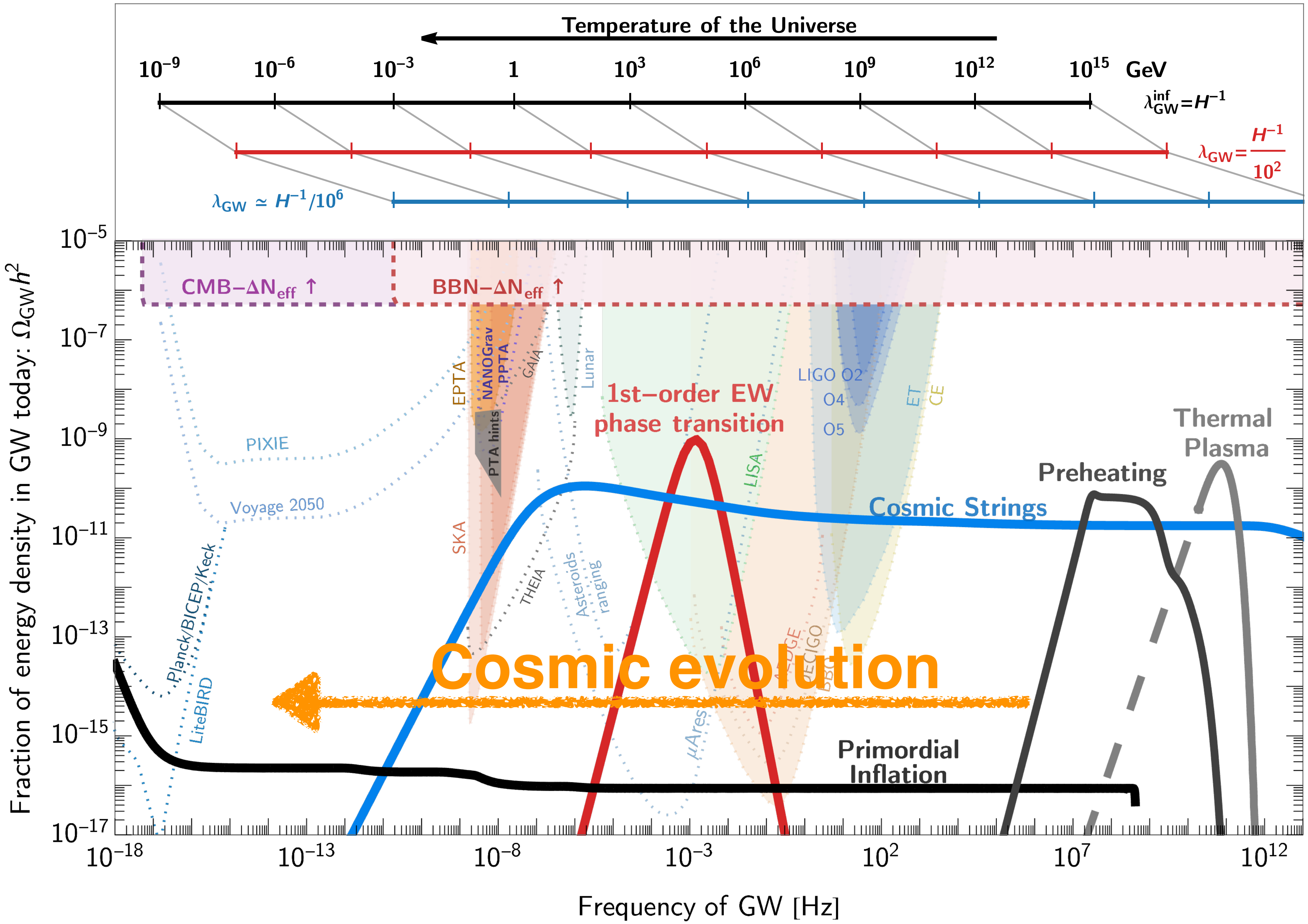

High-freq. limit

$f_{\mathrm{GW}}^{\max} \simeq 10^{13}$ Hz

$(\lambda_{\mathrm{GW}} \sim H^{-1} \sim M_{\mathrm{pl}}^{-1})$

[Simakachorn]

GW spectra are sensitive to the cosmological history.

frequency $f_{\mathrm{GW},0} \simeq \lambda_{\mathrm{GW}}^{-1}\left(\frac{a_{\mathrm{prod}}}{a_0}\right)$ **energy density** $\rho_{\mathrm{GW},0} \simeq \rho_{\mathrm{GW}}^{\mathrm{prod}}\left(\frac{a_{\mathrm{prod}}}{a_0}\right)^4$

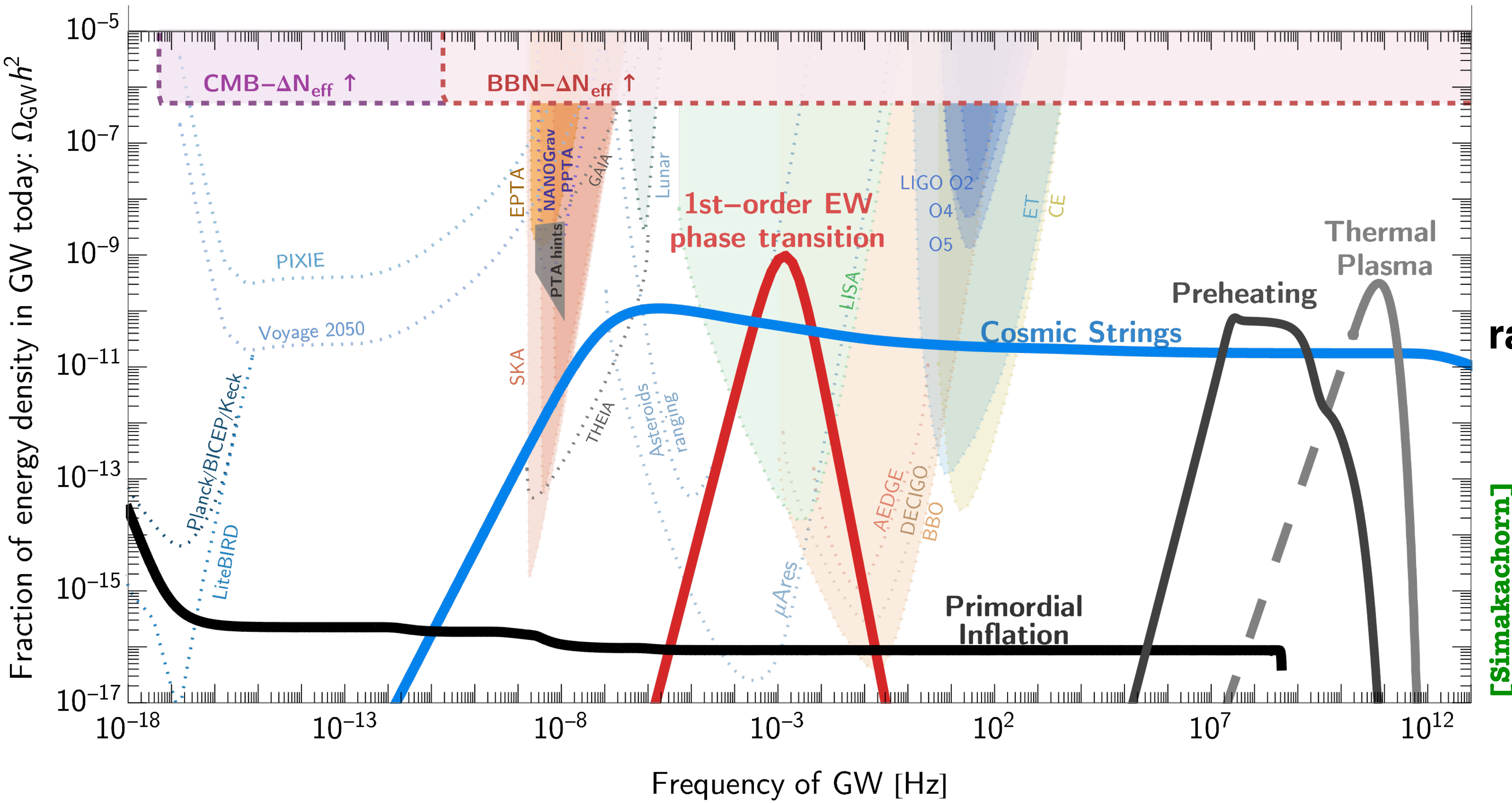

Standard Model radiation era at high energies

What if the universe is not radiation-dominated at high energies?

Effect of non-standard cosmology on the GW spectrum.

Standard cosmological history

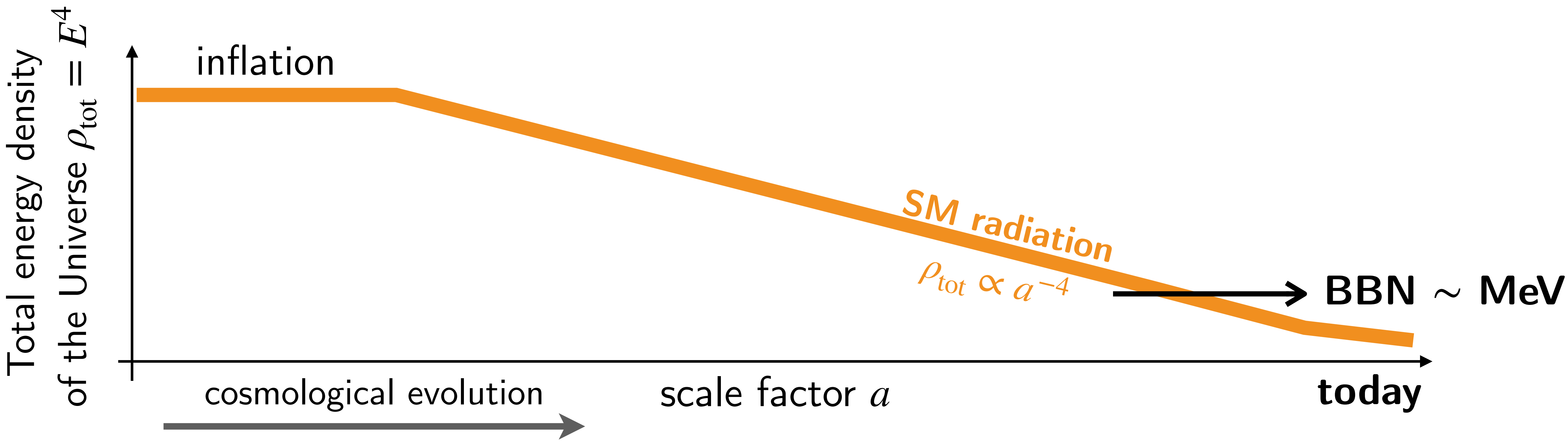

Early matter+kination era

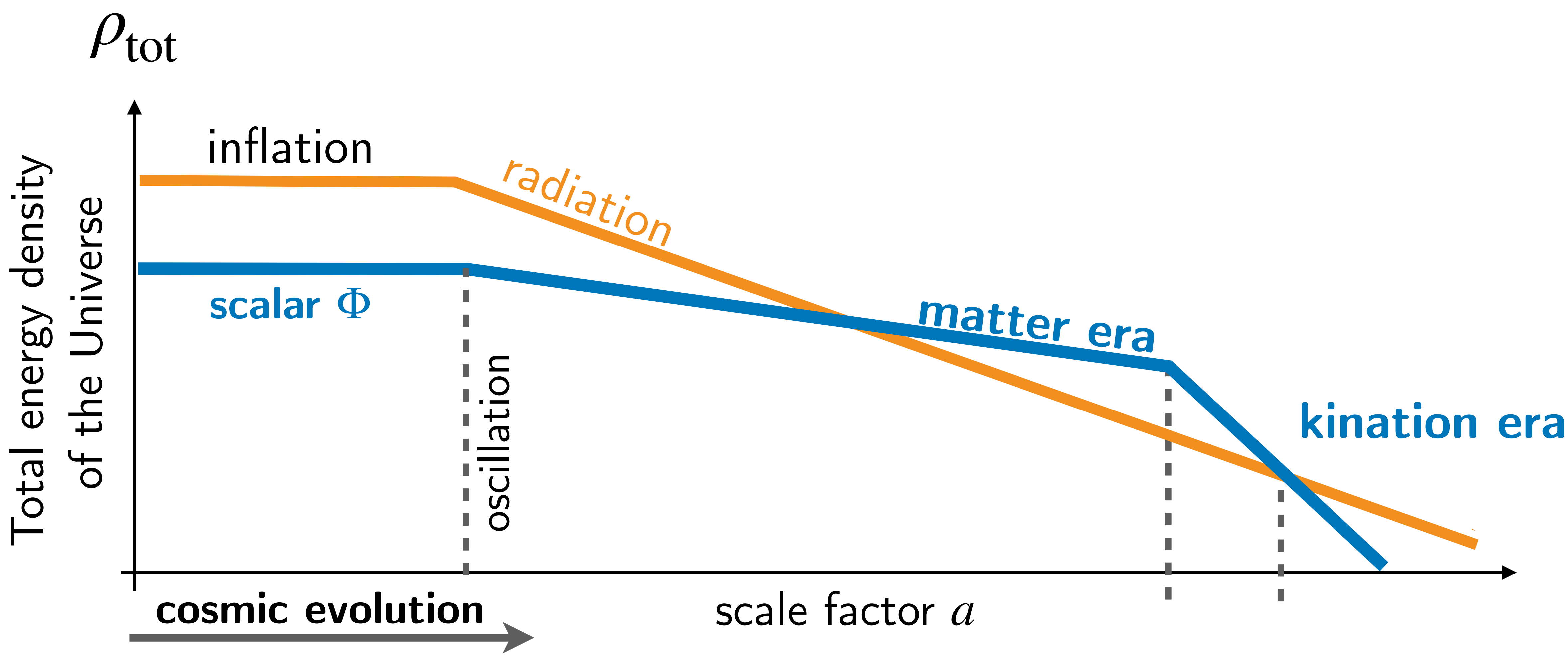

GW from cosmic strings and from inflation track the total energy density of the universe.

—> Significantly enhanced by a matter + kination era

Impact of the cosmological history on Gravitational Waves:

[1912.02569] [2111.01150]

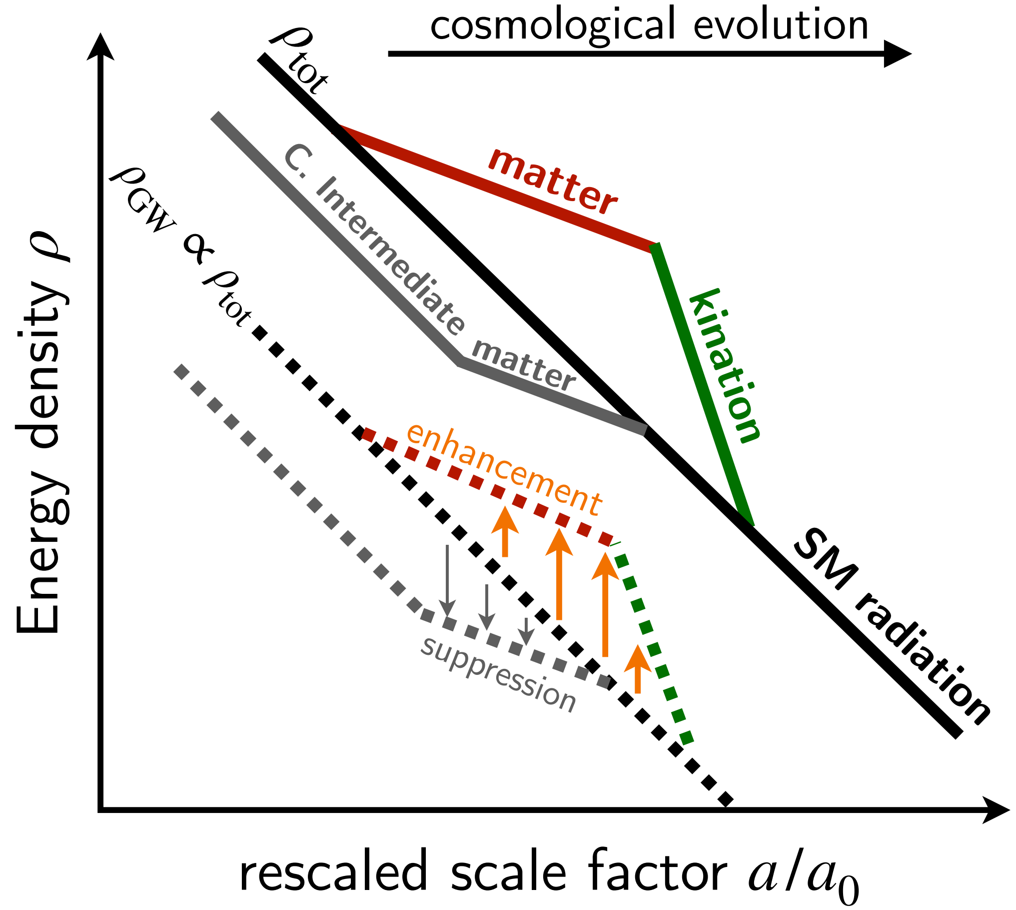

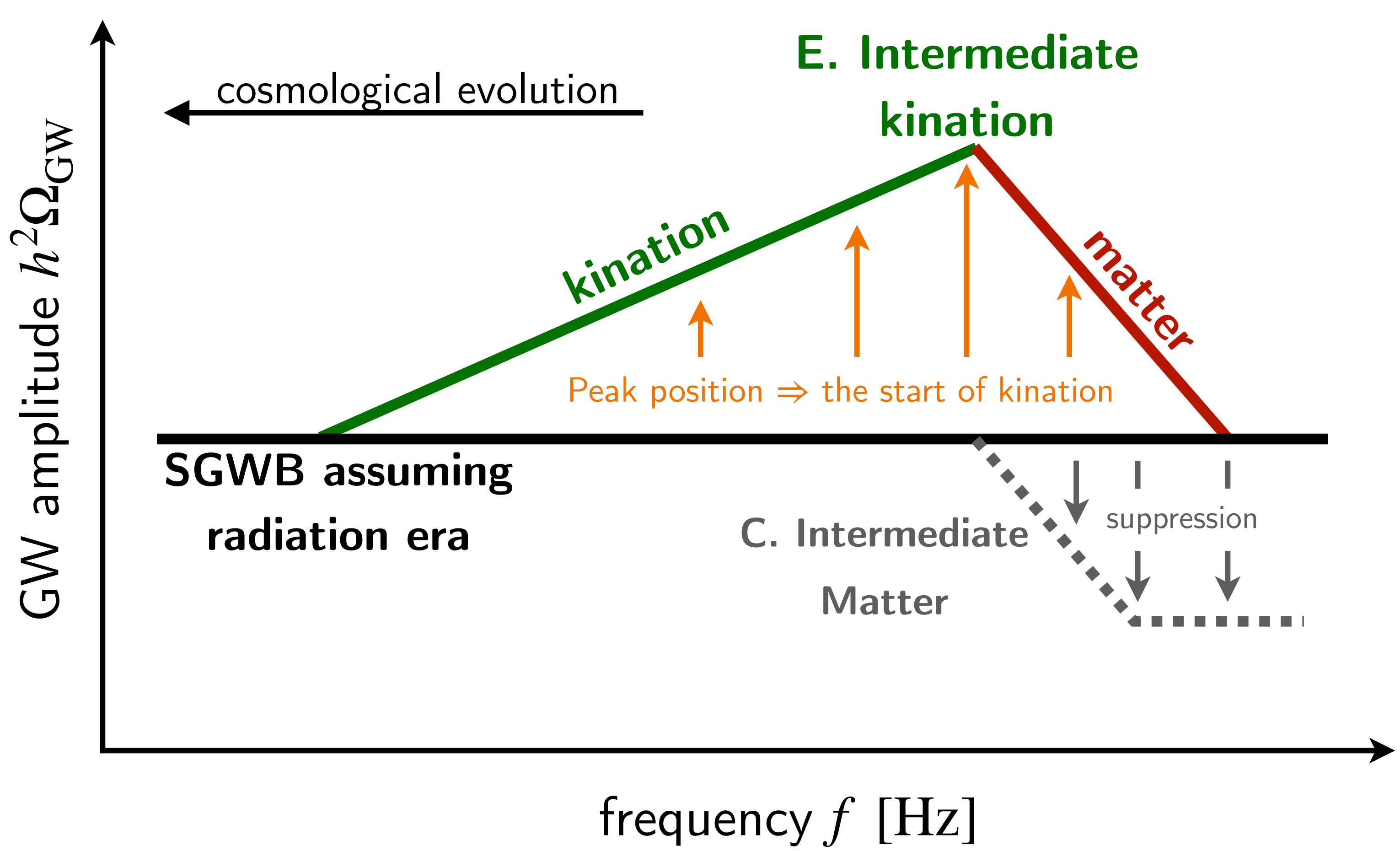

Fraction of energy density in GW today

$$\Omega_{GW,0} = \left(\frac{\rho_{GW,prod}}{\rho_{tot,0}}\right)\left(\frac{a_{prod}}{a_0}\right)^4 = \left(\frac{\rho_{GW,prod}}{\rho_{tot,prod}}\right)\left(\frac{\rho_{tot,prod}}{\rho_{tot,0}}\right)\left(\frac{a_{prod}}{a_0}\right)^4$$

Amplification of inflationary GW from axion-induced kination era.

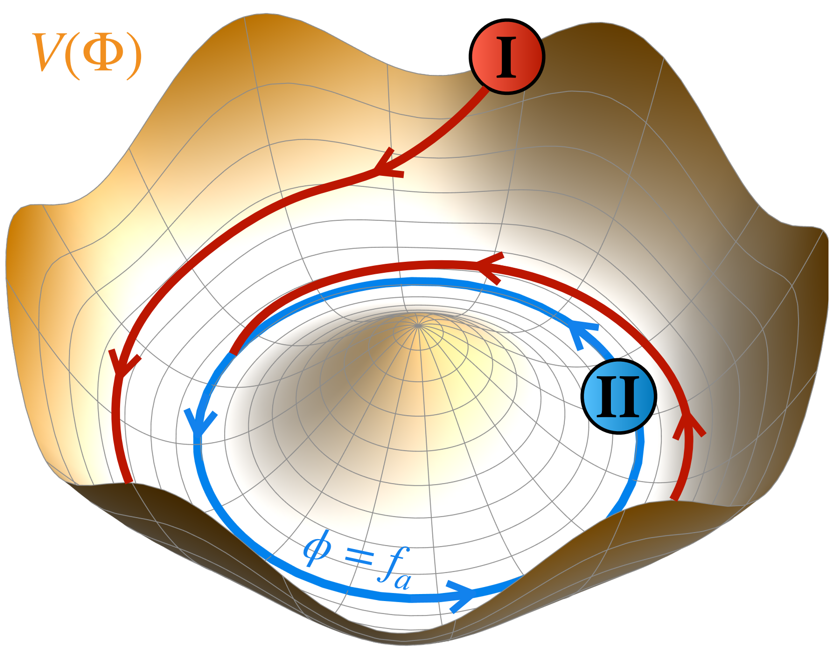

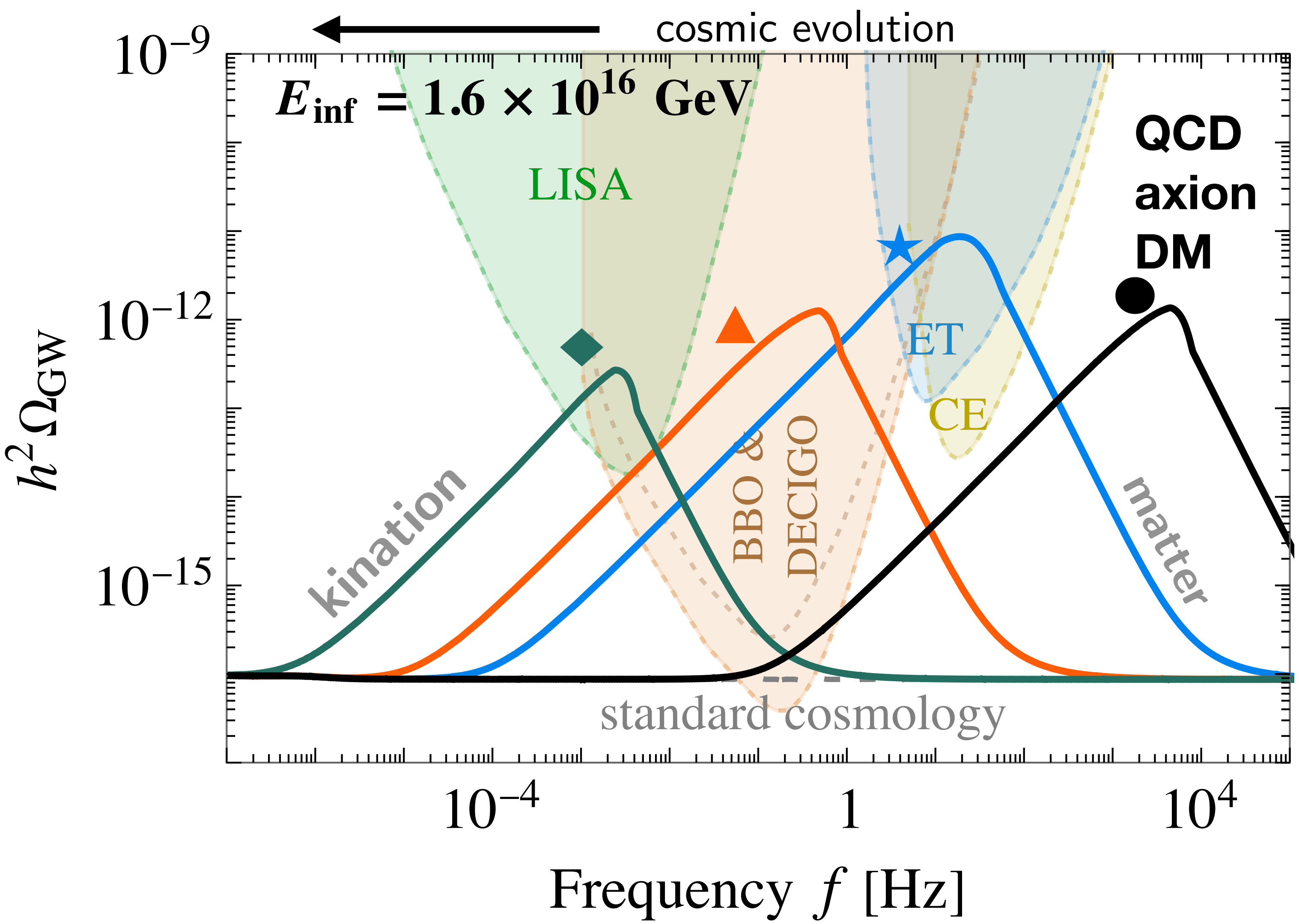

$f_a \sim 10^{10}$GeV
$N_{KD} = 5$

[Gouttenoire et al 2108.10328 & 2111.01150]

Amplification of GW from local cosmic strings due to an axion-induced kination era.

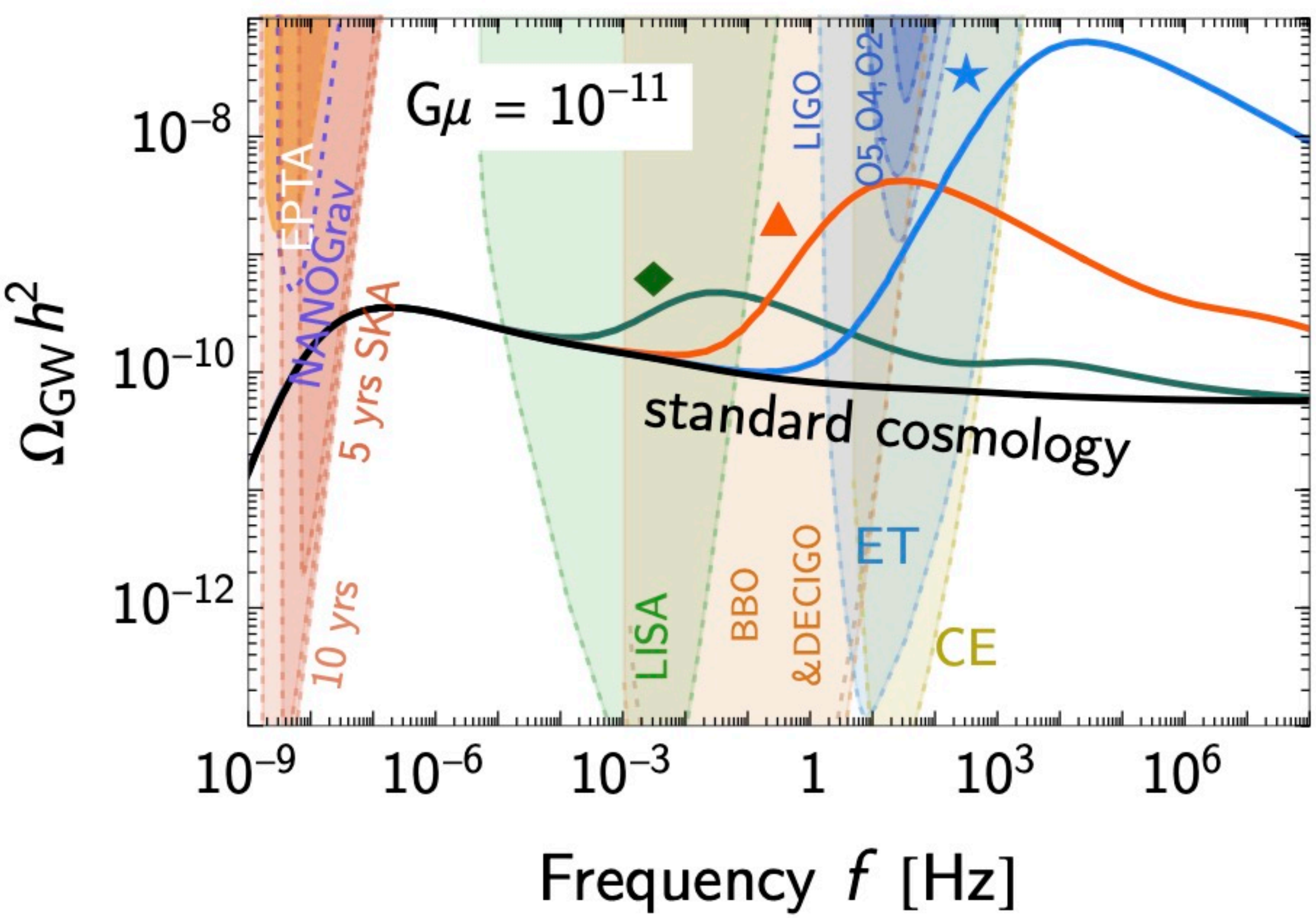

[2111.01150]

Amplification of GW from global cosmic strings due to an axion-induced kination era.

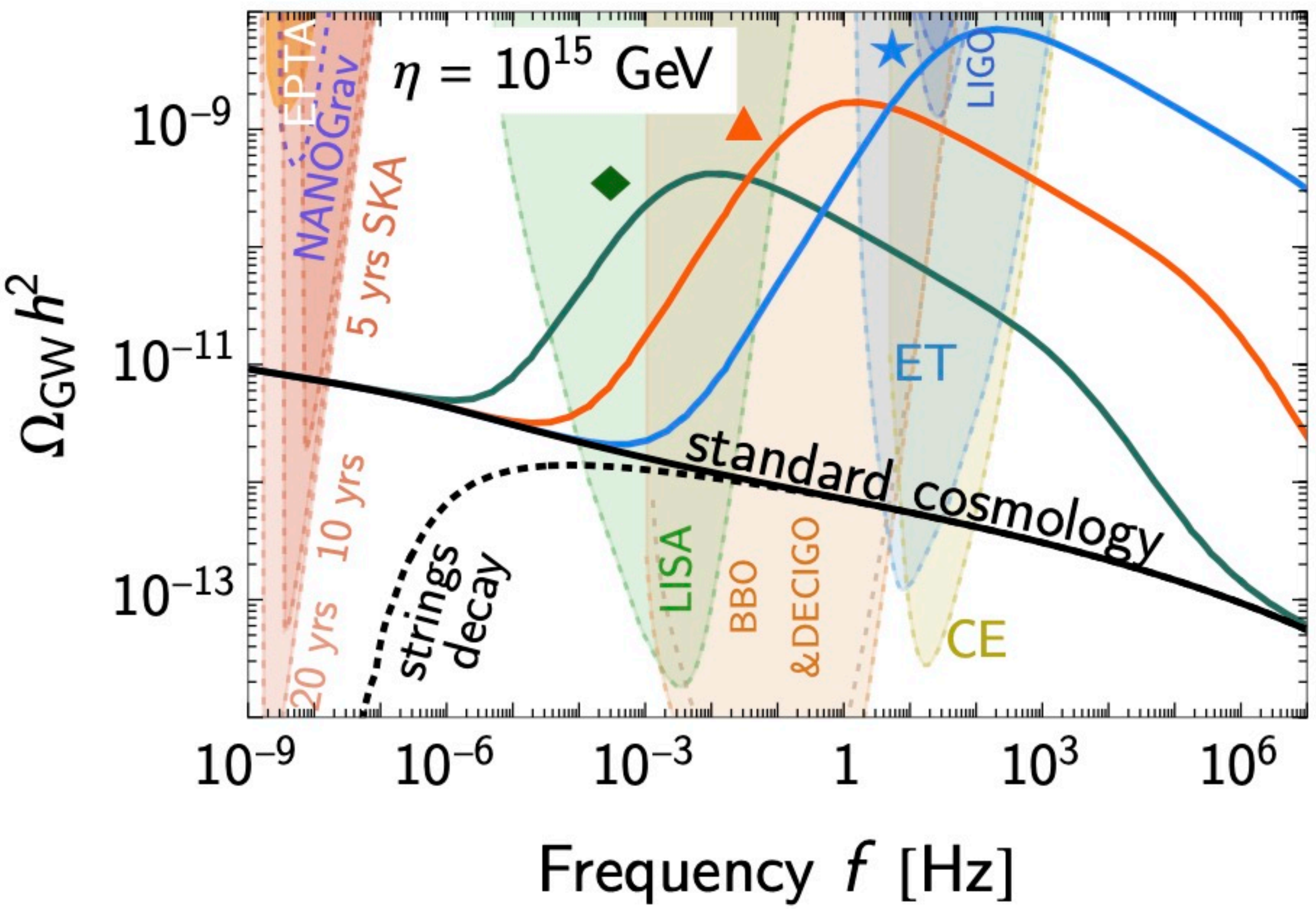

[2111.01150]

Gravitational Waves from inflation & local cosmic strings in non-standard cosmology induced by rotating axions.

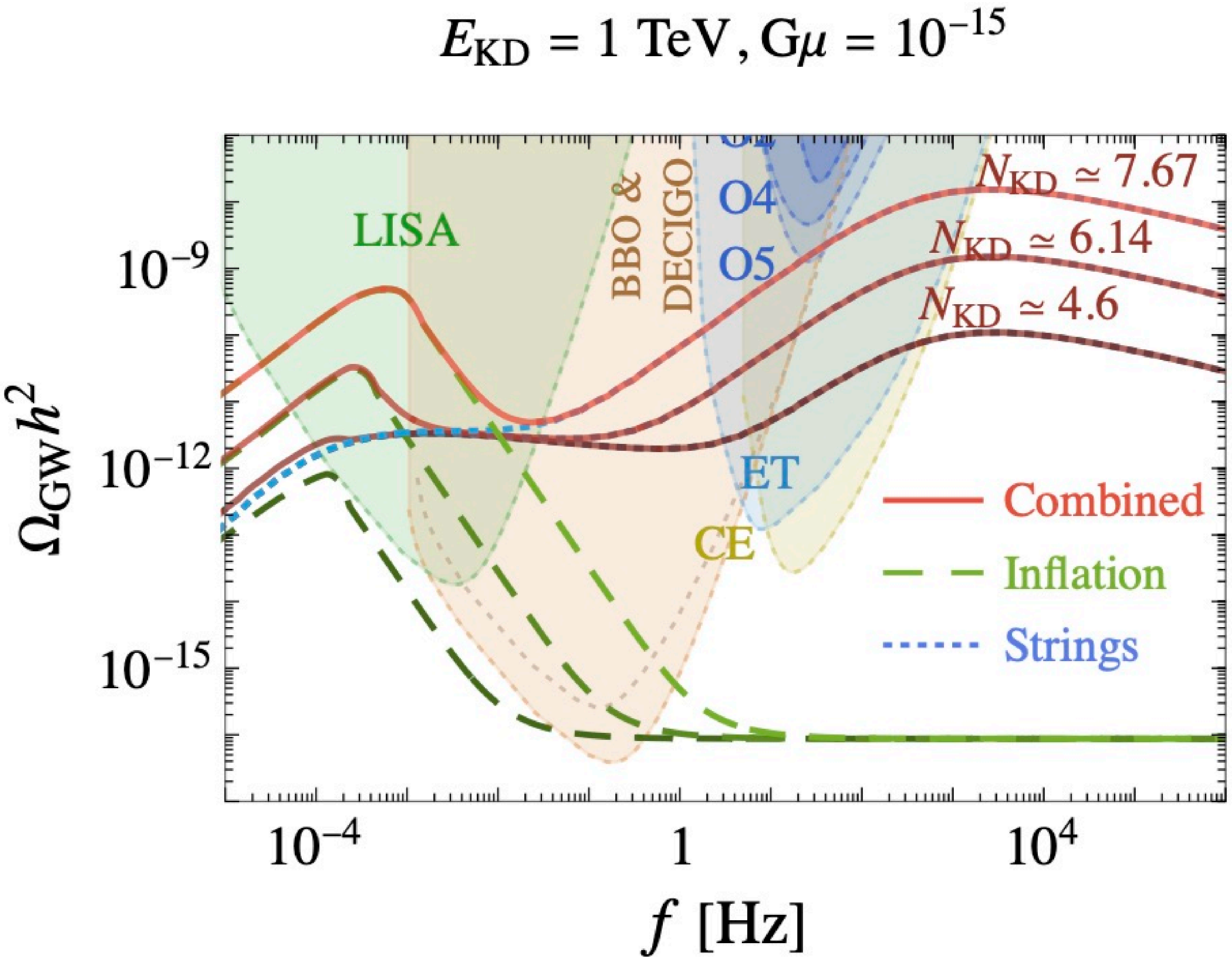

[2111.01150]

Gravitational Waves from inflation & global cosmic strings in non-standard cosmology induced by rotating axions.

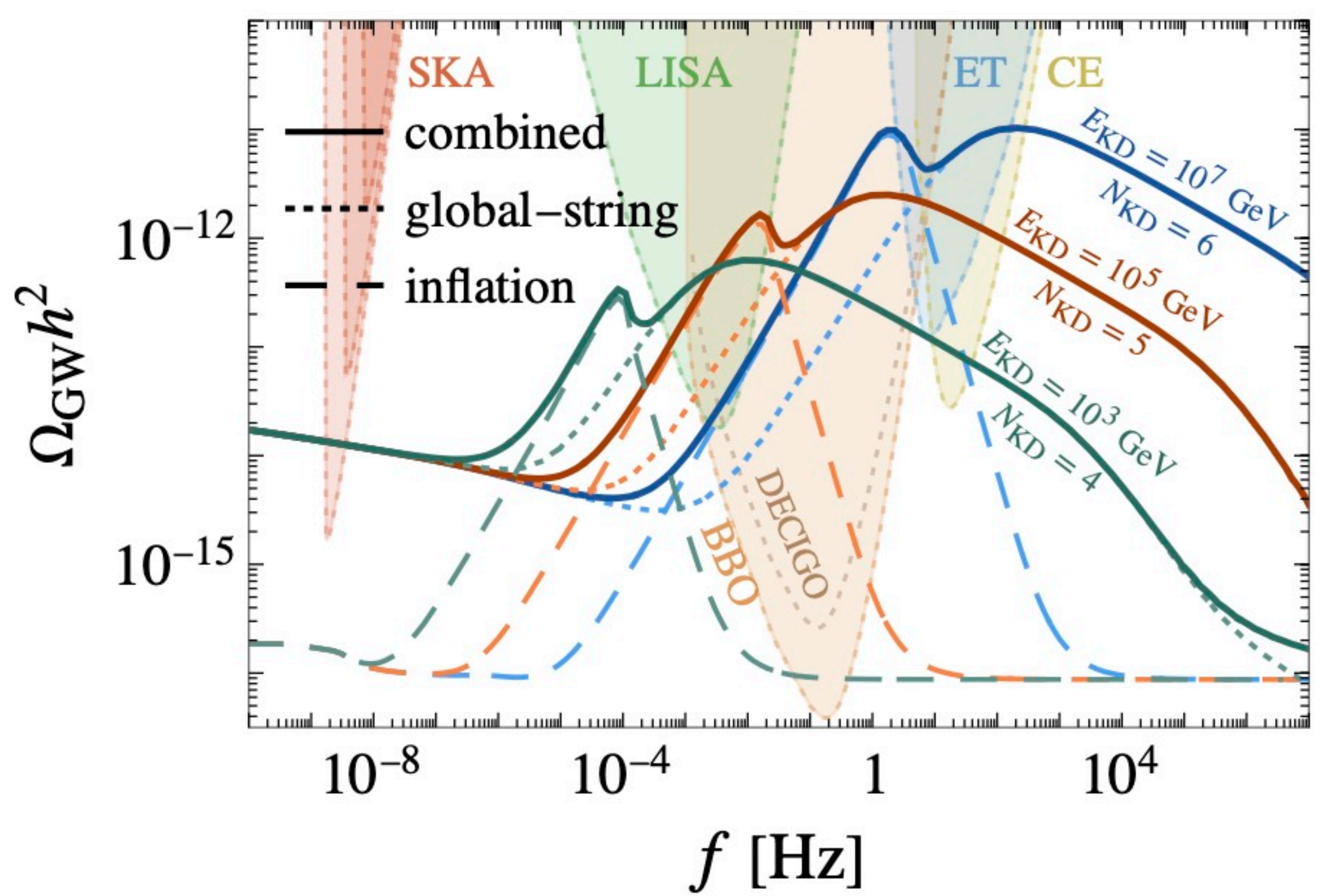

[2111.01150]